TÉCNICO LISBOA

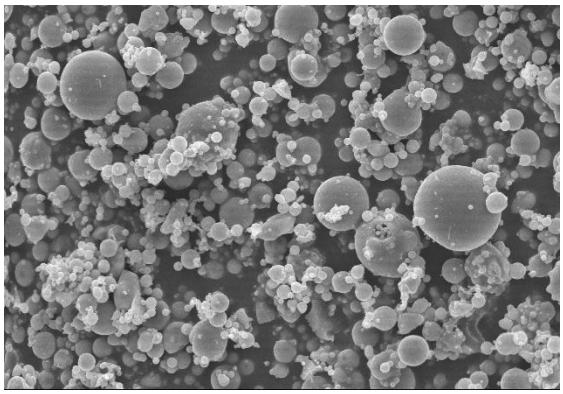

BIODIESEL PRODUCTION OVER FLY ASH-BASED CATALYSTS

JOÃO VICTOR DE OLIVEIRA PONTES

Thesis to obtain the Master of Science Degree in

Energy Engineering and Management

Supervisors: Prof. Ana Paula Vieira Soares Pereira Dias

Prof. Teresa Grzybek

Examination Committee

Chairperson: Prof. Edgar Caetano Fernandes

Supervisor: Prof. Ana Paula Vieira Soares Pereira Dias

Member of the Committee: Dr. Marta Susana Andrade Ramos

October 2020

AUTHOR'S STATEMENT

This thesis is based on the work conducted within the InnoEnergy Master School, in the MSc programme Clean Fossil and Alternative Fuels Energy. This programme is supported financially by the InnoEnergy. This author also received financial support from InnoEnergy, which is gratefully acknowledged.

InnoEnergy is a company supported by the European Institute of Innovation and Technology (EIT), and has the mission of delivering commercial products and services, new businesses, innovators and entrepreneurs in the field of sustainable energy through the integration of higher education, research, entrepreneurs and business companies. Shareholders in InnoEnergy are leading industries, research centres, universities and business schools from across Europe.

www.innoenergy.com

The MSc. programme Clean Fossil and Alternative Fuels Energy is a collaboration of:

AGH – University of Science and Technology, Kraków, Poland
SUT – Silesian University of Technology, Gliwice, Poland
IST – Instituto Superior Técnico, Lisbon, Portugal

(the MSc. thesis was prepared at the Instituto Superior Técnico - IST, Lisbon, Portugal)

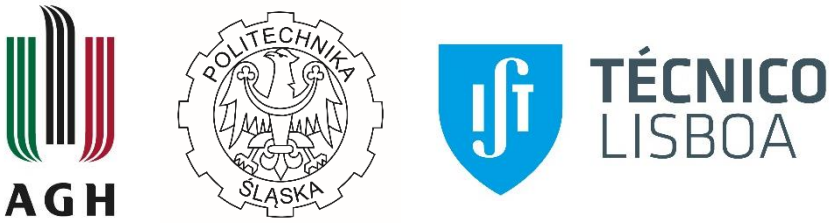

To my parents, Luís David and Daniela Virgínia, for all their love, support and patience.

To my grandparents, Celestino and Zilda Maria, for all their love, example and presence.

AKNOWLEDGEMENTS

First of all, I thank God, Holy Mary and Jesus Christ, for continuously taking care and never giving up on me, for continuously drawing the path of my life, for protecting and blessing me, and for allowing me to born in the right family.

I thank Pope and Saint John Paul II, whom I had developed care and love only by seeing and admiring him on TV in my childhood, and who stayed very close to me during my stay in the marvelous city of Kraków, his (almost) hometown.

I thank my parents, Luís David and Daniela Virgínia, for all their love, dedication, effort and patience to me, all of which shaped my personality, build my character and refined my principles to create the son, citizen and the professional I am today. Their ubiquitous example of strength and insistence are an inspiration and a continuous remembrance for me. I thank also to my three brothers, Brenno, David and Lucas for all their support, curiosity and incentive to me, besides all the uncountable memories that we built together mixed with discussions, happiness and friendship.

I thank my grandparents Celestino e Zilda Maria for their example, love, humanity, positiveness and continuous confidence that I will succeed, no matter what. Their lessons taught and presence were (and are) a gift and an unique opportunity to learn how to be a better person, to love unconditionally and to share the most sincere good with others.

I thank my great grandparents, Colonel Celestino and Maria Regina, for always care for me and receive me with purity and a smile. All the moments I was able to share with you were remarkable and are safe and recorded in my heart and mind. Grandfather Celestino, even with his traditional quietude and few words, became a true inspiration for his, unattachment, courage and dedication to leave his country to fight for freedom, democracy and peace in other lands during the 2nd World War. Thus, contributing to reshape the whole world and guarantee a brighter, better and more beautiful future for many generations to come.

I thank my great grandmothers, that God gave me the opportunity to meet and live together, Maria Eneida and Jacyra, for one of the most pure exemplifications of endless love someone can ever see and feel. Up in the sky, I am sure there is huge celebration for seeing their nephew reach this next step in the academic life.

I thank the friends that have a special place in my heart, Ícaro José, Antônio Flávio, Pablo, Pedro Yuri, Patrícia and Katarina, for all your care, love, patience and friendship. The Engineering brought us together to fight the good fight and created a bond that goes beyond the classroom and the walls of the university. Surely, we, together, are better and greater.

I thank to the very special friends I was blessed to meet and see a friendship flourish during the master's program. You share with me a true and sincere connection way beyond the sole classroom: the Pakistani Talal Ashraf and the Pole Maciej Sobczyk. You are, definitely, in my heart and mind forever. Your friendship is an unique gift that I carry in my heart.

I thank my *alma mater*, the Federal University of Ceará (UFC), dream-come-true of the inspiring Professor Antônio Martins Filho, for its excellent infrastructure, even during momentarily difficulties, and for all the available academic opportunities, a very relevant part of my shaping as engineer and citizen. Paraphrasing its motto, I affirm and reaffirm that I am compromised to cultivate the knowledge. As a student from UFC, I am compromised to serve the environment, doing the universal through the regional.

I thank, most sincerely, the European Institute of Technology and Innovation (EIT) and the KIC InnoEnergy Master school, both bodies of the EU Commission, for believing on me as a student and engineer, granting me a scholarship I never imagined I could get, and for all the great opportunities provided during the last 2 years. It, definitely, gave me new skills, made me settle principles and objectives, and made me grow as a person. All that focusing on to be a game-changer here and now.

I thank my new *almae matres*, my new home universities, Akademia Górniczo-Hutnicza im. Stanisława Staszica w Krakowie (AGH) and University of Lisbon (UL), for all the opportunities provided and the high quality pursued. Definitely, the good and relevant change to the world only can occur through knowledge, dedication, love, honesty and education. You are in my heart and I will honor your name, history and tradition through the knowledge.

I, specially, thank to my two beautiful advisors, one from AGH another from IST, prof. dr hab. Teresa Grzybek and Prof. Dr. Ana Paula Vieira Soares Pereira Dias. Two inspiring women that I am more than grateful to have built and shared this thesis research with. I am more than sure that I could not get (or want) any better supervisors. I cannot thank you enough for all your teachings, time donated and experience shared, all that besides the hours spent with the belly on the laboratory stand. This thesis is only at this stage due to you.

I thank all the professionals that dedicated themselves to make the Energy Transition MSc. program (formerly Clean Fossil and Alternative Fuels Energy, CFAFE) a great opportunity to shape new professionals and citizens. Specially to Mrs. Ewa Figórska from AGH, who was (and is) always ready to help, with care, education and a persistent smile, myself during (and after) my stay at AGH. Undoubtfully, without her, the difficulties and barriers faced would be harder to overcome.

I thank the friend I made at the laboratory in Kraków, Szymon Ratowicz, for his help and support during several weeks at the laboratory. Surely his advices and were applied in this work.

I thank the friends I made at the laboratory at the 9th floor of IST's South Tower in Lisbon, Daniela Spataru and Marta Ramos, for all the support, conversations and advices held in between the laboratory benches and the glass reactors, always watching the panoramic view of the city.

Ultimately and most sincerely, I thank, from the bottom of my heart, all the professors at AGH and IST that participated, directly or indirectly, in this MSc. program. After all, without them, I could not be graduating at all. Without the true care for teaching and love for the profession, easily observable by a glimpse of an eye, learning would not be the same. Vivid examples are prof. dr hab. Teresa Grzybek, prof. AGH dr hab. Joanna Kulczycka, prof. AGH dr hab. inż. Marek Ściążko, mgr Dariusz Kałuża, mgr Anna Małgorzata Gryboś and Prof. Dr. Ana Paula Vieira Soares Pereira Dias. I extend my gratitude, even, to those who dedicated only a little to my education and formation because it simply gave me even more incentive and energy to pursue my goal, regardless the challenges of the journey.

“Whoever you are, whatever social position you have in life, the highest or the lowest, always have as a goal a lot of strength, a lot of determination and always do everything with a lot of love and with a lot of faith in God, because someday you get there. Somehow you get there. “

(Ayrton Senna da Silva)

“You are not here merely to make a living. You are here in order to enable the world to live more amply, with greater vision, with a finer spirit of hope and achievement. You are here to enrich the world, and you impoverish yourself if you forget the errand.”

(Woodrow Wilson)

ABSTRACT

One of the major challenges for the current generation is to be capable of efficiently combine human development and advance with the support and protection of the environment. Many call this sustainability, which is based on three pillars: social, environmental and economic, and can be applied in different segments.

This work is dedicated to propose a novel economic and efficient coprecipitation-based methodology for heterogeneous catalyst synthesis focused in biodiesel production via transesterification. The major idea is to produce catalysts based on reduction of expensive reagents and valorizing residues, namely, coal fly ash (FA) and chicken egg shells (CES). Several FAES catalysts were synthesized via the same methodology (with slight variations) to evaluate the suitability of the crystalline material precipitated for biodiesel production from soybean-sunflower and WFO oils.

In terms of characterization, ATR-FTIR, XRD and SEM-EDS analysis were carried with all the catalysts. Data analyzed shows that FAES N° 6 and N° 7 calcined at 800 °C were the most efficient catalysts synthesized, reaching an average biodiesel conversion – measured via an ATR-FTIR methodology – of 80.59 % and 81.30 % respectively. This is a behavior superior even to traditional catalysts, such as NaOH, 77.60 %, and CaO, 80.60 %. These two FAES catalysts contain within their crystalline structure several minerals beyond just CaO, such as brownmillerite, andradite, mayenite, wadalite and periclase. All of which, after calcination, become mixed mineral oxides that are recognized as efficient biodiesel catalysts and can hold different active sites, alkaline or acidic.

Keywords: Biodiesel; Fly ash; Chicken egg shell; Residue valorization; Catalyst; Coprecipitation

RESUMO

Um dos grandes desafios da geração atual é ser capaz de aliar de maneira eficiente o desenvolvimento humano e o avanço com o apoio e a proteção do meio ambiente. Muitos chamam isso de sustentabilidade, que se baseia em três pilares: social, ambiental e econômico, e pode ser aplicada em diversos segmentos.

Este trabalho é dedicado a propor uma metodologia econômica e eficiente baseada em coprecipitação para síntese de catalisadores heterogêneos com foco na produção de biodiesel via transesterificação. A ideia principal é produzir catalisadores baseados na redução do uso de reagentes caros e valorização de resíduos, a saber, cinzas volantes de carvão e cascas de ovo de galinha. Vários catalisadores FAES foram sintetizados para avaliar a adequação do material cristalino precipitado para a produção de biodiesel a partir de óleos de soja-girassol e WFO.

Análises de ATR-FTIR, XRD e SEM-EDS foram realizadas com todos os catalisadores. Dados analisados mostram que FAES N ° 6 e N ° 7 calcinados a 800 ° C foram os mais eficientes, atingindo uma conversão média de biodiesel – medida por metodologia ATR-FTIR – de 80,59 % e 81,30 % respectivamente. Este é um comportamento superior até mesmo aos catalisadores tradicionais, como NaOH, 77,60 %, e CaO, 80,60 %. Esses dois FAES contêm em sua estrutura cristalina vários minerais além de apenas CaO, como brownmillerita, andradita, mayenita, wadalita e periclase. Todos os quais, após calcinação, se tornam óxidos minerais mistos, reconhecidos como catalisadores de biodiesel eficientes e podem conter diferentes sítios ativos, alcalinos ou ácidos.

Palavras-chave: Biodiesel; Cinzas volantes; Casca de ovo de galinha; Valorização de resíduos; Catalisador; Coprecipitação

STRESZCZENIE

Jednym z głównych wyzwań dla obecnego pokolenia jest umiejętność skutecznego łączenia rozwoju i postępu człowieka ze wsparciem i ochroną środowiska. Wielu nazywa to zrównoważonym rozwojem, który opiera się na trzech filarach: społecznym, środowiskowym i gospodarczym i może być stosowany w różnych segmentach.

Praca ta ma na celu zaproponowanie nowatorskiej, ekonomicznej i wydajnej metodologii opartej na współstrącaniu dla syntezy heterogenicznego katalizatora, ukierunkowanego na produkcję biodiesla poprzez transestryfikację. Główną ideą jest produkcja katalizatorów w oparciu o redukcję drogich odczynników i waloryzacji odpadów, a mianowicie popiołów lotnych ze spalania węgla (FA) i skorupek jaj kurzych (CES). Kilka katalizatorów FAES przygotowano przy zastosowaniu tej samej metodologiii z niewielkimi różnicami, aby ocenić przydatność otrzymanych krystalicznych materiałów do produkcji biodiesla z olejów sojowo-słonecznikowych i olejów WFO.

Jeśli chodzi o charakterystykę, przeprowadzono analizę ATR-FTIR, XRD i SEM-EDS dla wszystkich katalizatorów. Z analizowanych danych wynika, że FAES nr 6 i nr 7 kalcynowane w 800 ° C były najbardziej wydajnymi zsyntetyzowanymi katalizatorami, osiągając średni stopień konwersji biodiesla – mierzony metodą ATR-FTIR – odpowiednio 80,59 % i 81,30 %. Jest to zachowanie lepsze nawet od tradycyjnych katalizatorów, takich jak NaOH 77,60 % i CaO 80,60 %. Te dwa katalizatory FAES zawierają w swojej strukturze krystalicznej kilka minerałów poza samym CaO, takich jak brunmillerit, andradyt, mayenit, wadalit i peryklaz. Wszystkie z nich po kalcynacji stają się mieszanymi tlenkami mineralnymi, które są uznawane za wydajne katalizatory biodiesla i mogą zawierać różne centra aktywne, zasadowe lub kwasowe.

Słowa kluczowe: Biodiesel; Popiół lotny; Skorupka jaja kurzego; Waloryzacja odpadów; Katalizator; Współstrącanie

INDEX

LIST OF FIGURES

LIST OF TABLES

LIST OF ACCRONYMS, ABBREVIATIONS AND INITIALS

ABNT	Associação Brasileira de Normas Técnicas
AOCS	American Oil Chemists' Society
ASTM	American Society for Testing and Materials (nowadays ASTM International)
ATR-FTIR	Attenuated Total Reflectance – Fourier Transform Infrared Spectroscopy
BFS	Blast Furnace Slag
CCP	Coal Combustion Products
CHP	Combined Heat and Power
DAG	Diacylglycerol or Diglyceride
DIN	Deutsches Institut für Normung e.V.
EDS	Energy Dispersive Spectroscopy
EIA	United States Energy Information Administration
ER	Eley-Rideal Kinetic Mechanism
ESP	Electrostatic Precipitator
EU	European Union
FA	Fly Ash
FSS	First Source Solution
FGD	Flue Gas Desulfurization
FMM	Final Molar Mass
FT	Fischer-Tropsch
GC	Gas Chromatography
GHG	Greenhouse Gas
GTL	Gas-to-Liquid
HDT	Hydrotreatment
HPA	Heteropolyacid
HT	Hydrotalcite
Ht	Hattori Kinetic Mechanism
ICDD	International Centre for Diffraction Data
ICE	Internal Combustion Engine
IEA	International Energy Agency
ILUC	Indirect Land Use Change
IPCC	Intergovernmental Panel on Climate Change
ISO	International Standardization Organization
IUPAC	International Union of Pure and Applied Chemistry
JCPDS	Joint Committee on Powder Diffraction Standards
LDH	Layered-Double Hydrotalcite
LHHW	Langmuir-Hinshelwood-Hougen-Watson Kinetic Mechanism
LOI	Loss on Ignition

MAG	Monoacylglycerol or Monoglyceride
MM	Molar Mass
MMM	Mean Molar Mass
MSW	Municipal Solid Waste
MTOE	Million Tonnes of Oil Equivalent
PCC	Pulverized Coal Combustion
PDF	Powder Diffraction File
PET	Polyethylene Terephthalate
PLS	Partial Least Square
PNPB	National Biodiesel Production and Use Program
PTSA	Para-Toluene-Sulfonic Acid
PVA	Polyvinyl Alcohol
RDF	Refuse-Derived Fuel
RED	Renewable Energy Directive
RH	Rice Husk
RHA	Rice Husk Ash
RSC	Royal Society of Chemistry
SC	Supercritical
SCR	Selective Catalytic Reduction
SEM	Scanning Electron Microscopy
SG	Specific Gravity
SNCR	Selective Non-Catalytic Reduction
SSS	Second Source Solution
TAG	Triacylglycerol or Triglyceride
TCE	Tonnes of Coal Equivalent
TMM	Total Molar Mass
TOE	Tonnes of Oil Equivalent
TPES	Total Primary Energy Supply
UFC	Federal University of Ceará
UFO	Used Fried Oil
UN	United Nations Organization
VO	Vegetable Oil
WCA	World Coal Association
WCED	World Commission on Environment and Development
WFO	Waste Fried Oil
XRC	X-Ray Crystallography
XRD	X-Ray Diffraction

1 INTRODUCTION – CONNECTING EDGES

The broadest and more general idea or perception about energy is inherent to planet Earth since the constitution of the solar system until the condition that it presently has. The influence, impact and consequences of the solar energy are, decidedly, spread all around, for instance and indirectly, as fire. The time gap was proven to be very wide between the oldest recordings of fire identified on Earth – around 420 million years ago – and the first human ancestors' interactions with it, probably roughly 1.5 million years ago, as Scott (2018) informs.

It may not seem obvious but fire, among its control and manipulation, was able to lead off many major changes in behavior and habits of the early ancestors of the human being. Thus, they were able to extend the awake time during a day, not anymore following just the sunrise and sunset. Besides, they were able to use heat from fire as a tool against very cold winters, what allowed dwelling in colder areas of the planet. Likewise, enhancements were attained in safety, by repelling wild animals and insects, in quantity and quality of feeding, by making practicable to be eaten different types of food, and in general health, by reducing the occurrence of potential contaminations or diseases.

Those innovations in alimentation, directly, promoted an increment on the number of calories (or energy) available per unit of feed. In other words, what later was generally referred as cooking promoted a concentration of energy in food and, significantly, shrunk the time dedicated to obtain the same calories to support and sustain the whole body, as Herculano-Houzel (2012); Wrangham (2009) theorize. Associating these ideas with the logical sense that a more evolved brain requires more energy to function properly, in theory, the human ancestor's brain would need more hours of feeding to gather the extra demanded calories. Moreover, it would also be associated to a greater anatomy able to fit or store the more energy currently disposable.

Curiously, it is scientifically proven that the actual brain of the Homo sapiens in fact has a similar amount of neurons (around 86 billion) as other brains from primates having a proportional body size, according to Azevedo et al. (2009). Notwithstanding, it has a more evolved brain when it is considered the number of neurons and the body-brain size relation. Thus, as Herculano-Houzel (2012, 2016) proposes, the human brain thrived much more in comparison to what would be expected considering its body size. For instance, some primates who share the same evolutionary branch as humans, like orangutans or gorillas, are physically bigger but do not have a more evolved brain at all.

These last arguments may appear to be unsuitable or, merely, an irrelevance to this whole discussion regarding energy and its substantial role in the humanity pathway since the very early moments until present days. Nevertheless, the simple act of cooking is correlated to had favored a massive neurological development in human ancestors, allowing a marvelous rise in the number of brain neurons and its interconnections, as well as in its scale, specifically, between the Homo erectus and the Homo sapiens, according to Antón & Josh Snodgrass (2012); "Human Origins Initiative," (n.d.). Therefore, connecting all this with the idea that cognition – or ability of learning – is related to the brain

and its evolutionary level, the human being achieved an outstanding and pioneering stage. The need to spend many hours per day eating like other animals was diverted by cooking and yielded in more free hours per day to be dedicated to other activities, as debated by Herculano-Houzel (2012, 2016).

This distinction, associated with many other factors, acceded the Homo sapiens not to be just part of history but to have the conscious capacity of changing and writing his own. Considering the stage of evolution and development at that period, the advent of fire was surely a key element to support many of the transitions still to come, first as species, until become Homo sapiens, and then as an entirely communitarian animal, to institute the traditional concept of modern society. In fact, much of that due to its capacity to not only observe nature and its phenomena but also to analyze, question, hypothesize and, effectively, try to stablish rules, assumptions, definitions or equations, in a huge and constant effort to translate or interpret it.

An exemplification of that is the Great Navigations Era and what many identifies as Science Revolution. The first one was started by Portugal and Spain in the XVI century, that changed and shaped the whole world, transforming the human society entirely. It introduced the concept of worldwide commercial trades and mercantilism, aside to broadening the *mappa mundi* by reaching the so-called New World and discovering the American continent. The second one is solely an agglomerate of the uncountable events that historically marked the birth of modern science, represented by innumerous people that gained notoriety for their contributions, such as Nicolaus Copernicus and Isaac Newton.

The Homo sapiens reached a baseline where no other living being ever reached. However, the time, the sufferings and the sacrifices demanded from the very first ancestor towards reaching the level of development, evolution and knowledge found in the XVIII century was enormous. Contrastingly, after the advent of the First Industrial Revolution hatched in England and the others that would arise in the following years and centuries, humanity probably witnessed the biggest and quickest remodeling ever.

Coal and petroleum, were two constituents that, radically, reshaped the previously stablished conceptions and ideas believed to be eternal truths of a modern society. Definitely, the energy was in the focus point to characterize the human species' path to become a "Hydrocarbon Man", as Yergin (2008) coined the expression. Many men and women around the planet had their names written in the very dense, multifaceted and comprised of uncountable great challenges, history of oil. The polish pharmacists Jan Józef Ignacy Łukasiewicz and Jan Zeh, for example, are known as inventors of the kerosene lamp that started to be used safely as a substitutive to tallow candles with a rudely distilled oil. It begun to be used in July 31th, 1853 to brighten the general hospital at the, nowadays, Ukrainian city of Lviv, and, subsequently, some stations and trains of the Emperor Ferdinand Northern Railway.

The date of August 27th, 1859 is the milestone of the first oil well (21 meters deep) drilled with modern techniques – using drill bits and pipes – in the world, done by Edwin Laurentine Drake at the city of Titusville, in the US state of Pennsylvania. Oil that flowed from that well transformed forever the region near Oil creek and Oil city, sparkling a new era that lead the whole world to a brand-new revolution that extends until to this day and named "Petroleum Age" by Yergin (2008).

A growing perception of the damages caused by oil and coal in the environment started to be more and more focus of investigation and research. Much of that was triggered by the simple perception of changes in the environment and the rise of problems direct affecting human health, or even provoking negative impacts on the way-of-life or economic activities. As an exemplification there are the effects identified in metropolis and big industrial areas like smog1, acid rains and health diseases, with its multiple collateral effects.

As a major remarkable milestone, an experiment commenced in 1958 by the scientist Charles David Keeling, still to present day under operation at the Mauna Loa observatory2 in the American state of Hawaii, measured and brought into light to the world, for the first time, the carbon dioxide (CO_2) accumulation in atmosphere. The Keeling Curve, as it was baptized, is essentially an instant quantitative demonstration of CO_2 content in atmosphere. However, combining with data from ice core samples from North and South polar caps and mountain glaciers, it was possible to get a glimpse of Earth's climate history and attest the increase of CO_2 levels in atmosphere since the rise of fossil fuels.

There are many examples of concrete actions towards environment and pollution. The United Nations Organization (UN) Conference on the Human Environment, held in Stockholm, Sweden (1972), dedicated to discuss environment and human development as a whole, the Convention on Long-Range Transboundary Air Pollution (CLRTAP) agreement (1979), focused on developing tools and limiting the emissions produced by countries, and the Montreal Protocol (1987), created to protect the Ozone Layer via prohibition of use of many harmful compounds. Also examples are the World Commission on Environment and Development (WCED), also known as Brundtland3 Commission (1987), famous for creating the concept "Sustainable Development" and issuing the "Our Common Future" report, and the foundation in 1988 of the Intergovernmental Panel on Climate Change (IPCC), a body of the UN dedicated to provide technical and scientific support on climate change.

Undoubtfully, the traditional methods of producing energy were under questioning due to its side effects, much of those supported with concrete data and arguments. Examples of the amplitude of the challenge for alternatives to cohabit with fossil fuels are the electric, hybrid and hydrogen fuel cell cars, the pyrolysis, torrefaction and gasification, the Fischer-Tropsch (FT) synthesis, the gas-to-liquid (GTL) and methanol-to-gasoline (MTG) processes, the methanation and the hydrothermal liquefaction (HTL) Together with all that, a biofuel front also prospered recently. Ethanol is nowadays produced in different countries via a fermentation process of sugars using different types of plants, depending on the geographic location – sugar cane, in Brazil, corn, in the USA, and beet in Europe.

In Brazil, for instance a program to turn biodiesel a state policy and, parallelly, strengthen social support was conceived in 2004 and named National Biodiesel Production and Use Program (PNPB).

---

[1] Neologism created by the combination of two words, smoke and fog, to represent the atmospheric phenomena created by accumulation of gaseous pollution emitted by fossil fuels in big cities or industrial areas.
[2] Part of the Earth System Research Laboratory (ESRL) from the National Oceanic and Atmospheric Administration (NOAA), a scientific agency from the USA government.
[3] Gro Harlem Brundtland, born in April 20th, 1939 at *Bærum*, Norway. She was the chairperson of the WCED commission.

Currently, Brazil has a staggered plan until 2023 to increase the minimum biodiesel content in diesel from the current 11 % to 15 %, as regulated by CNPE (2018). In European Union (EU), following the Renewable Energy Directive (RED) issued by EU (2009), it is a mandatory target by 2020 to reach 10 % of renewable energy in the transport sector and 20 % for an overall share for renewable energy in the energy matrix.

Presently, the RED II directive issued by EU (2018) envisions to reach a minimum of 14 % of renewable energy in the transport sector and 32 % for an overall share for renewable energy in the matrix. Besides, it brought new requirements for Greenhouse Gases (GHG) emissions and sustainability criteria for biofuels used in transport to be eligible for government support an financing. Also, it also presented new conceptualizations and definitions like the Indirect Land Use Change (ILUC) concept, that relates to the use of agricultural areas for biofuels instead of food production.

This broad argumentation envisioned to bring light and connect the strings of the changes that energy sector is going through impelled by the needs of coupling modern civilization, development, and natural environment. The efforts to find new ways to keep promoting energy transformation are being challenged inside universities, research centers and industries towards much more elaborated ideas, many of them inspired by the human history and old experimentations. In common with all, there is this natural and constant human need to challenge himself and dare paths discouraged or never even explored by others.

All this humbly described panorama brings endorsement to the motivations and objectives of this present work in the academia and with the scientific community. The prime inspirations of this research, kindly nurtured for many months, and continuously pursued during its development, were the dream to combine sustainability and waste valorization (an unconscious eco-innovation approach) to improve the traditional biodiesel transesterification production route. All that involved with the desire to concretely contribute to the advancement of science and technology, and impact people's lives in a positive way.

1.1 General Objectives

Highlight the importance of biofuels and residues valorization to the current situation of world's energy matrix.

Investigate environmental and economically viable alternatives to minimize some of the most relevant and impactful limitations of the biodiesel sector.

Present strong based arguments to endorse the relevance of biodiesel production, use and support to the energy sector, no matter its generation (1st, 2nd, 3rd or 4th).

1.2 Specific Objectives

Propose a fiable, new and practical heterogeneous catalysts synthesis methodology for biodiesel production derived from two major residues, coal fly ash and chicken egg shells.

Avail the existent characteristics of the target residues to compose a synthesis methodology towards reducing expenses, increasing easiness of production and focusing on simplicity.

Evidence the effectiveness of biodiesel production and catalyst behavior with two different raw materials – refined and residual oils – via transesterification using the synthetized catalysts.

2 THE BIODIESEL

The known existence and uses of vegetable oils (VO) and later biodiesel is extensive and in fact connects different epochs of human civilization. For instance, it was very much utilized by the Egyptians as food, as illuminant and as an element for religious and mummification rituals according to Hardy & Finch (2017). This could be one of the reasons that could justify its presence inside pharaoh's tombs. The first scientist to describe the production of biodiesel via its nowadays most traditional production reaction, transesterification, was Friedrich Rochieder in 1846, focusing on the production of glycerol starting with castor oil, according to the work of Gupta & Demirbaş (2010) and Jachuck, Pherwani, & Gorton (2009). Later, in 1853, the scientists E. Duffy and J. Patrick, as inform Cleveland & Morris (2014), Demirbaş (2010), Feofilova, Sergeeva, & Ivashechkin (2010), Gupta & Demirbaş (2010) and Strezov & Evans (2014), were the first ones to carry an experiment to transesterify a vegetable oil to produce soaps and biodiesel.

All those events were previous even to the development of the diesel engine by Rudolf Christian Karl Diesel in 18934 and its display at the 1900 Paris Exposition, when the engine operated only with peanut oil. However the raw vegetable oils caused many problems such as fuel atomization, clogging, incomplete combustion and impurities accumulation, which led to a quick replacement by fossil fuels, as Strezov & Evans (2014); Knothe (2001); Ma & Hanna (1999) explains. Obviously, another reason for that would be the naturally rise of petroleum-derived fuels in a time that mostly all around the USA and Europe new oil fields were being discovered and prices were very low.

Those issues started to be worked around just after the proposition of a transesterification process that would transform a vegetable oil (palm oil in that case) into a derivative that could be used in diesel engines in 1937 by the Belgian scientist C. G. Chavanne from the University of Brussels and deposited under patent No. 422.877, as Knothe, Van Gerpen & Krahl (2005) highlight. Several other processes emerged as the interest in vegetable oils increased in the following decades, mostly influenced by the uncountable changes in petroleum prices, an iconic symbol of the XX century. In 1983, a Brazilian professor and researcher from the Federal University of Ceará (UFC) named Expedito José de Sá Parente5 was granted a patent No. PI – 8007957 (Production process of fuels from fruits or oleaginous seeds6) for the development of an industrial scale process for biodiesel production (deposited in 1977). It was claimed as the first methodology in the world to propose a large scale biodiesel production, as mentioned by Joo & Kumar (2019); Lin et al. (2011).

---

[4] British Patent GB189207241 – A process for producing motive work from the combustion of fuel from 1892, US Patent 542.846 – Method of and apparatus for converting heat into work from 1895, US Patent 607.845 – Internal combustion engine from 1898 and German Patent DE86633 – *Vorrichtung zum Anlassen von Viertakt-Verbrennungskraftmaschinen durch Umwandlung derselben in Zweltakt-Druckluftmaschinen* from 1895.

[5] He is considered the "father of biodiesel" in Brazil and, during his academic life, had worked with different biofuels and developed a biokerosene produced out of babassu (*Attalea speciosa*) oil intended to be used in airplanes.

[6] Patent "*Processo de produção de combustíveis a partir de frutos ou sementes oleaginosas*" registered at the National Institute for Industrial Property (INPI) from the Brazilian government.

The interest in biodiesel and biofuels is clear and raised sharply as they presented as a feasible alternative to fossil fuels used in transportation, mostly diesel and gasoline. At present, significant participation in the world matrix is associated to the growth of the renewable energies in general. The world's Total Primary Energy Supply (TPES) is a manner of attesting and sensing this behavior. Figure 1 presents that in 2016 out of the total amount of 13,761 million tonnes of oil equivalent (MTOE) of TPES, only 1,882 MTOE (13.7 %) resulted from renewable energies, which, compared to 2015, represents an increase of 63 MTOE. Thus, around 14 % of the total energy available in the world came from renewable sources of Primary Energy (PE).

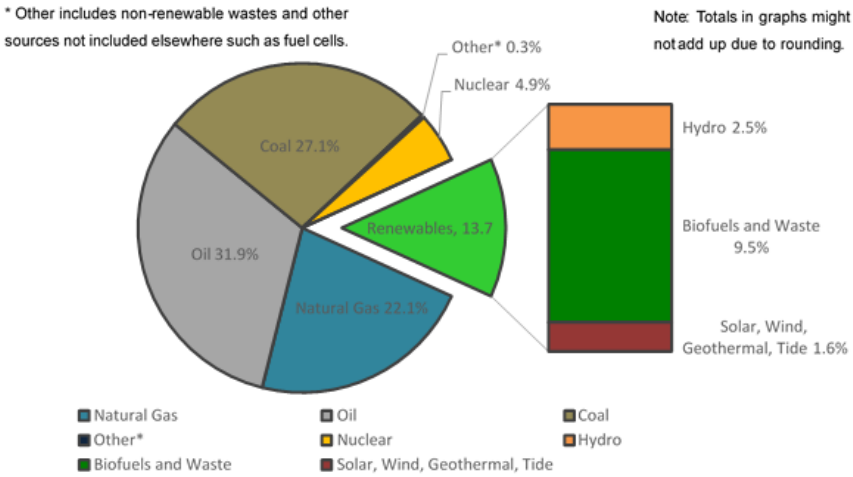

Figure 1 – Total shares of different energy sources for 2016's TPES. Adapted from: IEA, (2018b)

For a further comprehension of the role fulfilled by the renewable sources in nowadays world's economy, it is suitable particularizing the data so to identify the different types of technologies and to support a trustful analysis and discussion. Figure 2 illustrates the participation of different types of renewable energy.

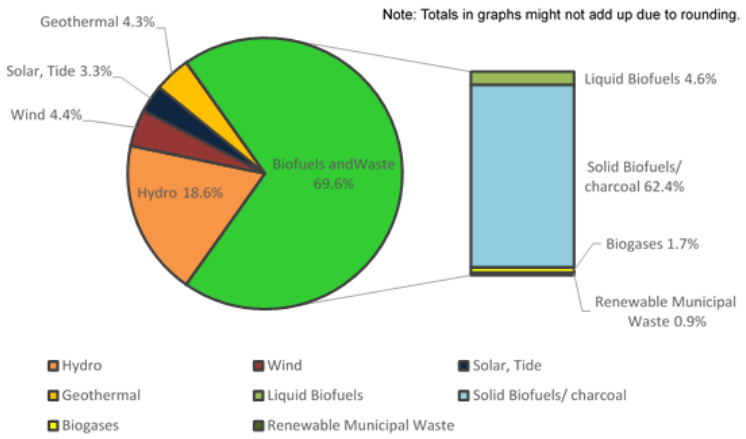

Figure 2 – Participation of different types of renewable energies for 2016's TPES. Adapted from: Adapted from: IEA (2018b)

The data indicates that liquid biofuels, as yet, do not, significantly, contribute to the worldwide TPES to the same extent as solid biofuels/ charcoal, which are responsible for 62.4 % of the total of renewable energies. It should be mentioned, contrastingly, that the annual growth rate of the use liquid biofuels was ca. 10 %, as in case of biogases (12.3 %) and solar thermal technology (11.5 %), and far beyond the worldwide TPES rate (1.7 %) or even the renewable energies rate (2 %).

As liquid biofuels dependent mostly of natural conditions such as arable areas and weather, some countries have better capacities to harness and to develop a biofuels sector. For instance, among the leaders in liquid biofuels production in the world, there are the USA, Brazil, Indonesia, Germany, China, France, Argentina, Thailand, The Netherlands and Spain, according to reports from the United States Energy Information Administration (EIA) and BP (2019). Figure 3 presents a historical data for biofuels and biodiesel production in the USA, Brazil and in the 28 constituent countries of EU in relation to production and consumption.

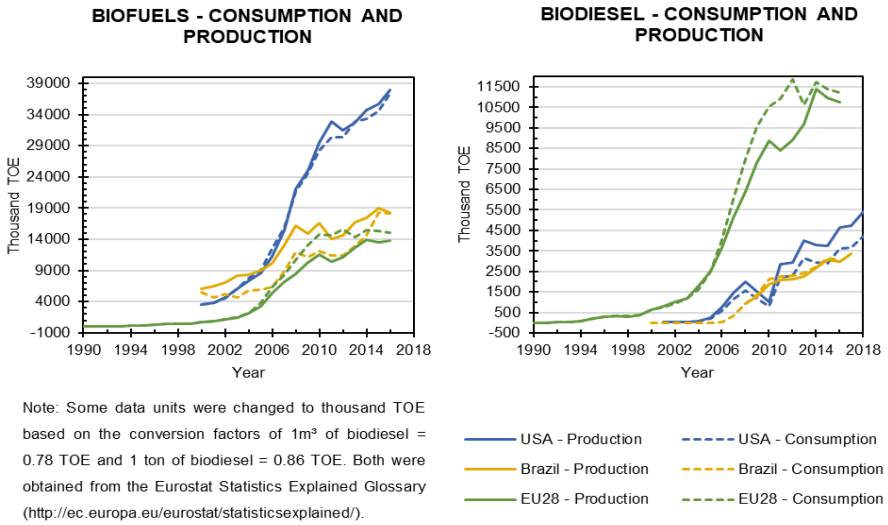

Figure 3 – Historical data of biofuels and biodiesel in the USA, Brazil and EU. Adapted from: EIA, (2019b); ANP (2018) and Eurostat

It is possible to observe a relevant raise in biofuels and biodiesel demand since the beginning of the XXI century, suggesting that effective policies were implemented towards its support. For biodiesel, specifically, Brazil almost consume all its production, while the USA produces more than its consumption and EU consumes more than its production but without much discrepancies.

2.1 Initial Definition and Basis

The EU Commission states in its regulation the definition of biofuel as liquid or gaseous fuel intended to be used for transportation and with an origin from biomass EU (2003). On the other hand, FAO (2015), the Food and Agriculture Organization (FAO) defines biofuel as a product originating from renewable sources such as plant, vegetable oils and treated wastes from domestic or industrial origin. Ultimately, EIA (2019a) characterize biofuels as being any kind of liquid fuel or blending products derived from biomass and intended to be used firstly as transportation fuel.

Biodiesel is defined by Krawczyk (1996) and Ma & Hanna (1999) as being produced from biologic materials, such as vegetable oils and animal fat that can be applied as a fossil diesel substitute. Gupta & Demirbaş (2010); Van Gerpen et al. (2010) refers to biodiesel as alkyl monoesters of vegetable oils or animal fats, while Meher, Vidya Sagar, & Naik (2006) as monoalkyl esters of long chain fatty acids (FA) obtained from renewable sources as vegetable oils or animal fats with direct application in Internal Combustion Engine (ICE).

Biofuels are classified into two main groups: the conventional or first-generation biofuels and the advanced biofuels, the latter subdivided into second, third and fourth generations. This discretization was done based on the type of technology implemented and the degree of development. Figure 4 presents the pathways that lead to biofuels.

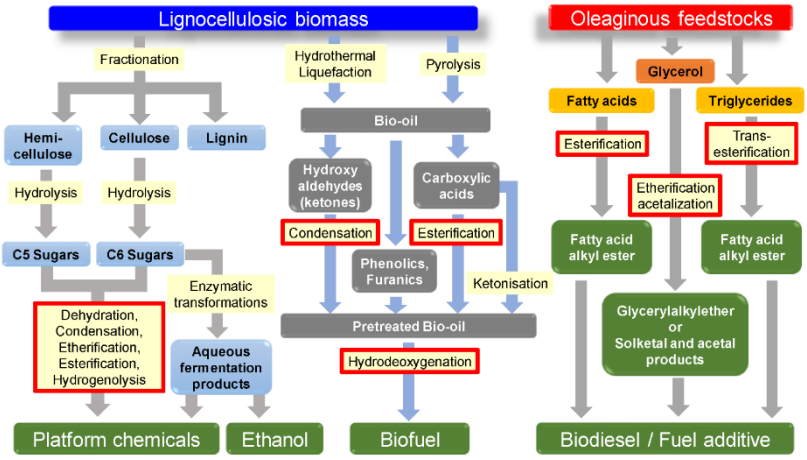

Figure 4 – Biologic feedstocks pathways. Source: Manayil, Lee & Wilson (2019).

2.1.1 Sources of Raw Materials

There is very wide variety of materials that can be used for biofuels production via different technology pathways depending on the generation. Narrowing the discussion upon the major focus of this work, which is biodiesel, it is clear that exists many opportunities for its production and development in different areas, a derivation of its flexibility and the advancement of ST & I. Examples are the vegetable derived from oleaginous plants like such as soybean (Glycine max), corn (Zea mays), palm tree (Elaeis guineensis), castor bean (Riccinus communis), sunflower (Helianthus annus), rapeseed (Brassica napus) and physic nut (Jatropha curcas).

Besides these, residues from different sectors can be also transformed into biodiesel like Waste Vegetable Oil (WVO), Waste Frying Oil (WFO) or Used Frying Oil (UFO), animal fat – tallows from chicken and cattle, and pork lard – fish viscera and Municipal Solid Wastes (MSW) – production of biogas and Refuse-Derived Fuel (RDF). Likewise, a raw material for 2nd generation of biofuels can be energy crops and agricultural wastes – branches, stems, leaves, straw, husks, nut shells and residues from forestry – defined by OECD (1997) as residues produced from different agricultural activities, among them farm and harvest wastes.

2.2 Fatty Acids Essential Structural Characteristics

An ubiquitous and essential component of vegetable oils and fats are the fatty acids (FA), which are composed of a Chemistry's functional group named carboxylic acid. It is attached to a single or several carbons connected to form a chain. The FAs exists in nature under different forms and constitute different compounds. For instance, among vegetable oils and fats, it exists in the form of triglycerides (TAG), which are classified, generically, as esters or, specifically, as tri esters. The TAGs are represented by (R'C(=O)(OR")), where R' and R" indicate different radicals composed of carbon atoms, as Figure 5 detaches.

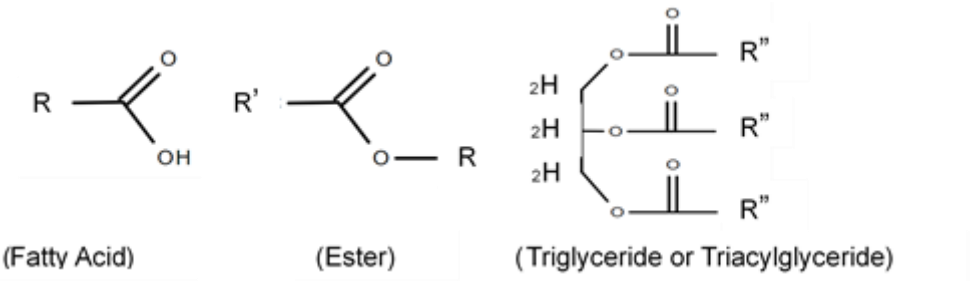

Figure 5 – FA, ester and TAG generic molecular structure. Note: drawings were made manually via an online tool from EPAM Systems Inc. provided by ChemSpider platform from Royal Society of Chemistry (RSC)

The FA, in view of its molecular structure, has very remarkable physical and chemical characteristics that enables it to be very useful to the biodiesel sector and to rise as an alternative to fossil fuels, mostly, diesel. As Figure 6 exemplifies, there are different types of FAs that, bonded with a glycerol molecule, create the TAG, an essential compound of vegetable oils.

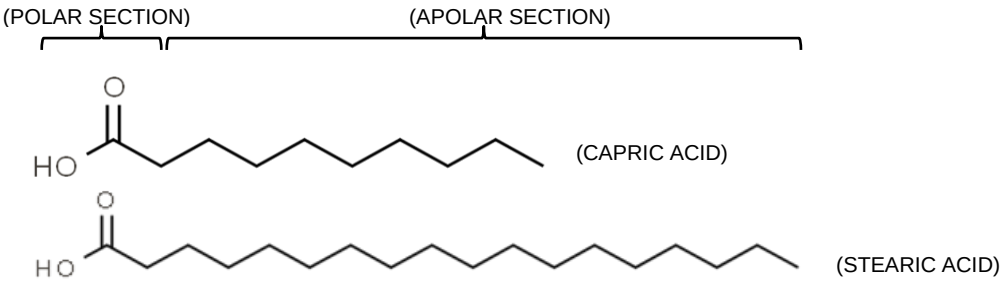

Figure 6 – Examples of fatty acids and its molecular structure with highlight to the polarity sections. Adapted from: ChemSpider platform from Royal Society of Chemistry (RSC).

Evaluating its structure, it is possible to observe clearly a difference in polarity promoted by the long apolar chain of carbons linked to the carboxyle and the other binders. This long apolar carbonic chain is precisely accountable for bringing properties like miscibility and interaction with the also apolar molecules of hydrocarbons. Among other things, this is what allows the addition of biodiesel in fossil diesel. By its time, the carboxyle is a strong focus of polarity and reasons for that are the presence of

the hydroxyl and the oxygen double-bonded to the carbon, which isolatedly is a carbonyl. This kind of characteristic is commonly known as amphipathicity or amphiphilicity.

The Table A1 (see Appendix A) broadly summarizes the major types of FAs, a topic very much presented by authors like Issariyakul & Dalai (2014); Aransiola et al. (2013); Thanh et al. (2012); Endalew, Kiros & Zanzi (2011b); Leung, Wu & Leung (2010); Narasimharao, Lee & Wilson (2007); Knothe, Van Gerpen & Krahl (2005); Barnwal & Sharma (2005); Baileys (2005); Srivastava & Prasad (2000); Kincs (1985); Goering et al. (1982). As to exemplify this variability of FAs among the various raw materials, the Table A2 (see Appendix A) summarizes some of the most known.

2.3 Biodiesel Production Pathways

There exists different technologies to produce biodiesel from raw materials like vegetable oils and fats. The most known are direct use and/ or blending, micro-emulsion, thermal cracking or pyrolysis and esterification/ transesterification, mentioned by innumerous researchers including Demirbaş et al., (2016); Ruhul et al. (2015); Agarwal (2007); Ma & Hanna (1999); Schwab, Bagby & Freedman (1987).

Furthermore, a process named hydroesterification is focus of research of different authors like Pradana et al. (2018); Aranda & Machado (2016); Dos Santos et al. (2015); Reyes et al. (2012); Silva et al. (2010); Encarnação (2007) and it is characterized by the combination of a hydrolysis reaction followed by an esterification reaction. Therefore, it is very suited to be used with low quality raw materials such as fats or WFOs and also with those contaminated with high water content.

Lastly, Hydrotreatment (HDT) is a promising alternative to transesterification or esterification to result in high quality bio-based products molecularly similar to fossil gasoline, diesel and jet fuel, as debated by Sotelo-Boyás, Trejo-Zárraga & Hernández-Loyo (2012); Aatola et al. (2008); Stumborg, Wong & Hogan (1996). The derivatives of this process are commonly named hydrotreated vegetable oil (HVO), hydroprocessed esters and fatty acids (HEFA) or even ‘green’ or ‘renewable diesel’.

2.3.1 Esterification

Esterification is a reaction of an alcohol (mostly methanol) with a FA molecule, resulting in an ester and a water molecule. Figure A1 (see Appendix A) presents its proposed reactional mechanism originally described by Fischer & Speier (1895) and explained in detail by Endalew, Kiros & Zanzi (2011b). It is carried in the presence of an acidic catalyst, usually of strong acidity, on a homogeneous or heterogeneous condition. Examples of possible catalysts are discussed further in chapter 3.

This process is mostly used as a bypass to situations the transesterification reaction does not proceeds as usually expected (i.e. in terms of conversion), commonly, with low quality raw materials such as animal fats and WFOs as Borges & Díaz (2012) mention. Contrastingly, this methodology is strategic to allow the harnessing and valorization of these residues within the biofuels sector.

2.3.2 Transesterification

The best known and most often applied methodology for biodiesel production from vegetable oils is transesterification. Interestingly, Rochleder (1847) already discussed this kind of reaction while preparing glycerol from castor oil, as Formo (1954) also highlights. This methodology uses as reactants TAGs and alcohol to result in other esters and glycerol. The transesterification reaction is also known as alcoholysis or, more specifically, methanolysis or ethanolysis when, respectively, methanol and ethanol are the chosen alcohols. Indeed, the reaction is named as it is due to the species involved as reagents and products, and the transformation of an ester into another.

The reaction occur in three separated steps until produce the esters, conventionally named fatty acid methyl esters (FAME) or ethyl esters (FAEE) depending on the type of alcohol used as reagent. The reaction is also reversible, which means it is needed a so-called “driving force” to steer it to the way desired (towards products), as depicted in Figure A2 (see Appendix A). It requires the presence of catalysts, either acidic or basic (also named alkaline), under either homogeneous, heterogeneous or enzymatic conditions, as massively evaluated by authors like Demirbaş et al. (2016); Atadashi et al. (2013); Aransiola et al. (2013); Thanh et al. (2012); Endalew, Kiros & Zanzi (2011b); Demirbaş (2009); Martino Di Serio et al. (2008); Meher, Vidya Sagar & Naik (2006); Knothe, Van Gerpen & Krahl (2005); Fukuda, Kondo & Noda (2001); Canakci & Van Gerpen (1999a). Examples of possible catalysts are presented and discussed further in chapter 3.

There is a pertinent and widely known rule of thumb to help define weather or not to carry transesterification. It is, specifically, related to the content of FFA in the raw material. This kind of requirement exists because the conversion of FFAs into esters happens using acidic catalysts. Thus, when basic catalysts are used to transesterify raw materials containing high levels of FFA, it enables the potential occurrence of side and undesired reactions like saponification. It results in the formation of soaps and emulsions, thus favoring a decrease in the total raw materials available to become biodiesel and in the FAME conversion and/ or yield.

2.4 Biodiesel Quality Standards

The existence of a reference parameter with an objective to standardize characterizations and favor comparison is very important for any field of knowledge, including the fuels and the biodiesel sectors, since it contributes to create a pattern of comparison between samples. For this, there are different technical standards created by institutions like the American Society for Testing and Materials (ASTM), nowadays known only as ASTM International, and the International Standardization Organization (ISO). Commonly, these standards serve as a major reference to many national institutions like the German Institute for Standardization (from German, DIN), the European Committee for Standardization (from French, CEN), the Brazilian National Standards Association (from Portuguese, ABNT) – and the American Oil Chemists’ Society (AOCS).

Worldwide, the two most relevant standards for biodiesel at present are the “ASTM D6751 – Standard Specification for Biodiesel Fuel Blend Stock (B100) for Middle Distillate Fuels” in the USA and published in 2002, and the “EN 14214 – Liquid petroleum fluids – Fatty acid methyl esters (FAME) for use in diesel engines and heating applications – Requirements and test methods” in Europe and published in October, 2003. The European standard was developed as an consequence of Directive 2003/ 30/ EC, EU (2003), based on the previously published German standard DIN 51606 published in 1997, as summarized by Joo & Kumar (2019); Prankl et al. (2004). In Brazil, the first technical standard for biodiesel was issue by ANP (2003) on September 15th, already referencing the ASTM, CEN and ISO standards for biodiesel. Later on, it was updated and substituted by others until the current legislation Resolution No. 45 ANP (2014).

Each of these technical standards lists the technical requirements and limits for each property, as it is summarized in Table A3 (see Appendix A). It is very interesting to extend this analysis to blended samples as to attest influences that biofuels could cause in the characteristics of a diesel fuel. This is briefly presented in Table A4 (see Appendix A) combining data from different researches.

2.4.1 Problems with Out-of-Standard Biodiesel

As biodiesel is produced by different processes and the raw materials used can be harvested in different areas of the world, it is most likely that some differences among its properties are observed. That is exactly the relevance of the previously commented technical standards. When they are not met in its entirety due to problems such as lack of efficiency in the reactional process, raw materials quality and contamination, many difficulties and technical impacts are envisioned when using biodiesel in engines. Diverse authors discussed about these issues, like Berrios & Skelton (2008); Faccini (2008); Agarwal (2007); Meher, Vidya Sagar & Naik (2006); Ma, Clements & Hanna (1998).

For instance, the most common problems with out-of-standard biodiesel are deterioration of natural rubbers gaskets, corrosion of aluminum and zinc, flash point influences due to high content of alcohol, formation of carbon deposits caused by poor combustion of compounds like FFAs, glycerin and monoacylglycerol (MAG), diacylglycerol (DAG) and triacylglycerol (TAG). These compounds can also induce formation of polymerization-derived deposits, as the combustion chamber temperatures are not enough to burn them and only favor its aggregation in bigger molecules. These residues can cause deposits inside the engine and even favor clogging of filters. Besides, FFAs is told to be a cause of poor atomization of the fuel. Water, for instance, if present in the fuel even in low quantities can even favor bacterial proliferation in storage facilities.

2.5 Biodiesel Purification Routes

The biodiesel production process consists of a reactional stage, to specifically modify the raw materials and generate FAMEs, and a purification stage designed to meet the requirements for biodiesel, following the technical standards previously cited. The main idea of this process is to remove unreacted alcohol, catalysts and TGs, glycerin, FFAs, moisture and any impurity that could damage the

quality of the final biodiesel. There are three major strategies for purifying the reactional product derived from a transesterification or esterification reaction using vegetable oils, wet washing, dry washing and membranes, as highlight Fonseca et al. (2019); Leung, Wu & Leung (2010); Berrios & Skelton (2008).

The latter, it is important to be highlighted, is usually composed of inorganic microporous ceramic materials, as Atadashi et al. (2011); Atadashi, Aroua & Aziz (2011) inform, and can be applied in two ways, together with the reactor or in a separate equipment. This type of purification shows high efficiencies and there are diverse experiences dedicated to this but not yet many industrial scale applications.

3 CATALYSIS IN BIODIESEL PRODUCTION

Catalyst is capable of providing an alternative path, with a, relatively, lower activation energy when compared to the regular one, to a certain reaction to occur. This, obviously, influences the rate of reaction. Hence, the catalyst is not part of a chemical reaction at all, not being consumed or produced during the entire process. Therefore, it should be, theoretically, possible to be completely recovered at the end of the reaction without losses or increases in mass. Usually, it is said that catalysts are, at the same time, reactant and product of a chemical reaction to reinforce this concept of not being part of the reaction.

As detailed further on and schematized in Figure 7, catalysts can have different physical and chemical characteristics and operate at different conditions. To this day, exists ample investigation streams towards developing catalysts of different natures to favor higher yields and overcome some of the major drawbacks currently faced by this sector in terms of separation and purification of products.

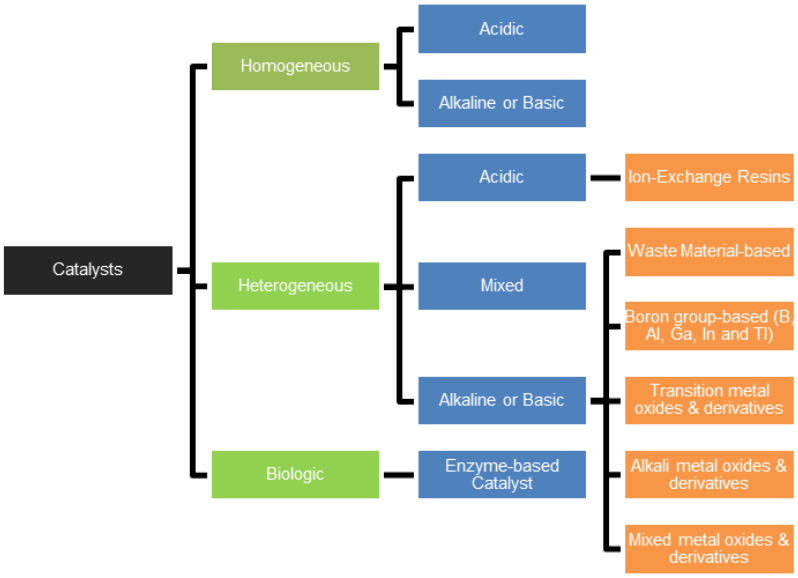

Figure 7 – Types of catalysts used in biodiesel production. Adapted from: Ruhul et al. (2015)

Independently of the nature inherent to the catalyst, the process it enables is governed by the acidic or basic strength existent, which defines in a ultimate analysis how the reactional mechanism will occur. To evaluate and characterize a catalyst as acidic or basic, there are two major modern acid-base theories, one proposed by the scientists Johannes Nicolaus Brønsted and Thomas Martin Lowry known as the Brønsted-Lowry theory, and another devised by Gilbert Newton Lewis and known as the Lewis theory. Each one has its assumptions and definitions and, by being like that, can coexist. Before deepening specifically on catalysts, it is worth it to detail and explain these theories as a tool to build knowledge and simplify the understanding of further debates that throughout this work.

3.1 Homogeneous Catalysis

This type of catalysis is defined and similarly characterized by being in the same phase as the reactional media, so either solid, liquid or gaseous. By its nature, the catalyst forms a single phase with the reagents forming a single phase medium. As for its physical characteristics, homogeneous catalysts are recognized by several positive and negative aspects but most widely as for possibly disfavoring purification and/ or separation processes aimed to remove it from the product stream, as debated by Abdullah et al. (2017); Ruhul et al. (2015); Chouhan & Sarma (2011); Yogesh C. Sharma, Singh & Korstad (2011b); Leung, Wu & Leung (2010); Helwani et al. (2009b). Besides, all those effects could be potentialized if there is an excess of catalyst in the reactional medium, therefore it is very important to follow the recommended conditions or perform a scientific investigation to determine the most suitable for a certain raw material.

3.1.1 Acidic Catalysts

Acidic homogeneous catalysis is carried in the same medium of the main reaction (i.e. biodiesel production reaction), hence in a liquid phase. As for its name, this type of catalysis utilizes acidic species to carry the reaction, mostly strong acids like hydrochloric (HCl), sulfuric (H_2SO_4), hydrofluoric (HF), phosphoric (H_3PO_4) and para-toluene-sulfonic acid (PTSA), also known as tosylic acid (TsOH). One of its major advantages, as reminded in a Table in the work of Abdullah et al. (2017) and by many other authors like Avhad & Marchetti (2015); Demirbaş (2008); Knothe, Van Gerpen & Krahl (2005); Ma & Hanna (1999), is its ability to catalyze both esterification and transesterification reactions. Even though for the second one, the reactional time is very much longer when compared with alkaline catalysts usage.

Besides that, acidic homogeneous catalysts does not favor the soap formation reactions and also can deal properly with FFA and water content in the feedstocks, not negatively impacting its activity. Negative aspects are focused on equipment corrosion, difficulty to recover and reuse, and the need of post reactional processes such as washing and cleaning to alkalinize the medium and remove traces of its use. All these above mentioned examples of acidic catalysts are recognized as “strong” acids, due to their ability or tendency to dissociate into ions in an aqueous medium, all of which are Brønsted-Lowry acids. This characteristic is relevant to biodiesel production since the acidic reactional mechanism is based on the proton H^+ starting initiative to conduct it.

Homogeneous Lewis acidic catalysts are in general metal complexes, stearates and acetates of calcium (Ca), barium (Ba), magnesium (Mg), cadmium (Cd), lead (Pb), zinc (Zn), cobalt (Co) and nickel (Ni), as M. Di Serio et al. (2005) indicate. Also, chlorides of Zn and Aluminum (Al) were investigated by Ferreira, Lemos Cardoso & da Silva (2012); Soriano, Venditti & Argyropoulos (2009). The reactional mechanism for homogeneous acidic-catalyzed transesterification is explained by Ambat, Srivastava & Sillanpää (2018); Thanh et al. (2012); D. W. Lee, Park & Lee (2009); Meher, Vidya Sagar & Naik (2006) and in Figures A1 (for esterification).

In essence, esterification and transesterification mechanisms resemble each other because they target, specifically, the carboxyle. For acidic catalysis, the proton H+ dissociated from the acid attacks the nucleophilic oxygen of the carboxyle, bonding with it and inducing the breakage of the double bond carbon-oxygen. By doing that, the carbon becomes electrophilic due to only having three bonds and is reached by the oxygen from the alcohol molecules, which are rich in electrons, thus stablishing a new bond (the fourth one). This creates a tetrahedron intermediate that is instable and, by transferring a proton H+ from the previous carboxyle oxygen to the other one bonded to the same carbon, the double bond carbon-oxygen is reestablished, and a FA molecule is freed out of the TG, together with a proton H+. Furthermore, the whole process is repeated until removing all three FAs and freeing a glycerol molecule.

3.1.2 Basic or Alkaline Catalysts

Alkaline (or basic) homogeneous catalysis is carried in the same medium of the main reaction (i.e. biodiesel production reaction), hence in a liquid phase. As for its name, this type of catalysis utilizes basic species to carry the reaction, mostly strong bases like sodium (NaOH) and potassium (KOH) hydroxides, two strong bases and Brønsted-Lowry basic catalysts. These two are the most widely used catalysts worldwide, argument cited by Yogesh C. Sharma, Singh & Korstad (2011b); Helwani et al. (2009a); Knothe, Van Gerpen & Krahl (2005); Ma & Hanna (1999) but also by different authors in reference literature.

In fact, NaOH and KOH are relatively cheap reagents massively produced yearly worldwide that can reach very high yields of biodiesel production under mild conditions and shorter times, as investigated by Demirbaş (2009). In terms of Na and K methoxides, even though having a higher cost, they perform very efficiently and readily dissociate in solution when compared to the ordinary catalysts. Furthermore, the basic homogeneous transesterification reaction is told to be nearly 4000 times quicker than the acidic one, as cited by Reid (1911) apud Fukuda, Kondo & Noda (2001); Freedman, Pryde & Mounts (1984); Formo (1954). Authors like Freedman, Pryde & Mounts (1984) recommend 0.5 % of NaOH for laboratory scale and 1 % of NaOH for industrial scale, while Issariyakul & Dalai (2014) says that it is very common to use between 1 % and 2 % of H_2SO_4 for transesterification.

These discrepancies between homogeneous transesterification (i.e. acidic and basic) could be attested in a wide variety of published papers from different years available in the literature and in the brief summary done by Issariyakul & Dalai (2014). Even though the required amounts of catalysts are slightly different, a major discrepancy is noted in the reactional time and the temperature, both much higher than for acidic ones. This, in fact, is one of the arguments that favors alkaline catalysts and its milder conditions to be widely used in small and industrial scales as Agarwal (2007) comment. As an exemplification of this discrepancy that enables the homogeneous alkali-catalyzed reaction to be widely utilized, Canakci & Van Gerpen (1999b) conducted experiments with soybean oil, methanol and sulfuric acid at different temperatures for 48 h and 96 h to reach conversion of 87.8 % and 95.1 % respectively. As a comparison, a standard alkali-catalyzed transesterification reaction produces similar conversion levels right after 1 h, as investigated by Tomasevic & Siler-Marinkovic (2003); Foidl et al. (1996).

In terms of negative aspects, the alkaline compounds are sensitive to water content in the medium, as soap production can be favored together with emulsion formation. Both of these side effects reduce the amount of final product available and even impede post reactional procedures (e.g. separation and purification). Ultimately, homogeneous alkaline catalysts are very hard to be recovered and reused, and induce the production of relevant amounts of waste water as a result of catalyst removal and cleaning. In relation to reactional mechanisms for homogeneous basic-catalyzed transesterification, it is explained by the drawings of Thanh et al. (2012); D. W. Lee, Park & Lee (2009); Meher, Vidya Sagar & Naik (2006); Lotero et al. (2005) and in Figure 10.

The basic catalysis, for instance, instead of acting on the oxygen of the carboxyle, focus on the carbon itself by enabling it to be attacked by the alkoxide ion derived from the alcohol (usually methoxide). Hence, is creates a fourth bond to the carbon and, indirectly, dismantling the double bond of the carboxyle. This results in an unstable tetrahedron intermediate with an oxygen very much nucleophilic (due to the actual single bond carbon-oxygen). Then it contributes to the reestablishment of the double bond in the carboxyle and freedom of a FA molecule. Besides, the TAG becomes a DAG molecule with a nucleophilic center, quickly, compensated by a proton H+ from the solution. By comparing both mechanisms it is possible to understand the difference in reactional time evidenced to achieve a similar conversion. The acidic one is naturally slower than the basic one, so reaction rates are also different.

3.2 Heterogeneous Catalysis

This type of catalysis, as the name indicates, is characterized by a catalyst and reagents occurring in a different medium (e.g. transesterification or esterification). Theoretically, this catalysis is carried out at the interface of the two phases such as solid-liquid, solid-gaseous or liquid-gaseous and, for that, active sites are needed since molecules will need to adsorb on them to start reaction. Therefore, in pursuance of a faster reactional proceeding, the phenomenon of adsorption of reagents and desorption of products need to occur on the surface. This type of catalyst is composed of active sites of two kinds, Brønsted-Lowry or Lewis, thus capable of being acidic and/or alkaline, or even bifunctional, as highlighted by Yogesh C. Sharma, Singh & Korstad (2011b); Helwani et al. (2009a); Martino Di Serio et al. (2008).

Notwithstanding heterogeneous catalysts present a lower activity when compared to homogeneous, its catalysis requires the usage of a material that is not miscible at all in the reactional medium, thus being separable and even recyclable, depending on the specific situation, as (Mardhiah et al. (2017); Yogesh C. Sharma, Singh & Korstad (2011b) address. This is associated with reducing the steps after the reaction, namely washing and neutralization (the latter in the case of homogeneous acidic catalysts) and with avoiding side reactions, such as soap formation and emulsions. They can be easily separated from the liquid medium by filtration. This constitutes one of their major advantages in comparison to homogeneous catalysts. Besides that, there exist benefits associated to a reduced investment on post-reactional proceedings, such as separation and purification, and, beyond that, much

lower waste water production. Ultimately, the disfavoring for soap and emulsion formation and corrosion damages are also envisioned.

Clearly, associated to these advantages there are some drawbacks connected to a requirement for longer duration of reaction, higher amount and frequently higher alcohol: oil ratio. This, in fact, is exacerbated by the coexistence of three phases in the reactional medium, one solid, from the catalyst, and two liquid, from the two reagents, alcohol and FA or TAG, initially immiscible. This more complex environment can bring issues related to diffusion and mass transfer, as Leung, Wu & Leung (2010) discuss. Likewise, the slower conversion is a negative aspect discussed by Ambat, Srivastava & Sillanpää (2018); Abdullah et al. (2017); Mardhiah et al. (2017); Ruhul et al. (2015); Lourinho & Brito (2014); Banković-Ilić, Stamenković & Veljković (2012); D. W. Lee, Park & Lee (2009), and requires relatively harsher reactional conditions.

To mention an example concerning reactional aspects, D. W. Lee, Park & Lee (2009) suggest temperatures between 100 °C and 250 °C, catalyst content of 3 % to 10 % in weight (wt.) and methanol: oil molar ratio between 10:1 and 25:1. However, in fact, this is variable throughout the literature depending on the type of catalyst, type of oil and methodologies defined. Besides the above cited restrictions, the major drawback of its application, as, for instance, Ruhul et al. (2015); Banković-Ilić, Stamenković & Veljković (2012); Yogesh C. Sharma, Singh & Korstad (2011b); Leung, Wu & Leung (2010); Helwani et al. (2009a) mention, is the need of tailoring the design and preparation of an efficient catalyst.

Furthermore, there are two main types of deactivation of heterogeneous catalysts impacting the possibility of recycling and reuse: a direct removal and leaching of components from the catalyst to the liquid phase (which may promote homogeneous catalysis) or a blockage of active sites by adsorption of acidic hydrocarbons on basic sites, as D. W. Lee, Park & Lee (2009) reminds. This effect can even induce the co-existence of homogeneous and heterogenous catalysis in the medium, depending on the components of the catalyst and its active species. The deactivation is, nowadays, focus of many different researches, dedicated to different materials and production methodologies since it may contribute to a more sustainable catalyst development process and reduce the economic impact of production. Sivasamy et al. (2009), indicate that besides only leaching there exists poisoning, sintering and even coking which also cause noxious effects and, as such, need to be avoided.

3.2.1 Reactional and Kinetic Mechanisms

The reactional and kinetic mechanism of a heterogeneous catalysis is a topic under research by different authors and, as D. M. Marinković et al. (2016); Kapil et al. (2011); Endalew, Kiros & Zanzi (2011b); Martino Di Serio et al. (2008) describe, it is hypothesized as based on the Eley-Rideal (ER), Langmuir-Hinshelwood-Hougen-Watson (LHHW) or Hattori (Ht) mechanisms. Each of these proposals differentiate in terms of which molecule adsorbs on the catalyst (namely either alcohol or FA/ TG) and which and how each sequential chemical reaction occurs towards obtaining the products. So, since each of them are composed of a series of reactions, it raises the question of the existence of a rate-

determining chemical reaction (the slowest one) that governs the overall velocity of the product formation. It is important to highlight that, as it is possible to use acidic or alkaline heterogeneous catalysts, there exist different mechanisms for each Brønsted-Lowry and Lewis types.

3.2.2 Acidic Catalysts

There are several types of heterogeneous acidic catalysts presently studied with success in biodiesel production via esterification. Martino Di Serio et al. (2008) mention that Brønsted-Lowry catalysts are more active in esterification while Lewis catalysts in transesterification. The disadvantages of the latter are the long duration of the transesterification reaction and the need for harsher reactional conditions, as highlighted by Mansir et al. (2017). Furthermore, Yogesh C. Sharma, Singh & Korstad (2011b) indicate that water formed as product in esterification damages the acidic Lewis catalysts, thus making them more advantageous for transesterification.

Several types of heterogeneous catalysts were proposed for biodiesel production, as reviewed by Aransiola et al. (2013); Atadashi et al. (2013); Banković-Ilić, Stamenković & Veljković (2012); Borges & Díaz (2012); Thanh et al. (2012); Endalew, Kiros & Zanzi (2011b); Narasimharao, Lee & Wilson (2007). Likewise, Helwani et al. (2009a) highlight commercial products like Nafion NR50 ®, heteropolyacids (HPA), which are very strong Brønsted-Lowry acids, and superacid catalysts like sulfated (S-ZrO_2) and tungstate (WO_3/ ZrO_2) zirconia, also cited by Mansir et al. (2017); Mardhiah et al. (2017); A. F. Lee et al. (2014); Helwani et al. (2009b); Zabeti, Wan Daud & Aroua (2009).

Besides that, de Almeida et al. (2008) highlight that metal oxides like pure and sulfated tin oxide (SnO_2) supported on alumina or silica, Beta zeolite (β) promoted with Lanthanum (La), rich in Brønsted-Lowry sites, ZSM-5 zeolite, rich in Brønsted-Lowry and Lewis acidic sites, and mordenite zeolite were used for biodiesel production and reached relevant conversions.

Singh & Gaurav (2018); Yogesh C. Sharma, Singh & Korstad (2011a) review those catalysts together with ion-exchange resins such as Dowex ® and Amberlyst ®, polyvinyl alcohol (PVA) crosslinked and silica functionalized with sulfonic groups. Conversions and yields obtained were different depending on the studied feedstocks, either FFA or TAG with different acidity levels, and reactional conditions. Furthermore, certain examples of this type of catalyst can be found in Table A6 (see Appendix A).

3.2.3 Basic or Alkaline Catalysts

There are several types of heterogeneous acidic catalysts presently used with success in biodiesel production, many summarized by Aransiola et al. (2013); Atadashi et al. (2013); Banković-Ilić, Stamenković & Veljković (2012); Thanh et al. (2012). Although several types of heterogeneous acidic catalysts were studied, some authors like Endalew, Kiros & Zanzi (2011b) indicate the importance of heterogeneous alkaline catalysts , that can be classified into five main types: single metal oxides, doped

and mixed metal oxides, zeolites, supported alkali and alkaline earth metal oxides and hydrotalcites (HT).

Examples for this type of catalyst are presented in Table A6 and by Singh & Gaurav (2018); Kesić et al. (2016); Ruhul et al. (2015); A. F. Lee et al. (2014); Atadashi et al. (2013); Chouhan & Sarma (2011); D. W. Lee, Park & Lee (2009); Zabeti, Wan Daud & Aroua (2009); Hattori (2004). In general, they are single alkali and alkaline earth metals (e.g. sodium (Na), potassium (K), Lithium (Li), Barium (Ba) and Mg) supported on γ-alumina (Al_2O_3), as well as oxides of these species such as CaO and MgO. Basic zeolites and single and mixed oxides not supported or supported on γ-alumina (Al_2O_3) were also applied as catalysts for biodiesel.

The alkali and alkaline earth metal oxides possess in their structure both Brønsted-Lowry basic sites (oxygen species) and Lewis acidic sites (metal species). The number of basic sites available varies among the different catalysts as MgO > CaO > SrO > BaO, while the basic strength varies as MgO < CaO < SrO < BaO, according to Endalew, Kiros & Zanzi (2011b); Tanabe & Fukuda (1974). Zeolites can be tuned in terms of the silica/ alumina content ratio (SiO_2/ Al_2O_3), which, directly, influences the acidity (lower ratios) or basicity strength (higher ratios). This can result in improved FAME conversion according to Kiss, Dimian & Rothenberg (2006).

Besides those, Helwani et al. (2009a) summarize examples from different authors like potassium nitrate (KNO_3) supported on alumina, Mg-Al HT, also cited by A. F. Lee et al. (2014), calcined HTs, SBA-14 promoted with CaO and mesoporous silica loaded with MgO. Mardhiah et al. (2017) in their review work, highlighted some of the above mentioned catalysts successfully used for FAME production by a myriad of authors, together with KNO_3 supported over alumina, sole and doped with Li and CaO from different sources (e.g. chicken eggshells) and TiO_2. All of them were capable of reaching remarkable FAME yields, all above 71 % and many close to 100 %.

The review of A. F. Lee et al. (2014) discusses other types of alkaline catalysts such as sodium silicate (Na_2SiO_3) and potassium carbonate (K_2CO_3) supported on different materials, such as activated carbon, MgO and silica, with yields of 99.6 % and over 86 % depending on the support chosen.

3.2.4 Bifunctional Catalysts

As its name suggests, this type of catalyst possess both acidic and basic active sites. H. V. Lee, Juan & Taufiq-Yap (2015); Farooq, Ramli & Subbarao (2013); Endalew, Kiros & Zanzi (2011a), for instance, explain that a bifunctional catalyst can be composed by a metal oxide that has Brønsted-Lowry and/ or Lewis acidic sites derived from, for example, transition metals like zirconium (Zr), zinc (Zn), iron (Fe), tin (Sn), Ti, molybdenum (Mo) and tungsten (W) metals, and a metal oxide that has Brønsted-Lowry basic sites from earth metals like Ca, La and Mg. The works of Mansir et al. (2018) and Ramli et al. (2017) list a wide variety of bifunctional catalysts synthesized and applied in biodiesel production by different researchers. This remarkable characteristic of combining two types of catalysts (acidic and basic) creates a material capable of catalyzing both transesterification and esterification.

Hence, it may be of interest when processing low quality feedstocks, such as WFOs or unrefined vegetable oils, since they usually have high acidity index, which is associated with side reactions (e.g. soap and emulsion formation) and limitations or reactional problems in transesterification, as previously discussed.

In terms of low quality feedstocks like WFO or highly acidic vegetable oils, which contain both FFA and TAG molecules, the bifunctional catalyst can facilitate their incorporation into the biofuels sector on a larger scale since it is capable of converting simultaneously both. Definitely, the application of a catalyst capable of carrying both esterification and transesterification due to the presence of acidic and basic active sites is a major advantage since a single step process has both economic and environmental aspects. For instance, Mardhiah et al. (2017) reviewed several so-called bifunctional catalysts, such as bismuth oxide (Bi_2O_3) supported on lanthanum oxide (La_2O_3), and La_2O_3 supported on CaO, zinc oxide (ZnO) and alumina. Further examples can be found in Table A6 (see Appendix A).

3.3 New Possibilities of Catalysts

Considering all that was explained above about biodiesel and heterogeneous catalysts, including their advantages and disadvantages, there exists a true motion to new or ameliorated types of catalysts. This is even more the case when associating with some of the modern world demands such as the legitimate need to reduce costs, impacts and improve properties, the appeal and strength of sustainability and waste valorization, and the necessity to make use, in an intelligent way, of the available resources and/ or wastes produced in different sectors of the economy.

Thereby, the development of new heterogeneous catalysts for biodiesel production using as major source residues is on the front of a new set of innovation and technologic advancements being harnessed in different universities and research institutes across the world. This is coined focusing on adding value to roughly zero-valued residues from agriculture and energy sectors.

3.3.1 Low-cost Catalysts

This is a general name for a whole sort of materials presently being utilized to produce biodiesel catalysts. Since they are derived from industrial residues or even from dwelling wastes, they discern from the most traditional sources of catalysts, which comes from industrial processes and currently are available on a commercial scale. In fact, there are several research papers and reviews on this topic, e.g. Marwaha et al. (2018); Shan et al. (2018); Tang et al. (2018); Abdullah et al. (2017); Cao, Sun & Sun (2017).

As examples, agricultural residues, such as husks and seed hulls, cellulosic materials in general, and vegetable oil extraction cakes can be mentioned. For instance, Li et al. (2014) studied a pyrolyzed rice husk (RH) catalyst sulfonated with H2SO4 for biodiesel production from WFO. Both FFA and TG were converted (the catalyst presented bifunctional characteristics) and FAME yield was nearly 90 % (FFA was around 98 %) at 110 °C, methanol: oil ratio of 20:1 and 5 % wt. of catalyst for 15 hours.

Ho et al. (2014) researched palm oil mill ash as a support for CaO to transesterify crude palm oil. A FAME yield of 79.76 % was reached with a 45 % wt. loading catalyst at 45 °C, methanol: oil ratio of 12:1 and 6 % wt. of catalyst for 3 hours. Mendonça et al. (2019) evaluated the application of calcined hulls of *Astrocaryum aculeatum*, a palm tree from South America, as a catalyst for soybean transesterification. A yield of 97.3 % of FAME was reached at 80 °C, methanol: oil ratio of 15:1 and 1 % wt. of catalyst for 4 hours.

Dai et al. (2016); Roschat et al. (2016b) evaluated the efficiency of rice husk ash (RHA), naturally rich in silicon compounds, in biodiesel production. The former authors used it combined with lithium carbonate ($LiCO_3$) to synthesize a calcined Li4SiO4 and applied to soybean oil (and other oils) transesterification, reaching a conversion of 98.8 % for a catalyst calcined at 800 °C. The reaction was carried out at 65 °C, methanol: oil ratio of 12:1 and 1 % wt. of catalyst for 3 hours. Roschat et al. (2016b) used NaOH with RHA to synthesize $Na2SiO_3$ for palm oil transesterification, obtaining, respectively, 97 % and 94 % of FAME yield at 65 °C and 0.5 hour, and room temperature and 2.5 hours. Both conditions used a methanol: oil ratio of 12:1 and 2.5 % wt. of catalyst.

Other possibility for catalyst preparation originates from the application of animal industry residues, such as sea shells from a variety of animals (mollusk, mussel, crab, lobster, shrimp, scallop, clam shells and fish scales) as cited by Marwaha et al. (2018), and animal bones and egg shells from birds (duck and chicken), as reviewed by Mansir et al. (2018). Moreover, ash from gasification or pyrolysis (biochar), fly ash (FA) from combustion of several materials, such as biomass and coal, ash materials from iron industry – blast furnace slag (BFS) – and aluminum industry (red mud), mineral residues from construction, specific types of rock like lime, bentonite, kaolinite or dolomite and even sea sand, were considered, as indicated by Shan et al. (2018).

Vargas et al. (2019) compared the use of four different residues as catalysts for WFO and refined rapeseed oil transesterification: FAs from residual forestry biomass (dried and calcined), dolomite rock (pure or impregnated with H_2SO_4), egg shells (calcined and impregnated with Na_2SiO_3 and further with H_2SO_4) and polyethylene terephthalate (PET) plastic bottles (heated at 450 °C and impregnated with H_2SO_4 and fuming H_2SO_4). The catalysts behaved differently when existing FFA in the medium but the one with a true efficient bifunctional capacity was the dried FA, with around 96 % FAME yield 60 °C, methanol: oil ratio of 9:1 and 10 % wt. of catalyst for 3 hours.

An interesting remark is that a chicken egg shell catalyst impregnated with sodium silicate (Na_2SiO_3) and calcined at 800 °C under the same reactional conditions were capable of carrying transesterification only to ca. 40 % yield. Only when treated with H_2SO_4 2M for 6 hours and calcined at 500 °C led to FAME yield of ca. 70 %. Notwithstanding, PET catalysts were not so much successful in transesterification. The one pyrolyzed at 450 °C for 2 hours and impregnated with H_2SO_4 98 % for 2 hours only reached 24.5 % FAME yield for WFO and 4.3 % for rapeseed oil. The same PET catalyst, when treated with fuming H2SO4 at 150 °C for 10 hours under N2 atmosphere presented improved FAME yield for WFO and rapeseed oil of 38.5 % and 5.3 % respectively. Both presented better efficiency to esterify FFAs of WFO, holding yields of 70.8 % and 86.9 % respectively.

Wilson et al. (2008) evaluated the use of dolomitic rocks (composed of Mg and Ca carbonates layers) calcined at 900 °C for olive oil transesterification. Conversion was up to 90 % at 60 °C, 0.16 g of oil, 9.7273 g of methanol and 15.625 g of catalyst for 3 hours. D. Kumar et al. (2018) researched the use of concrete and mortar (cement) wastes from construction calcined at 850 °C as catalyst for karanja oil processing. The results were 76.03 % FAME conversion for cement at 60 °C, methanol oil ratio of 30:1 and 2 % wt. of catalyst for 3 hours. Even though like that, leaching of CaO to biodiesel was registered.

Bottom ash from wood biomass gasification, mostly containing calcium carbonate ($CaCO_3$), was studied by Maneerung, Kawi & Wang (2015). At 65 °C, methanol: oil ratio of 20:1 and 5 % wt. of catalyst for 6 hours, transesterification of palm oil resulted in a biodiesel yield of above 90 %. Similarly, M. Sharma et al. (2012) calcined waste wood ash pure or activated with K_2CO_3 and $CaCO_3$ and investigated them as catalysts for Jatropha curcas oil transesterification. Both materials led to between 97 % and 99 % FAME conversion at 65 °C, methanol: oil ratio of 12:1 and 5 % wt. of catalyst for 3 hours. Kotwal et al. (2009) researched a similar catalyst with KNO_3 supported on FA for sunflower oil transesterification. A conversion of 87.5 % was reached with 5 % KNO_3 containing catalyst under the following reactional conditions: 170 °C, methanol: oil ratio of 15:1 and 15 % wt. of catalyst for 8 hours.

FA was also used as support for CaO, obtained from waste egg shells to transesterify soybean oil, as evaluated by Chakraborty, Bepari & Banerjee (2010). A FAME yield of 96.97 % was reached with a catalyst containing 30 % wt. of CaO in the reaction at 70 °C, methanol: oil ratio of 6.9:1 and 1 % wt. of catalyst for 5 hours. Ashes from a biomass-fed power plant, calcined at 550 °C, were also utilized as a catalyst for biodiesel production from Jatropha curcas oil by P. Kumar et al. (2015). A FAME yield of 93.9 % was reached in a batch reactor under pressure of 3.2 MPa at 225 °C, methanol: oil ratio of 9:1 and 5 % wt. of catalyst for 3 hours.

A. F. Lee et al. (2014); Aransiola et al. (2013) dedicated part of their review work to consider the use of carbon-based catalysts prepared from wastes from different sources, such as agricultural crops, algae and biodiesel production solid residues. These residues after treating with a H_2SO_4 acid turned into good quality material for FFA esterification. Dawodu et al. (2014) prepared a catalyst from seed cake residues (after oil extraction) from *Calophyllum inophyllum*, a typical plant from Africa, Asia and Australia. The material was incompletely carbonized under N2 atmosphere at 400 °C, followed by a treatment with sulfuric and PTSA acids. A FAME yield of 99 % was reached with the sulfonated catalyst under optimized conditions at 180 °C, methanol: oil ratio of 30:1 and 7.5 % wt. of catalyst for 4 hours. Utilizing a similar procedure, Zeng et al. (2014) developed a sulfonated carbon-derived catalyst (Brønsted-Lowry acidity) from partially carbonized peanut shell wastes. The biodiesel produced from cottonseed oil reached a FAME yield of 90.2 % at 85 °C, methanol: oil ratio of 9:1 and 2 % wt. of catalyst for 2 hours.

4. COAL AND FLY ASH

Energy is an ubiquitous topic to the modern society since it is harvested from different sources and from different technologies. Some of most traditional and even historic sources of energy are human and animal physical work, water and wind, massively utilized to move mills as to enable water pumping and aggregate value to other tasks in domestic agriculture (e.g. milling, cutting, pressing and crushing of products).

Advancing through the marvelous history of mankind, as briefly debated in the early parts of this present work, to those primal sources of energy was added the steam, responsible for boosting the transformations and revolutions in industry, society and market since the XVII century. Following that, the discovery and understanding of the full potentialities of fossil energy sources like coal, oil and, later on, natural gas reframed the concepts of development and globalization, and revolutionized the idea of modernity.

Up to this day, the century XXI stands as a strenuous time for humanity since there are multiple challenges associated to sustainability, development, innovation, environmental impact and opportunities. In terms of energy, it is obvious the changes being undertaken in terms of fossil fuels and GHG emissions, support for alternative and renewable energies such as hydroelectric, solar, wind and biomass and biofuels. Appendant to it, the dependency of fossil fuels, notably, oil, coal and natural gas, are still existent and, in fact, very much substantial.

4.1 The Coal Relevance

Coal is, definitely and presently, a strategic commodity and an energy source responsible to supply the world with a relevant share of the energy needed. In 2017, according to IEA (2019), coal solely was responsible for approximately 38 % of the total electric energy produced worldwide in TOE, as Figure 8 indicates. More than that, this source, historically, has not lost much of its global importance at least since 1990 as it always varied between not more than 40 % and not less than 37 %.

Within the EU, there is a trend, attested by IEA (2018a), for the reduction in coal consumption between 2000 and 2017, since it lowered from 451 million tonnes of coal equivalent (TCE)[7] to 323 M TCE, and, for 2023, further diminishment is expected to 280 M TCE. The same behavior is observed in the USA, while a more stabilized pattern is envisioned to Japan and South Korea. On the other hand, other parts of the world are not pursuing the same dwindling trends as demand has been increasing and is forecasted to keep the same behavior for 2023. China, Southeastern Asia and India are the major carriers. As an example, for the last country, the increase in coal consumption skyrocketed from 208 M TCE in 2000 to 563 M TCE in 2017 and is pictured to reach 708 M TCE in 2023. This is, unequivocally, linked to the progress of development, economic and social indexes – even though still not enough in

[7] One TCE is equivalent in terms of energy to 0.7 TOE.

terms of the country's present challenges – that have been enabling more citizens to improve their lives, climb the economic pyramid and then consume and demand more.

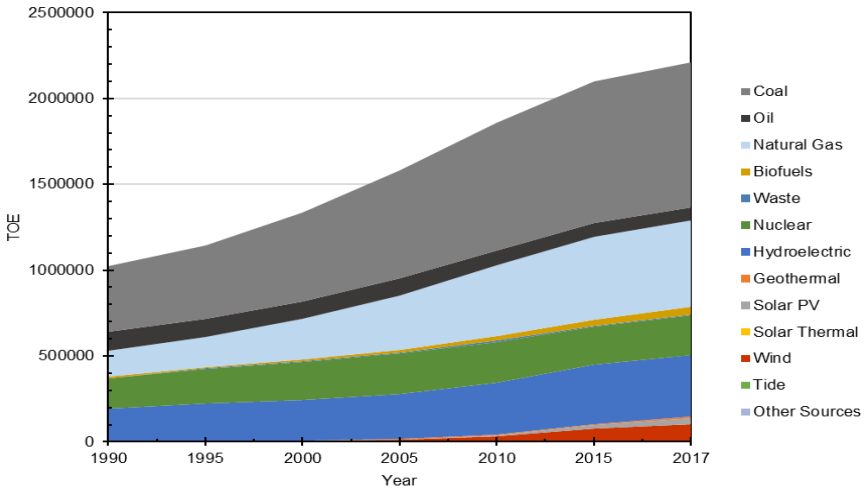

Figure 8 – Electricity generation by energy source worldwide between 1990 – 2017. Source: IEA (2019)

According to EU (n.d.), the community in 2017 accounted 34.8 % of gross inland energy consumption from fossil fuels, 13.6 % derived from solid fossil fuels (i.e. coal in general). In terms of coal, as cited by IEA (2018a), there scenario is multivariate and bonded to each country's specificities. For instance, Poland, the biggest among the 5 EU coal producing countries (together with Czech Republic, Germany, Spain and the UK), has a share of 80 % for coal in power generation while, Portugal, Sweden, Italy and Greece have, respectively, 21 %, 1 %, 13 % and 35 %.

This aspect is discrepant when compared to oil since it clearly lost importance for, particularly, electric energy generation as time passed and technology improved, enabling other sources to gain relevance like nuclear, hydroelectric, natural gas and, lately, wind and solar. Other way to explain it is since oil is very much demanded for transportation liquid fuels production and petrochemical derivatives, wasting it, so to say, in electric energy production was not always the most clear and economically intelligent strategy at all.

Expanding this debate furthermore with the intent to better understand and indicate robust arguments to the real relevance of coal to the modern society, Figure 9 combines perfectly with this objective. It indicates which sectors of the economy are responsible for demanding the biggest shares of coal and, in fact, it is possible to see that industry and residential are the top leaders, even though, in between themselves, they are very discrepant. This indicate the massive role played by coal to the industry sector since it is responsible for approximately 80 % of the total coal consumption in 2017 and, since 1990, was never lower than 61 %.

This sector is interrelated to different industries and manufactured products such as electric energy generation (via thermal power plants or more modern technologies such as gasification), cement

and iron and steel industries. According the Fernandez Pales, Levi & Vass (2019), in 2017 the steel sector was depended on coal to supply 75 % of its entire energy demands.

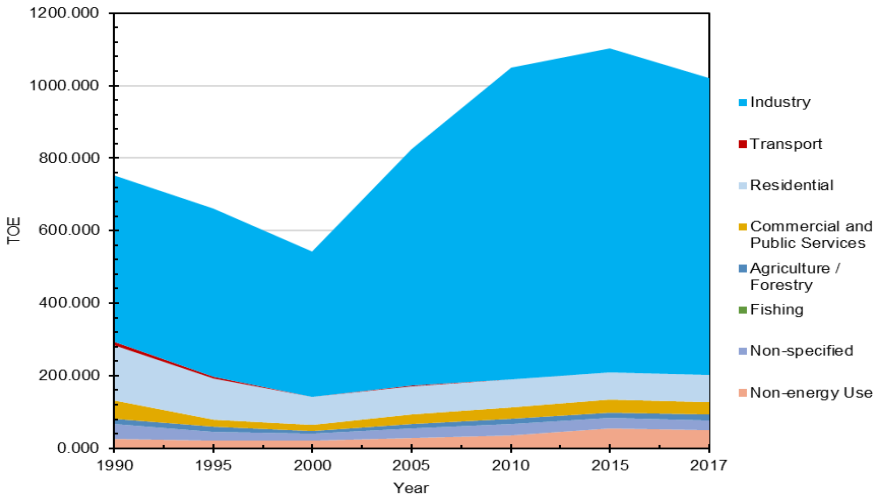

Figure 9 – Coal final consumption by sector worldwide between 1990 – 2017. Source: IEA (2019)

The residential sector, by its time, even though the second biggest consumer of coal in 2017, is only responsible for 7 % of the total, mostly associated to residential heating in countries with harsher winter seasons. Notwithstanding, this sector is, currently, showing a clear reduction trend, being in 2017 less than the half of 1990s levels, what can be linked to fuel shifting for natural gas or wood pellets, or even district heating networks based on Combined Heat and Power (CHP) plants.

This brief and general panorama indicates the prevailing challenge for coal as part of the energetic matrix. Mainly because, associated to its use, there are residues connected to its mining processes. Primarily, can be cited the GHG emissions within flue gases, what should be properly treated and cleaned depending on the enforced regulations, and solid residues, ordinarily named coal combustion products (CCP). This kind of material consists of Coal Fly Ash (CFA or FA), also known as Pulverized Fuel Ash (PFA), Bottom Ash (BA), Boiler Slag (BS) and flue gas desulfurization (FGD) residues such as gypsum, as ACAA (n.d.) highlights.

Worldwide, coal ash as a whole was forecasted to 2010, according to data from Joshi & Lothia (1997) and cited by Ahmaruzzaman (2010), at 600 million tonnes, being approximately 75 % – 80 % (500 million tonnes) of only FA. Focusing only on the EU, according to estimates from the European Coal Combustion Products Association, ECOBA (2016), in 2016, the EU15 produced in its powerplants 40.333 million metric tonnes of CCPs, with 63.8 % (25.741 million tonnes) only of FA, 8.97 % (3.618 million tonnes) of bottom ash and 23.63 % (9.531 million tonnes) of FGD residues. Widening their data, the organization was capable of forecasting, based on the coal consumption data available, the production of CCPs for the EU28 to be above 105 million tonnes in 2016, 88 being only ashes. Considering the entire European continent, it could reach beyond 145 million tonnes of CCPs produced, 124 being only ashes.

4.2 Fly Ash

Its formation out of raw coal origins from submitting the material to high temperatures near 1300 °C – 1700 °C via different types of technology like pulverized coal combustion (PCC), a subcritical steam technology, and supercritical (SC) and ultra-supercritical (USC) steam coal combustion technology. The usual name fly ash was coined, exactly, in relation to its light weight that enables it to leave the combustion zone inside a boiler carried by the flue gases and then only being captured and retained in electrostatic precipitators (ESP), bag filters or scrubber (dry or wet) equipment installed in power plants. This is the opposite to what occurs with, for instance, bottom ash or boiler slag, which are heavy ash residues – at least in comparison to FA – and stay inside the boiler.

This material is currently very much relevant as it is a byproduct of a fundamental economic sector – energy industry – that is spread throughout the world and it still is fundamental to guarantee electric energy access. Besides that, due to its light weight, if not very well disposed and taken care of in landfills, it can be carried by wind easily and become a health issue for populations. Commonly, FA is associated to eyes, throat and skin irritation and more serious respiratory complications and diseases, as Yao et al. (2015) indicate. It is a relevant aspect of many debate and researches, as presented by Belviso (2018); Yao et al. (2015); Ahmaruzzaman (2010), and, in fact, fly ash constitutes a strong argument for supporting Science, Technology & Innovation as a way to valorize this hazardous waste and propose innovative alternatives for its recycling, reuse and disposal.

Furthermore, FA is a potential soil, underground water reservoirs, rivers and lakes contamination if not treated well since it is, generally, rich in a wide variety of chemical elements and compounds such as Zinc (Zn), Aluminum (Al), Silicon (Si), Iron (Fe), Copper (Cu), Manganese (Mn), Boron (B), Phosphorus (P) and Potassium (K), and also traces of other elements possibly noxious to human and animal health such as Lead (Pb), Mercury (Hg), Chromium (Cr), Nickel (Ni), Vanadium (V), Selenium (Se) and Arsenic (As). In fact, this hazardous aspect of FA has been called to the attention of researchers and the industry for some decades, as the work of Murtha, Burnet & Harnby (1983) already presented some concerns and proposed viable alternatives, in place at that time.

4.2.1 Structure, Composition and Major Characteristics

Fly ash is defined, according to ASTM International (2019a), as fine residues produced from coal (under grounded or powdered condition) combustion and transported via flue gases. Hence, it is considered a byproduct from coal.. More specifically, FA, as depicted in Figure 10, is a pozzolanic material, which means that it is composed of silica and alumina materials that, after chemically interacting with water, have cementitious properties.

This is a fact massively discussed in the specific literature and highlighted by Bhatt et al. (2019); Ahmaruzzaman (2010); Iyer & Scott (2001); Murtha, Burnet & Harnby (1983). Generally, in accord to the work of Fisher et al. (1978), FA contains spherical particles of different aspects, such as cenospheres, which are hollow (empty inside), or plerospheres, which are filled with other smaller

sphere or solids. The cenospheres, for instance, are a very special byproduct existent within FA composed of an external aluminosilicate shell and empty in the inside. Thus, it is light, inert and thermal resistant since it is produced at high temperatures above 1200 °C through a process similar to glass production (i.e. occurrence of sintering), as debated by Ranjbar & Kuenzel (2017); Żyrkowski (2014).

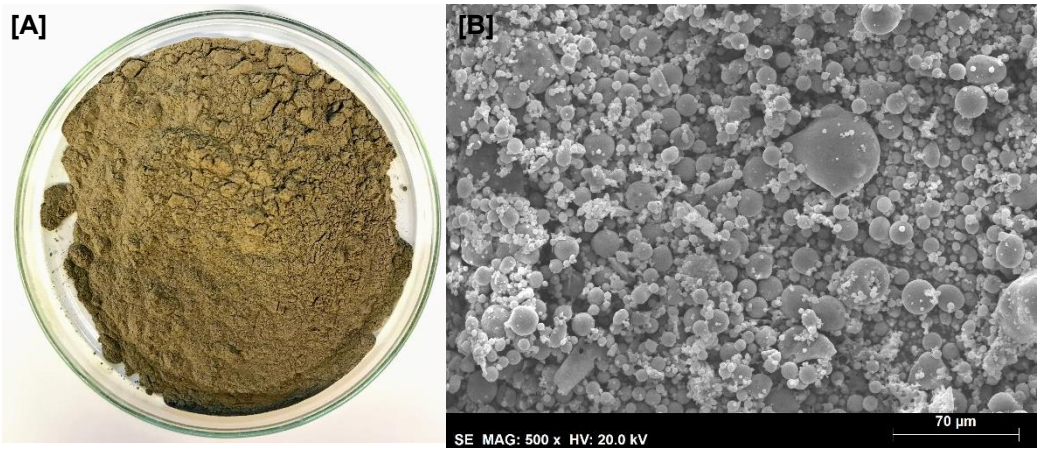

Figure 10 – Fly ash sample in natura [A] and its microscopic image [B]. Source: Author

Fly ash, according to data from Summers, Rupp & Gherini (1983), cited in the work of Mattigod et al. (1990), has a specific gravity (SG) within the range of 1.59 – 3.10, a dry bulk density of 1.01 – 1.43 · 106 g/ m³ and a specific surface area of 200 – 3060 m²/ kg. Yao et al. (2015) indicate that FA has a mean particle size of below 20 µm, a surface area of 300 – 500 m²/ kg and an average bulk density for FA is 0.54 – 0.86 g/ cm³ (alternatively, 10-6 g/ m³). Snellings, Mertens & Elsen (2012), for instance, cites that the Specific Gravity (SG) for FA is in average estimated to be 2.2, possibly varying of 0.3. Ahmaruzzaman (2010) indicate several references and states that FA SG is within 2.1 – 3.0 and the surface area can oscillates between 170 – 1000 m²/ kg.

Ultimately, within similar ranges, Bhatt et al. (2019) cites that the SG of FA is near 2.0 but can reach values between 1.6 – 3.1 depending on its source material and combustion processes. In terms of color, FA usually has a gray-like color but it can change to darker tones in relation to the amount of unburned carbon and iron existent, as Yao et al. (2015); Ahmaruzzaman (2010) discuss. In relation to pH, the work of Hower et al. (1996) indicates that FA has a wide range, roughly between 2 – 12.5. Even though very much changeable, Yao et al. (2015) indicate that in function of the Ca/ S ratio and the pH it is possible to classify FAs as strongly alkaline (pH 11 – 13), mildly alkaline (pH 8 – 9) and acidic.

The broad work of Vassilev & Vassileva (2005) indicates that near 316 minerals and 188 mineral groups already have been found, respectively, in coals and FAs, a fact that can give a glimpse of the degree of complexity associated to FA composition. The same authors divide FA composition into three (3) major parts, inorganic components (90 % – 99 %), organic components (1 % – 9 %) and fluidic components (< 0.5 %).

Among the biggest share, 34 % – 80 % are glassy and amorphous spherical and spherical-like particles, and their debris. The rest, around 17 % – 63 %, contains crystalline materials, such as silicates, oxides, hydroxides, chlorides, sulfates, carbonates and phosphates. The organic share is mostly associated with unburned carbon and chars, and the fluidic one is moisture and gaseous organic and inorganic compounds. In relation to the amorphous material, the work of Fisher et al. (1978) identified and classified, via light microscopy, 11 different types of FA particles, from completely spherical until rounded, angular-like and vesicular-like ones.

Focusing on the type of mineral existent within a FA sample, Vassilev & Vassileva (1996a, 1996b) debated that they can be divided into three (3) classes in relation to the way they were synthesized. Other authors like Kruse et al. (2012) discussed the similar aspects.

- Primary constituents: primeval compounds already existent in the raw coal, hence without any phase transformation after the combustion process. Examples are silicates (quartz, clays, mica, feldspar and zircon), oxides (hematite, chromite and corundum) and carbonates (calcite and dolomite).

- Secondary constituents: compounds synthesized as a result of the physical and chemical processes during coal combustion. Examples are silicates (quartz, cristobalite, metakaolinite, mullite and melilite), oxides (magnetite, hematite, lime, periclase, ilmenite, spinel, magnesioferrite and several oxides of different chemical elements, such as Ce, Cr, Cu, Mn, Zn and Zr), sulfates (sulfates) and carbonates (calcite).

- Tertiary constituents: compounds synthetized after the combustion phase, specifically, during transportation and storage. Examples are brucite, portlandite, gypsum, iron sulfate, calcite and Fe and Al hydroxides.

At this point, it is fundamental to comprehend that FA does not have a fixed composition or chemical formula since it is, straightforwardly, related to the type of raw material that was combusted. Even though coal is mainly composed of carbon, it also holds relevant amounts of hydrogen, oxygen, nitrogen and even sulphur, and may – often do have – a wide variety of impurities and other compounds that influences its physical and chemical characteristics. Ultimately, these so-called impurities are found in the CCPs.

In terms of classification, shown in Figure 11, coal is divided into four (4) different categories or ranks referred to volatile matter and energy content (heat value), both directly or indirectly affiliated to the carbon content and the impurities present, as proposed by Parr (1922). Some researchers refer also to peat or turf, which is the precursor of coal and is an agglomerate of organic matter commonly found near the surface and prior to pressure, temperature, depth and time influences to, properly, transform into coal.

Since it is made of aluminosilicates, FA can be classified also in relation to its composition and, in this sense, there exist two most recognized technical standards for that, one proposed by ASTM International (2019a) and another introduced by the American Association of State Highway and Transportation Officials, AASHTO (2019).

It is important to highlight that both have roughly similar requirements for physical and chemical classification of coal ash, with minor discrepancies. In summary, FA is divided into 3 different classes, more importantly, in terms of the content of SiO_2, Al_2O_3 and Iron Oxide (Fe_2O_3), but also related to the presence of moisture, sulphur trioxide (SO_3) and a property named Loss on Ignition (LOI). In the 2019 update, the ASTM standard included a requirement for calcium oxide (CaO).

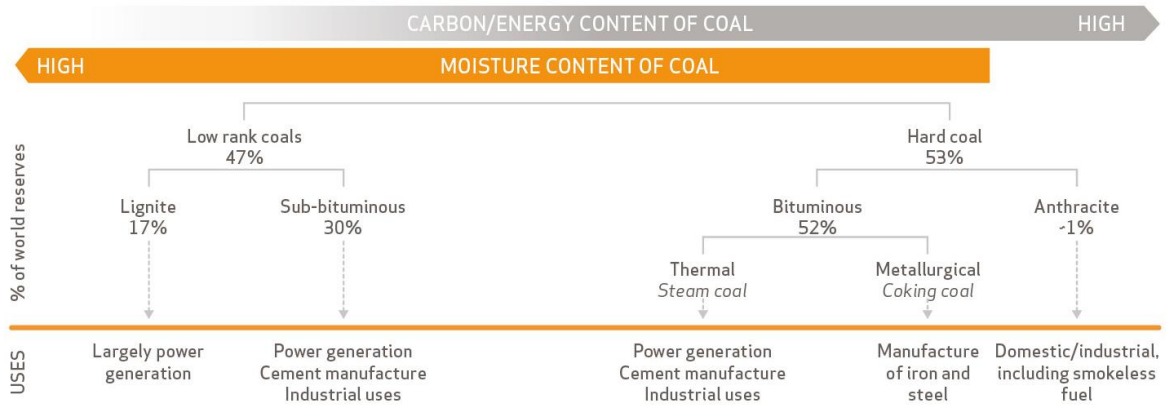

Figure 11 – Coal classification diagram. Source: World Coal Association (WCA)

Usually, it is important to highlight, even with those limits for CaO established, in reality, the type of coal will very much influence it since the high ranking coals have much less than the others. For instance, Ahmaruzzaman (2010) indicates that class F FAs contains CaO in the range 1 % and 12 %, while class C is between 30 % and 40 %. Belviso (2018), similarly, affirms that CaO content in class F usually is less than 5 % since it is derived from anthracite and bituminous coals, while class C content is above 20 %, as lignite and peat are its major raw materials. For a better understanding, Table A5 (see Appendix A) presents a brief summary of the different coal ranks and their composition.

Furthermore, the variations in chemical composition are also attested relative to the geographical source of coal. Hence, to illustrate the certain difficulty faced to classify properly the coal ashes, the review work of Bhatt et al. (2019) contribute to shed light on this important aspect. It is relevant to discuss the variability as it can, directly, influence the combustion processes but also researches dedicated to propose new strategies to make use of FAs. Thus, Table A7 (see Appendix A) concisely lists the characteristics of coal fly ashes from several countries.

4.2.2 Applications

Fly ash has been changing its major destination throughout the time as, instead of being simply a waste destined to be dumped in landfills, it started to be considered as a qualified raw material for

different activities and industries. Figure 12 gives several alternatives indicating that FA can be used as a valuable raw material because of its ubiquitous availability, high production, potential and cheap price –considered as a negative valued residue since producers spend money to properly manage it, and then can be turned into a costless raw material. Traditionally, fly ash is being used in the civil construction industry as construction products, such as bricks and tiles, and as an additive to cement and concrete, exactly, due to its natural pozzolanic properties, facts fully recognized in the specific literature and emphasized by Asl et al. (2018); Ahmaruzzaman (2010); R. Kumar, Kumar & Mehrotra (2007); Wang & Wu (2006); Murtha, Burnet & Harnby (1983); ACAA (n.d.). Depending on the type of coal the FA came from, the incorporation as a replacement for cement is very strong.

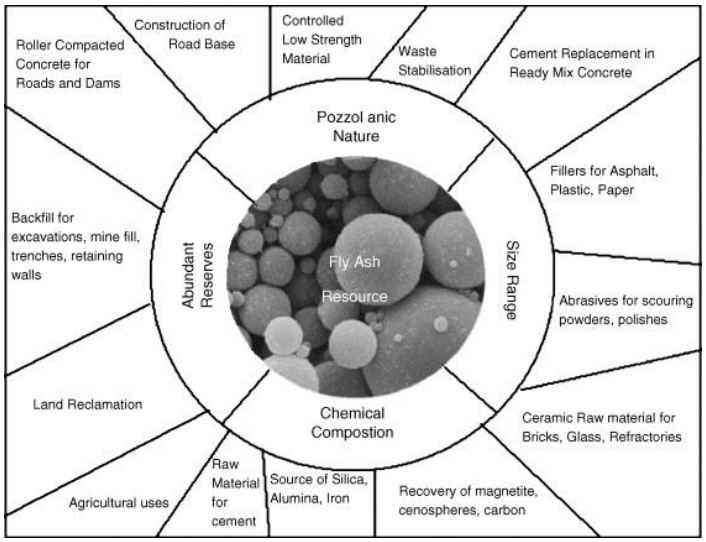

Figure 12 – Application potentials of fly ash. Source: Wang & Wu (2006)

For instance, Ahmaruzzaman (2010) says that 15 % – 25 % of cement can be replaced by bituminous coal FA, while for high lime FA this can reach levels of 25 % – 40 % and even 75 %, depending on the final application (parking lot and streets pavements). Furthermore, the broad of FA applications in construction has been widening throughout the time since technology and researched advanced as to, safely, enable its incorporation for buildings, skyscrapers, hydroelectric dams, bridges and robust highways. The same author says that a cost reduction of 10 % – 20 % is envisioned when FA is used in road construction and pavement. Furthermore, FA valorization and use can be done as soil amelioration and fertility boosting, as stressed by Yao et al. (2015); Basu et al. (2009), mostly, for soil texture and pH correction (acidity diminishment) due to its content of lime, and also as a source of minerals for plants (e.g. P, N, K, Mg and Mn). Obviously, FA needs to be pretreated to guarantee the elimination and/ or removal of any kind of toxic chemical elements and heavy metals possibly existent.

Currently, there have been proposed several new possibilities, with an even higher added-value for FA valorization as adsorbent for flue gas cleaning, mainly for mercury (Hg) and nitrogen oxides (DeNOx) and sulphur oxides (DeSOx) removal processes. The former consists of processes, such as Selective Catalytic Reduction (SCR) and Selective Non-Catalytic Reduction (SNCR) techniques. The latter consists of FGD technologies such as wet, dry and spray-dry scrubbing. For Hg and nitrogenous

compounds removal, the work of Rubel et al. (2005) indicates certain potential of FA-based processes. In relation to FGD systems, FA be used as a substitute for activated carbon (AC), a costly raw material responsible for a huge share of the investments, to remove SO_2 from exhaust gases. An example can be the work of Davini (1996), who achieved positive results by mixing FA with $Ca(OH)_2$ and water for SO2 removal.

FA have been evaluated as an adsorbent due to its physical and chemical characteristics, mainly, surface area and porosity. As for exemplification, FA was used to remove toxic compounds from wastewaters, such as heavy metals, inorganic compounds like phosphates and fluorides, and organic compounds like phenols, pesticides and dyes and colored pigments contained in painting materials and massively by textile industries and commonly present in clothes. Ahmaruzzaman (2010); Basu et al. (2009) have a broad summary of different researches towards these applications of FA.

Another interesting path for FA valorization is to use it as catalyst support or as a heterogeneous catalyst itself, as reviewed by different authors including Galadima & Muraza (2020); Asl et al. (2018). Alumina and silica, rich phases among FAs, are commonly used to sustain active components for catalysis and the metallic oxides formed during coal combustion and retained in FA are traditional catalysts for different types of reactions. The work of Chakraborty, Bepari & Banerjee (2010) used FA as a support for CaO derived from eggshells for biodiesel production. FAME yields of 96.97 % were reached with a 30 % wt. CaO loading catalyst at 70 °C, methanol: oil ratio of 6.9:1 and 1.0 % wt. of catalyst for 5 hours.

Other authors, e.g. Manique et al. (2017), used fly ash to synthesize materials capable of transesterifying vegetable oil. They adapted a precipitation methodology proposed by Petkowicz et al. (2008) to synthesize a FA-based zeolite (sodalite) reaching 95.5 % of soybean conversion into FAME at 65 °C, methanol: oil ratio of 12:1 and 4 % wt. of catalyst for 2 hours. Bhandari, Volli & Purkait (2015) proposed three zeolites, A, X and KX, that showed successful efficiency towards yielding biodiesel up to 81.2 % at 65 °C, methanol: oil ratio of 6:1 and 3 % wt. of catalyst for 8 hours. Lastly, Volli & Purkait (2015) developed a HTlc and a zeolite catalyst from FA residues following a precipitation method using also pure, reagent grade materials. Final results indicate that mustard oil was transesterified to FAME with the HTlc catalyst up to a conversion of 67.1 % at 65 °C, methanol: oil ratio of 12:1 and 5 % wt. of catalyst for 8 hours.

Through a similar objective, Xiang, Wang & Jiao (2016) utilized FA after a treatment with KOH and nitric acid for WFO biodiesel production under ultrasound influence. The final results were positive since the supported alkaline catalyst promoted a FAME conversion of 95.57 % at 70 °C, methanol: oil ratio of 10.71:1 and 4.97 % wt. of catalyst for 1.41 minutes. Furthermore, Jain, Khatri & Rani (2011), for instance, evaluated the behavior of a FA-derived catalyst, subject to a thermal and a chemical (with a 50 % wt. NaOH solution) activation processes, for condensation reactions with cyclohexanone and benzaldehyde. The final results indicate higher conversion (> 70 %) and selectivity (> 80 %) to the desired products.

Likewise, fly ash can be applied as a source of materials for zeolites production – notedly types A, X, Y, sodalite and ZSM-5, as reviewed Yao et al. (2015); Wdowin et al. (2014); Ahmaruzzaman (2010). For instance, Pavlović et al. (2020) developed a zeolitic basic catalyst (cancrinite-sodalite-zeolite-like material) based on FA and chicken egg shell residues. FAME yields of 97.8 % was obtained at 60 °C, methanol: oil ratio of 6:1 and 6 % wt. of catalyst for 0.5 hour. Furthermore, zeolite materials were also evaluated as adsorbents of heavy metals and, as mentioned by Z. Zhang et al. (2017) for carbon dioxide capture.

5. EXPERIMENTAL PROCEDURES

The practical part of this entire work, following its objectives previously stated, focus on the biodiesel with a special dedication towards the valorization of residues. Accordingly, it is, essentially, divided into two major sections: Heterogeneous Catalyst Development, Synthetization and Improvement, and Biodiesel Production. The following sections describe in a proper and comprehensive way all the assumptions, definitions, methodologies, references and calculations done as a way to achieve the final results presented and discussed in the forthcoming chapter.

5.1 Heterogeneous Catalyst Development, Synthetization and Improvement

The FA-based heterogeneous catalyst was synthetized via a novel methodology, a result of inspiration, rework and combination of the positive and negative aspects from several others, formerly, proposed by several authors from different fields, all of which aligned with the objective of developing a successful heterogeneous catalyst starting from different types of wastes and aiming to create different materials.

Olfs et al. (2009); He et al. (2005); Cavani, Trifirò & Vaccari (1991) reviewed broadly (HT) and highlighted that coprecipitation is often chosen as preferred path for synthetization. It is, well recognized as the most utilized methodology due to the ease of preparation as it is an “one pot” direct synthesis, as mentioned by (Othman et al. (2009); He et al. (2005).

Kuwahara et al. (2009, 2010) used industrial residues and developed, respectively, a hydroxyapatite-zeolite composite from steel slag residue, and a HT-like compound (HTlc) and a zeolite from BFS residue. Both were based on a comprehensive coprecipitation process fundamentally dedicated to extract the metallic ions existent in such residues – Al, Si and Ca. These authors proposed a simple and low cost methodology, comprised of three major steps, an acid leaching, an alkaline addition (to alter pH and promote the precipitation of a solid phase) and an aging step (of different duration).

In fact, the work of Kuwahara et al. (2010) was a key support to other works, Kuwahara & Yamashita (2015, 2017); Kuwahara et al. (2012, 2013), focused on developing suitable heterogeneous catalysts and, as the third one investigated, for biodiesel production. Muriithi et al. (2017) applied the same methodology, now using fly ash as raw material, and came up with a HT heterogeneous catalyst successful for biodiesel production.

Finally, the works of Valente et al. (2009); Valente, Sánchez-Cantú & Figueras (2008) and their derivative works (Patent No. US000007807128B220101005, 2008; Patent No. US000007740828B220100622, 2010), considering the reality that HTs materials are synthesized via coprecipitation methods using as reagents metallic salts (e.g. nitrates, phosphates, chlorides) of, for

instance, Ca, Al, Mg or Zn, proposed an inexpensive and, as they state, easy, environmentally friendly and economical methodology for Layered-Double Hydrotalcite (LDH) production.

The methodology implemented in this work is a combination of three separated phases to be properly executed. Namely, they are source solutions preparation step, precipitation step and aging/ crystallization step.

The first phase requires the production of two source solutions, hereafter named 1st Source Solution (FSS) and 2nd Source Solution (SSS), composed, respectively, of metallic cationic species and alkaline active species. The major role of FSS is to supply the metallic species needed to crystallize the catalyst, while the one of SSS is to enrich the medium with Ca and nitrate (NO_3^{2-}) ions. Hence, both solutions are responsible to promote the formation of hydroxides and precipitation of solid phases later on. Figure 13 graphically describes the FSS preparation.

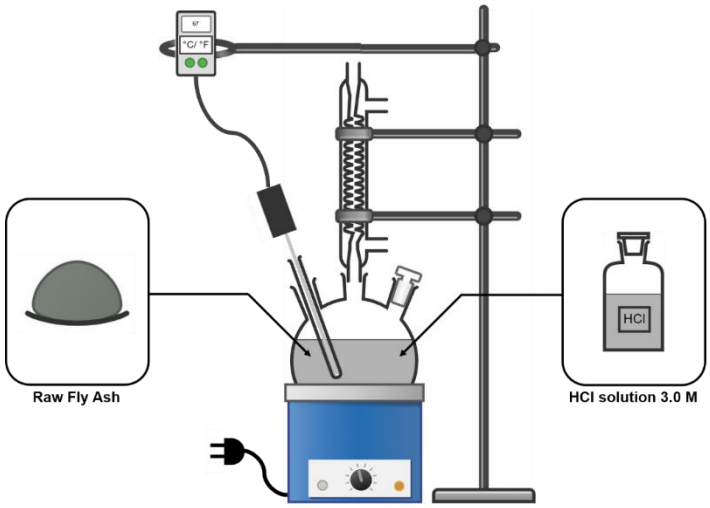

Figure 13 – FSS preparation system. Source: Author and Chemix Lab Diagrams

The FSS is produced from fly ash residues from bituminous coal collected from the Skawina power plant, located in the municipality of the same name in southern Poland and owned by the Czech electricity conglomerate ČEZ Group ®. Further details about its properties and composition are given in the following chapter. This procedure is done by contacting 20 grams of raw and in natura FA with 400 ml of a 3 M solution of HCl for 2 hours. This solution was made by adding 99.3712 milliliters of reagent-grade HCl from Panreac AppliChem ® 37 % in 400 milliliters of distilled water. Its major objective is to extract or lixiviate the metallic ions naturally contained in FA and produce an acidic leachate fully enriched with 2+ and 3+ species.

The second source solution, with the due procedure depicted in Figure 14, is made of another waste, chicken egg shells (ES). The ES, mostly composed of calcium carbonate ($CaCO_3$), were collected from a local restaurant near the IST Alameda campus in Lisbon, Portugal and, to become a suitable raw material for the source solution, requires a pre-processing stage. The ES were thoroughly washed with soap and water to remove dust and residues, dried at 60 °C in a laboratory oven for 24 hours and manually milled in a ceramic mortar with pestle until becoming a white-like fine powder.

Finally, 10 g of the powdered ES were added to 200 milliliters of a ≈ 0.7 M solution of HNO_3. This solution was made by adding 10 milliliters of reagent-grade HNO_3 from Honeywell Fluka ® ≥ 65 % of purity in 190 milliliters of distilled water.

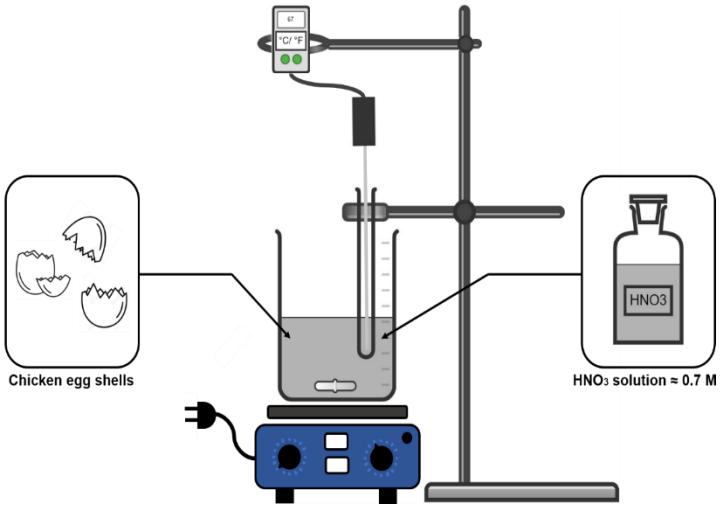

Figure 14 – Second source solution preparation. Source: Author and Chemix Lab Diagrams

Care is needed while mixing the ES in the solution as an acid-base reaction is promoted, transforming the $CaCO_3$ into calcium nitrate ($Ca(NO_3)_2$) and freeing CO_2 to the atmosphere. This process is represented by Equation (I) and promotes the formation of high amounts of bubbles and, sometimes, thick foams which, as time passes, disappear entirely leaving a clear transparent aqueous medium.

$$\underset{\text{(Carbonate)}}{CaCO_3\,(s)} + \underset{\text{(Acid)}}{2\,HNO_3\,(l)} \rightarrow \underset{\text{(Salt)}}{Ca(NO_3)_2\,(s)} + CO_2\,(g) + \underset{\text{(Water)}}{H_2O\,(l)} \qquad \textbf{(1)}$$

The second phase of the methodology is the precipitation step, which is focused on associating the previously prepared source solutions and conditioning for the nucleation of crystals and precipitation of a solid phase, a further base for the heterogeneous catalyst. Figure 15 summarizes the whole procedure.

It consists of combining 200 milliliters of each source solution prepared – FSS and SSS – in a beaker at 50 °C with vigorous agitation. Further, an alkaline species is added to the aqueous medium dropwise together with a pH controlling measure via stripes – Hydrion ® papers from Micro Essential Laboratory ® until reaching the value of 10.0 (± 1.0).

Depending on the catalyst preparation sample, different alkaline species were chosen to be added to the aqueous medium. The objective was to evaluate the variability of precipitated solids formed in the procedure towards the catalyst synthesis process in association with its cost for preparation. Namely, they are the following ones:

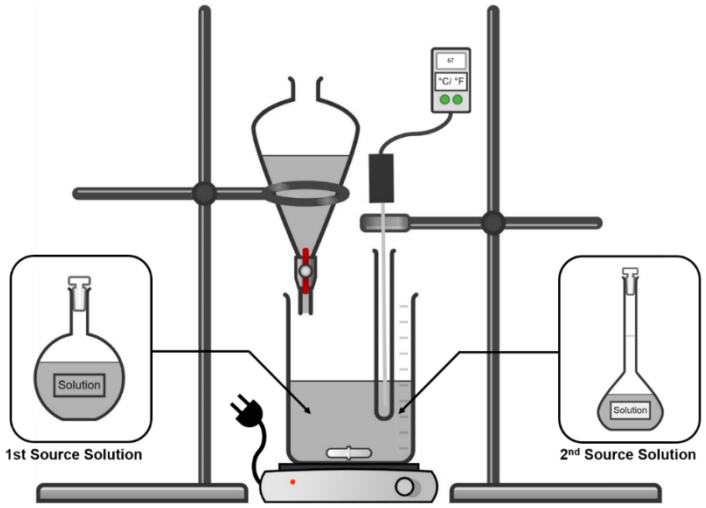

Figure 15 – Heterogeneous catalyst synthesis. Source: Author and Chemix Lab Diagrams

2M solution made of reagent-grade KOH 86 % minimum purity from EKA Chemicals ® (currently Akzo Nobel ®).

Reagent-grade ammonium carbonate ($(NH_4)_2CO_3$) with ≥ 99.99 % of purity from Honeywell Riedel-de-Haën ®.

Suspension of calcium hydroxide ($Ca(OH)_2$) made from chicken egg shells (ES).

The last alkaline species – a suspension – as being a derivative of ES, requires a specific procedure to be prepared. The final manually milled white-like fine powdered ES was submitted to calcination in a laboratory muffle furnace Nabertherm ® L9/ 12 at 800 °C for 3 hours in a static atmosphere to convert from $CaCO_3$ to CaO, as Figure 16 highlights.

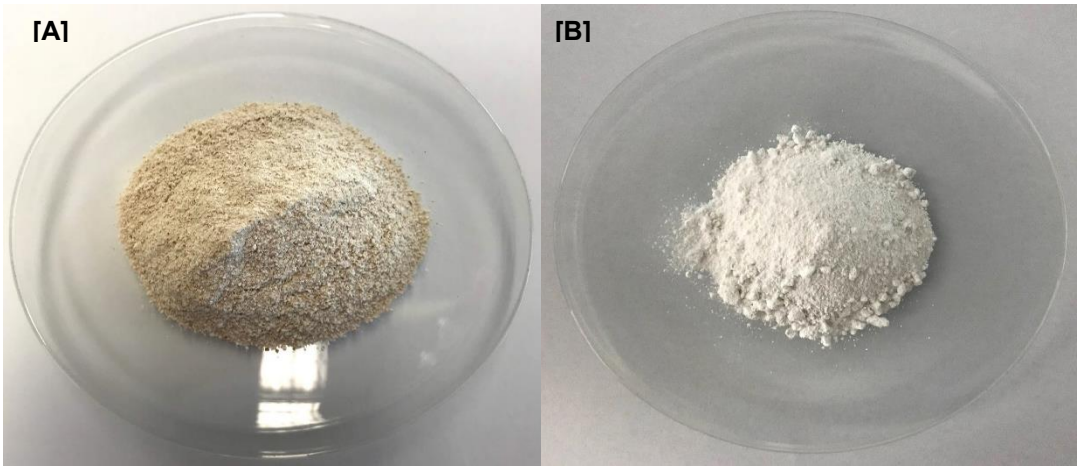

Figure 16 – Powdered [A] and calcined [B] egg shells

This final powdered material, CaO, was used to make the alkaline suspension used to raise the pH during the precipitation phase of the methodology. It was made by mixing 10 g of CaO in 270

milliliters of distilled water. Thus, containing ca. 3.6 % wt. (3.5714 %) of $Ca(OH)_2$ in suspension. The Equation (II) indicates the occurring chemical reaction.

$$\underset{\text{(Calcium oxide)}}{CaO\ (s)} + \underset{\text{(Water)}}{2\ H_2O\ (l)} \rightarrow \underset{\text{(Calcium hydroxide)}}{Ca(OH)_2\ (s)} \qquad \textbf{(2)}$$

The third and last phase of the methodology is the aging/ crystallization step. It consists, basically, of allowing the final aqueous medium, obtained after adding the alkaline species, to crystallize under a vigorous agitation at 50 °C for 6 hours in the same beaker. This crystallization time was standardized at 6 hours but for certain samples it was modified. The main objective is to allow the recently nucleated crystals to combine and grow the crystals as to form the solid minerals. This is a very complex process which can involve agglomeration of particles, crystal growth, deconstruction of crystallites, redissolution and even Ostwald ripening process. After that, the agitation is ended and the whole recipient is moved to a laboratory oven at 60 °C for 24 hours in a static atmosphere to promote the aging of the material and its precipitation.

After that, the material is vacuum filtered together with a thorough washing with distilled water and then left to dry at 60 °C in a laboratory oven. This is the final material that will be tested as a heterogeneous catalyst.

The present work prepared the following catalysts samples via the above described methodology, henceforth, named Fly Ash – Egg Shell (FAES) catalysts. Since there are small differences between them, details are provided below:

- FAES N° 1 – FA and ES added directly to the HNO_3 solution, without preparation of FSS and SSS. Alkaline species used: $(NH_4)_2CO_3$. pH final: 10.0 (± 1.0). Crystallization time: 6 hours.
- FAES N° 2 – Alkaline species used: $Ca(OH)_2$. pH final: 5.0 (± 1.0). Crystallization time: 6 hours.
- FAES N° 3 – Alkaline species used: KOH. pH final: 10.0 (± 1.0). Crystallization time: 6 hours.
- FAES N° 4 – Alkaline species used: $(NH_4)_2CO_3$. pH final: 10.0 (± 1.0). Crystallization time: 6 hours.
- FAES N° 5 – Alkaline species used: KOH. pH final: 10.0 (± 1.0). Crystallization time: 168 hours.
- FAES N° 6 – Alkaline species used: $Ca(OH)_2$. pH final: 10.0 (± 1.0). Crystallization time: 6 hours.

- FAES N° 7 – Alkaline species used: $Ca(OH)_2$. pH final: 10.0 (± 1.0). Crystallization time: 6 hours.

- FAES N° 8 – FA added directly to FSS and 10 ml of HNO_3 ≥ 65 % of purity. Alkaline species used: $Ca(OH)_2$. pH final: 10.0 (± 1.0). Crystallization time: 6 hours.

The last requirement to arrange the synthetized catalysts for the second section of this work is to submit each sample to a calcination process at 800 °C in a laboratory muffle furnace Nabertherm ® L9/ 12 at 800 °C in a static atmosphere. The heating process was standardized and preprogrammed in the equipment holding two parts, a heating ramp from room temperature until 800 °C during 3 hours and a proper calcination at 800 °C for more 3 hours.

Other heterogeneous catalysts were also prepared to serve as a comparison parameter with the FAES synthesized catalysts. Namely, CaO, calcined at 800 °C and 900 °C. In natura FA was also utilized as a catalyst for FAME conversion to attest its capacity. Exceptionally, the catalyst FAES N° 1, due to its specificities in synthesis, was also calcined at 900 °C. Lastly, It NaOH was also used as a homogeneous catalyst for vegetable oil conversion for further comparisons and discussions.

Hence, this present work developed 13 different types of catalyst samples to carry transesterification reactions.

5.2 Biodiesel Production

The biodiesel production was done with a soybean – sunflower mixed vegetable oil from Manuel Serra S.A. ® (Serrata ® brand) and WFO collected from one canteen at IST. Both raw materials were used for a transesterification methodology in a laboratory scale scheme, as described in Figure 17.

The reactional parameters and conditions were defined and standardized throughout the whole experiments. It was based on the reference literature previously cited and discussed in the preliminary chapters. Specifically, it was defined a pre-conditioning step for the raw material of 1 hour at 100 °C and a reactional temperature at 67 °C – methanol total reflux condition – under vigorous mixing. The methanol: oil molar ratio is 12:1 (meaning a molar excess of 200 %), the catalyst amount in % wt. is 2.5 and the reactional time is 6 hours. For the samples using CaO and NaOH, a preconditioning step (also named contact step) at 65 °C for 1 hour between methanol and the catalyst is required as to promote the formation of methoxide ionic species.

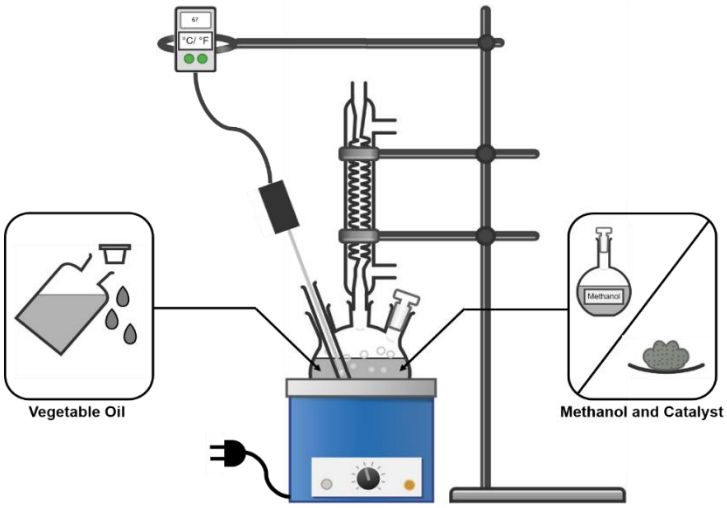

Figure 17 – Biodiesel production setup. Source: Author and Chemix Lab Diagrams

Each experiment was repeated three (3) times, meaning four records for each catalyst, as to evaluate and confirm the repeatability of the results. These conditions are summarized in Table 1. It is important to highlight that for both homogeneous and heterogeneous reactions, the conditions were exactly the same, with only one exception which is the catalyst amount of NaOH. This had to be like that as to avoid the occurrence of side reactions, as already discussed in previous chapters.

Table 1 – Biodiesel production reactional parameters summary

Parameter \ Sample	Heterogeneous Reaction		Homogeneous Reaction
	FAES	CaO	NaOH
Temperature (°C)	67	67	67
Time (hour)	6	6	6
Methanol: oil Molar Ratio	12:1	12:1	12:1
Catalyst Content (% wt.)	2.5	2.5	0.5
Pre-mixing Temperature (°C)	–	65	65
Pre-mixing Time (hour)	–	1	1
Agitation (rpm)	1000	1000	1000

To calculate the amount of methanol used in the experiments, stoichiometric calculations based on the fundamental transesterification chemical reaction is required. For that, obviously, it is needed to know the Molar Mass (MM) of the vegetable oil used. Notwithstanding, it is difficult to account the total MM of the material since there is a natural and huge variability in the feedstock in terms of TAG composition. Besides that, the current vegetable oil used is made of a mixture of soybean and sunflower oils not fixed and thus not announced by the producer. A point to stress is the different content of TAGs and its associated FAs exert direct influence in the Total Molar Mass (TMM) of the vegetable oil. Therefore, it constitutes an influential aspect in the chemical reaction and its stoichiometry.

To overcome these difficulties and avoid the use of any precise analytical method for quantification, i.e. chromatography techniques, which are somewhat expensive and require a continuous analysis for each and every vegetable oil utilized, an alternative procedure was resorted to.

Basically, a Mean Molar Mass (MMM) was calculated for each vegetable oil individually – soybean and sunflower – based on compositional data previously reported by Hammond (2003); Demirbaş (2002); Kincs (1985); Goering et al. (1982) via the application of a method proposed by Pighinelli (2007) and expressed in Equation (III). Furthermore, the data for several FA molar masses were obtained from RSC (n.d.) chemical structure database.

$$MMM_{Vegetable\ Oil} = [3 \cdot (\sum \%_{Fatty\ Acid} \cdot MM_{Fatty\ Acid})] + MM_{Glycerol} + MM_{Water} \quad \textbf{(3)}$$

Where,

$MMM_{Vegetable\ Oil}$: Mean molar mass of vegetable oil.

$MM_{Fatty\ Acid}$: Molar mass of each fatty acid.

$MM_{Glycerol}$: Molar mass of glycerol.

MM_{Water}: Molar mass of water.

The complete references for the MMM calculation is presented in Table A8 (see Appendix A) for a better comprehension.

Then, an average of the four MMMs derived from Equation (3) was calculated for each vegetable oil and used for a final calculation of a single MM for several combinations of potential mixtures. This has the objective of taking into account the influence of soybean and sunflower oil mixtures within the raw material used in the experiments. Therefore, combinations of both from 0.0 % to 100 % with a step factor of 10 % were made. Hence, 10 potential mixtures were made – and a weighted molar mass in terms of the content of each oil was calculated. Ultimately, an average of those 10 MMs was done and this constituted the Final Molar Mass (FMM) applied to all the stoichiometric calculations of transesterification. In detail, as given in Table 2.

The entirety of calculations for the transesterification experiments are presented in Table 3 and were standardized for 100 grams of vegetable oil but, throughout the work, certain experiments were carried with 50 g and 10 g of oil. This was aimed at a reduction of raw materials consumption, and to allow a further look and discussion in terms of reactional behavior and repeatability.

After each transesterification reaction experiment, the medium was vacuum filtered with a Büchner funnel to remove the catalyst (for the heterogeneous ones) and transfer the liquid phase to a separatory/ decantation funnel to promote the segregation of glycerol and the transesterification liquid product (formally not possible to be called biodiesel prior to the characterization analysis). After certain time, usually 24 hours, but less depending on the behavior of the sample, the glycerol and the transesterification product were separated and safely stored for further characterizations.

Table 2 – Vegetable oil final molar mass data

Mean Molar Mass (g/ mol)	Composition of Mixtures (%)		Mixtures Weighted Molar Mass (g/ mol)	Final Molar Mass (g/ mol)
	Soybean	Sunflower		
Soybean	0.1	0.9	878.43	873.75
869.07	0.2	0.8	877.39	
	0.3	0.7	876.35	
	0.4	0.6	875.31	
	0.5	0.5	874.27	
Sunflower	0.6	0.4	873.23	
879.46	0.7	0.3	872.19	
	0.8	0.2	871.15	
	0.9	0.1	870.11	
	1.0	0.0	869.07	

The heterogeneous catalyst after filtration was dried in a laboratory oven at 60 °C during 24 hours to promote the evaporation of unreacted reagents (e.g. methanol) and traces of water if existent. After that, it was stored for further analysis, mainly, connected to evaluate its physical aspect, loss of crystallinity and the possible reuse after a simple cleaning procedure to remove any retained residues, such as TAG, DAG, MAG and glycerol.

Table 3 – Transesterification reaction stoichiometric calculations

Vegetable Oil Mass, gram	100	50	10
Vegetable Oil Specific Gravity, g/ cm³	–	–	–
Vegetable Oil Volume, milliliter	–	–	–
Vegetable Oil Mean Molar Mass, g/ mol	873.75	873.75	873.75
N° of mols of Vegetable Oil	0.11	0.06	0.01
Theoretical N° of mols of Methanol (stoichiometric)	0.34	0.17	0.03
Reactional Excess of Methanol (%)	300	300	300
N° of Mols of Reactional Excess	9	9	9
N° of mols of Reactional Methanol	1.37	0.69	0.14
Mass of Methanol, gram	44.00	22.00	4.40
Methanol Specific Gravity, g/ cm³	0.79	0.79	0.79
Methanol Molar Mass, g/ mol	32.04	32.04	32.04
Volume of Methanol Utilized, milliliter	55.56	27.78	5.56

5.3 Analytical Techniques

The experimental part of this work resulted in a relevant amount of samples and, towards supporting all the due discussion and debate related to the proposed methodology and the efficiency of the catalysts, several characterization analysis were carried. In relation to biodiesel, as previously

explained, there are two major technical standards, namely the ASTM and the EN 14214, thus the following methodologies briefly detailed and explained as based on those.

5.3.1 Acidity Index

In this work, it was utilized a titrimetric acidity index method from IAL (2008), a adapted version from the AOCS official method Cd 3d-63 – “Acid value of fats and oils”, formerly known as Cd 3a-63.

This method is applicable to animal and vegetable oils, crude or refined, and animal fats. It consists of titrating an oil sample mixed with neutralized ethanol 97 °GL min. with a alkali solution of NaOH of known molarity. To obtain the AI value in milligram of KOH per gram (mg KOH/ g), the Equation (4) should be used.

$$AI = \frac{56.11 \cdot v \cdot N \cdot f}{m} \qquad \textbf{(4)}$$

Where,

v: Titrated volume of NaOH solution (in milliliter).

N: Molarity of the NaOH solution.

f: NaOH solution correction factor (related to a standardized potassium biphthalate titration).

m: mass of the sample (in gram).

In this work it was standardized the use of NaOH solutions with 0.1 M and 0.01 M molarity to be used depending on the degree of expected FFA content. In other words, for higher quality oils (with a very low FFA content) a lower molarity solution will be used. Thus focusing on giving more precise and trustful data and to reduce the operational visual error while attesting the color change from colorless to light pink. As color indicator 1 % aqueous solution of phenolphthalein was used. The alcohol neutralization was done by adding 2 – 3 drops of phenolphthalein and adding NaOH until reaching a pink color. It is important to highlight that the pink color cannot be very strong or almost nonexistent, it needs to be at the right tone to be mixed with the sample and change color, even with very low acid contents. Each analysis for each sample was repeated three times, thus totaling four measurements.

5.3.2 X-Ray Powder Diffraction (XRD)

The X-Ray Crystallography (XRC) is a field of knowledge dedicated to study and comprehend the crystalline structures of the solid matter. As its name indicates, the investigation is very much based on the use of x-rays and, among the varied analytical methods, there is XRD. The main focus is understanding the contained phases, the crystalline structure and the existent atomic organization.

X-ray wave has a determined wave length (λ) between 0.01 nanometer (nm) and 10 nm, and, while reaching a solid material, energy is transferred to the atoms, more specifically, to the electrons. Whereas this increase of energy is not enough to excite and remove the electrons out of the atoms, two patterns can occur: diffraction of part of this extra energy as other x-rays in a process named scattering, or transmission of the electrons (or the rest of it) through the material entirely. These scattered waves are, what is captured, measured and interpreted by an XRD equipment.

Furthermore, there are two main possibilities of behavior for the diffracted x-rays, a destructive or constructive interference. The former is ubiquitous in x-rays analysis as uncountable waves interact indistinctly and then cancel partially each other or not, resulting in almost insignificant detection by the equipment. Contrastingly, the special condition to occur a constructive interference of x-rays is the synchronism of two waves that reach the material in phase, which means having a certain wavelength, amplitude and frequency, at a certain angle and with a specific distance between them. This creates a relevant amplification of the signal detected by a x-ray equipment and forms a XRD diffractogram.

This constructive interference of the waves is expressed mathematically by the famous Bragg's law, presented in Equation (5), and developed by the British scientists William Henry Bragg and William Lawrence Bragg, father and son respectively.

$$n \cdot \lambda = 2 \cdot d \cdot \sin(\theta) \quad \textbf{(5)}$$

Where,

n: Multiplication positive integer proportionally related to the atomic plane and wavelength.

λ: Wavelength of the x-ray.

d: atomic plane interdistance.

θ: X-ray incidence angle.

This equation can be directly derived with the support of geometry by evaluating the path required by a x-ray wave to go as to cause a constructive interference, as detailed in Figure 18. It is clear that when the first wave reach the atom in the plane, the second wave still need to continue for a certain distance to reach the respective atom in another plane. This length difference needs to be proportional to the wavelength to secure that both waves are still in phase (i.e. parallel and adjacent) and is represented by the sum of $\overline{CB}$ and $\overline{BD}$ segments, which are of equal length. Finally, the chart produced by the equipment is in terms of 2θ angle and intensity.

For identification of crystallographic phases among the sample it is needed to apply the Bragg's law and calculate the d parameter for each intense peak observed and compare to the very wide database of diffraction data existent for pattern compounds. A very well-known document for XRD patterns or reference standards is the Joint Committee on Powder Diffraction Standards (JCPDS)

currently named as International Centre for Diffraction Data (ICDD). Alternatively, a freely available database for XRD matching is the American Mineralogist Crystal Structure Database, developed by Downs & Hall-Wallace (2003).

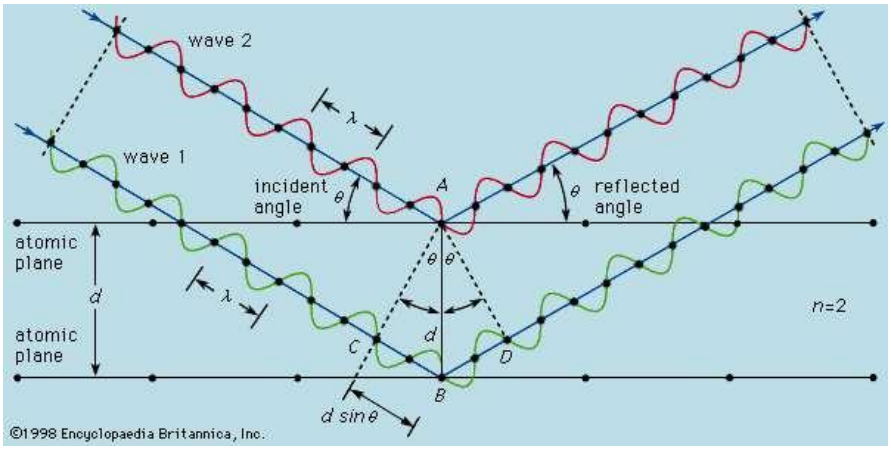

Figure 18 – Bragg's law graphic description. Source: Augustyn et al. (2016)

For the XRD experiments developed throughout this work, a Bruker ® D8 Advance equipment of 6.5 kVA, 50 Hz and containing copper with a Kα = 1.5418 Å of wavelength was used. The analysis for all samples were carried out within a 2θ angle range of 5° to 70°. The step size for each measurement was of 0.048718°. All XRD analysis were controlled using a Diffrac Plus XRD Commander ® and characterized using a Diffrac.EVA ® version 5.0.

The raw XRD diffractogram obtained throughout this work was previously treated with the objective of adjusting the baseline and set it to a constant value at zero (0), the initial value in the chart. This procedure was done manually using a standardized Microsoft Excel ® file, prepared by the author, consisting of plotting a new curve using 32 data points within the 2θ angles range – 5° to 70° – and values, specifically, set to get the most close to raw XRD diffractogram curve. This curve is referred as baseline. Then, a trendline as a power function, generally, expressed in Equation (VI), is automatically generated by the software related to the baseline and then a new intensity value is calculated.

$$y = A \cdot x^B \qquad \textbf{(6)}$$

Where,

A: Positive integer.

x: Power function base.

B: Exponent or power that can be a positive or negative integer.

The difference between the real experimental data and the trendline-derived data is computed, which means calculating the intensity residuals existent. Furthermore, a normalization of the data is

done as to standardize all values in the range 0 – 1. To do this, the highest intensity residual is identified and a simple division of each data point by it is computed. These is the dataset utilized to build all the XRD charts presented and debated in the following chapter and, afterwards, named “baseline-adjusted”. In the situation that a specific data point is negative instead of positive, meaning that the baseline created surpassed the experimental data, it is substituted by a zero. Hence, avoiding the occurrence of negative values in the final XRD chart.

5.3.3 Scanning Electron Microscopy (SEM) with Energy Dispersive Spectroscopy (EDS)

The SEM is a well-known technique based on the use of an accelerated (i.e. high kinetic energy carrier) electronic beam to allow the superficial analysis of solid materials, such as morphology (or texture), chemical composition (with the aid of EDS) and crystallographic information (mostly structure and orientation). The existence of SEM is justified since the most traditional microscopic technique used, the optical microscope, is limited in terms of lens magnification (up to around 1000 times) and the characteristic (i.e. wavelength) of the light beam used to illuminate the sample. Furthermore, with the need to evaluate new materials in micro or nano scales or to obtain more detailed information of surfaces, the optical microscope became limited.

The electronic beam is capable of providing much higher wavelengths and produce various signals, as Nanakoudis (2019) explains. Depending on the type of interaction between the electron and the material, different responses are observed and then utilized to obtain the desired information. For instance, an incident electron can be transmitted (i.e. pass through the sample directly), diffracted (i.e. pass through the sample in a different angle than the original) or be reflected as secondary electrons (SE) – the ones utilized for SEM imagery formation –, backscattered electrons, characteristic x-rays and Auger electrons (AE) – used for superficial atomic elements composition identification via an EDS equipment combined with SEM. The EDS tool is dedicated to evaluate and divide the different x-rays (characteristic x-rays) emitted by the source electronic after reaching the sample material.

The SEM technique is understood as a non-destructible analysis, so it is possible to carry it several times using the same material. Besides, it is a mere qualitative technique in terms of superficial analysis. Notwithstanding, in terms of EDS tool, it is understood as a semi-quantitative technique, as discussed by Makhlouf & Aliofkhazraei (2016), since it is capable of detecting major (amounts higher than 10 % wt.) and minor elements (amounts between 1 % wt. and 10 % wt.) but has a minimum detection limitation of 0.1 % wt. Therefore, it is not capable of, for instance, identify trace elements in general. In this work, In order to carry out analysis an analytical SEM equipment Hitachi ® S2400 with Bruker light elements EDS detector was utilized.

5.3.4 Attenuated Total Reflectance (ATR) – Fourier Transform Infra-Red (FTIR) Spectroscopy

The spectroscopy is a field of knowledge dedicated to comprehend all the aspects related to the interaction – absorption and emission – of electromagnetic radiation (i.e. microwaves, infrared, visible light, ultraviolet, x-ray and gamma ray) within the existing matter. Furthermore, there exists a

series of different analytical techniques based on spectroscopy to allow identify the nature of the compounds in a certain material. One of these techniques is FTIR.

This specific methodology is essentially based on using infrared waves since the molecular vibration range is very similar to its operational range (between 700nm – 1 mm of wavelength). Thus, the vibrational aspect of each molecule is the base for IR to be properly used to identify them, since a molecule – or part of it, i.e. a certain chemical bond – holds a vibrational pattern that is inherent and characteristic to each one, standing as an unmistakable molecular fingerprint.

An straightforward effect of absorbing extra energy – i.e. when it matches with the frequency of the molecule's natural vibration – is the stimulus to move to a new energetic level, inducing changes in the way the molecule vibrates and rotates. This energy absorption in a molecule can be of three major levels in terms of the progressive amount of energy brought: rotational, vibrational and electronic In general terms, the vibration patterns can be differentiated between stretching and bending, and, for diatomic and triatomic molecules, these movements are divided in 6 types. Symmetric, Asymmetric and Twisting stretches and Wagging, Scissoring and Rocking bends.

Finally, a FTIR equipment operates based on the infliction of IR waves with a wide range of wavelengths simultaneously towards a sample. This varied wavelengths are produced by an equipment named interferometer. It has the responsibility for dividing an original IR wave produced by a source in two different beams that will go through two different paths with a mirror in its end. One of the paths is of constant distance as there is a mixed (immovable) mirror, while the other is of variable path since the mirror is moveable. Then, both beams are combined, causing constructive or destructive interferences, and resulting in a wide range of wavelengths that are inflicted towards the sample, considering the varied positions the moveable mirror can have. Therefore, it is possible to carry the measurements of which wavelengths were absorbed by the sample under analysis in the FTIR and build an interferogram, the direct result from the equipment that quantifies light absorption versus mirror position in its axes. By applying the Fourier's Transform mathematical tool to modify the raw data obtained into the traditional and well known FTIR spectrum that quantifies light absorption (or transmission) versus wavelength.

Ultimately, a FTIR spectrum can be expressed in two (2) ways, as transmittance or as absorbance. The former is associated to the amount of energy that is transmitted by a sample material, or in other words, trespassed it and measured by the detector. Hence, as Silverstein, Webster & Kiemle (2005) indicate, it is a defined as a rough ratio between the transmitted energy and the total inflicted energy, as Equation (7) highlights.

$$\text{Transmittance} = \frac{Transmitted\ Energy\ by\ the\ Material}{Total\ Inflicted\ Energy\ to\ the\ Material} \qquad \textbf{(7)}$$

The latter, by its time, is basically defined by a logarithmic function in terms of transmittance. This is properly indicated by Equation (8).

$$A = \log_{10}(\frac{1}{T}) \qquad \textbf{(8)}$$

Where,

A: Absorbance

T: Transmittance

In essence, the ATR method is based on directing the IR beam through a specific crystal – commonly named Internal Reflection Element (IRE) – and provoking a reflectance internally and a evanescent wave or field that invades the sample, which is directly located on its top. The IR beam after traversing the whole crystal and the sample and then is directed to a detector inside the FTIR. Measurements are made based on the attested changes of reflectance (attenuation of the initial value) in the crystal, exactly, caused by the absorption of some energy from IR wave by the sample (at the specific wavelengths it vibrates). Then, an interferogram and, later on, a FTIR spectrum is produced as the final result of analysis. An ATR-FTIR measurement is done by pouring a drop big enough to cover the small crystal or by pressing a certain amount of a solid sample against it. This crystal needs to express a chemical compatibility (i.e. not reacting with the samples at all) and a high refractive index (bigger than the sample).

For the experiments developed throughout this work, a Perkin Elmer ® Spectrum TwoTM spectrometer with a universal ATR (UATR) equipment was utilized. The ATR-FTIR equipment houses a diamond crystal (where samples are placed). The ATR-FTIR is managed by a SpectrumTM IR software version 10.6.1.942. The measurements were carried under a fixed spectral range of 600 – 4000 cm^{-1} with a resolution of 1 cm^{-1}, 8 scans and a single bounce per measurement. Prior to each analysis, performed at room temperature, the proper cleaning (with acetone and isopropanol) was done, followed by a background (blank) measurement to assure it, done by measuring the air and evaluating the shape of the spectrum. For liquid samples no preparation was done, while solid samples were manually milled in a ceramic mortar with a pestle.

In relation to experimental data treatment, the CSV file obtained from the software was exported to a Microsoft Excel ® software and a Kubelka-Munk (K-M) transform was applied, as discussed by Larkin (2011). It is derived from a mathematical model related to diffuse reflectance (scattering) of inhomogeneous materials (*e.g.* powders and papers), as expressed by Equations (IX) and (X), and applied to all data points. After that, the FTIR experimental data set was prepared for further analysis and discussions.

$$R\infty = 1 + \frac{k}{s} - \sqrt{\frac{k}{s} \cdot (2 + \frac{k}{s})} \qquad \textbf{(9)}$$

$$\frac{k}{s} = (1 - R\infty)^2/(2 \cdot R\infty) \quad \textbf{(10)}$$

Where,

$R\infty$: Diffuse reflectance coefficient.

k : Absorption coefficient.

s: Scattering coefficient

$\frac{k}{s}$: Kubelka-Munk transform. Sometimes referred as simply K-M.

5.3.5 FAME Yield

In this work, the accountability of FAME yield was done by an analysis of the FTIR spectra produced, since there are big differences between a vegetable oil spectrum and a transesterification product spectrum.

The FTIR methodology is an attested and widely used method of quantifying the FAME content in a sample, with strong references in the literature. Moreover, there already exist technical standards by ASTM International (2014) and DIN (2014) for FAME determination via FTIR, respectively, the "ASTM D7371-14 – Standard Test Method for Determination of Biodiesel (Fatty Acid Methyl Esters) Content in Diesel Fuel Oil Using Mid Infrared Spectroscopy (FTIR-ATR-PLS Method)", and the " DIN 14078 – Liquid petroleum products – Determination of fatty acid methyl ester (FAME) content in middle distillates – Infrared spectrometry method".

The methodology applied for FAME yield measurement in this work is somewhat different from the two above described in relation to the spectrum range and the procedure utilized. However, the though reference literature is rich in review like the ones from W. B. Zhang (2012); Monteiro et al. (2008), but also researches aiming to propose alternative, cheaper and easier (e.g. in terms of operation and calculations) methodologies to quantify FAME in biodiesel samples. Examples are the works of Torres et al. (2020); Rosset & Perez-Lopez (2019); Cruz et al. (2019); Matwijczuk et al. (2017); Kollar et al. (2017); Rabelo et al. (2015); Natalello, Sasso & Secundo (2013); Aliske et al. (2007); Siatis et al. (2006); Dubé et al. (2004); Knothe (1999).

Presently, notwithstanding Mahamuni & Adewuyi (2009); Soares et al. (2008) cite the existence of a so-called biodiesel "fingerprint" region, respectively, at 1000 – 1300 cm^{-1} (since it is totally nonexistent in fossil diesel) and 900 – 1300 cm^{-1},different parts of a FTIR spectrum can be the chosen one for FAME yield quantification, in many cases discrepant from the band chosen by ASTM or DIN. Siatis et al. (2006) say that the 1060 – 1300 cm^{-1} spectral region is used for FAME percentage measurement and the peak at 1200 cm^{-1} is the most characteristic for FAME since it refers to the methanol added during the transesterification. In the same spectrum range, the author indicates that

the peak near 1170 cm^{-1} is related to C-O stretching vibrations composed of 2 asymmetrical coupled vibrations, C-C(=O)-C and O-C-C, the former being the most important, but both existent in TAG and biodiesel. Furthermore, Siatis et al. (2006) indicate that the peak around 1445 cm^{-1} is supposed to be used for FAME quantification as it is outside of the quantitative region, even though this specific is very characteristic as it indicates the occurrence of CH_3 groups in FAME mixtures.

Mahamuni & Adewuyi (2009) defined two regions in biodiesel FTIR spectrum, segment I from 1425 – 1447 cm^{-1} and segment II from 1188 – 1200 cm^{-1}. These two were utilized for FAME yield calculations with a software. Dubé et al. (2004) quantified FAME conversion using the sole peak of 1378 cm^{-1}, which is attributed to terminal CH_3 groups in TAG, DAG, MAG, FFA and FAME, and to the O-CH_2 groups in glycerol moiety of TAG, DAG and MAG, as also discussed by Colthup, Daly & Wiberley (1990). The authors highlighted that the errors between theoretical and experimental measurements of FAME were small enough to not need a calibration curve for ATR-FTIR. However, a disadvantage of this technique is the lack of capacity for quantifying MAG and DAG individually (when compared to gas chromatography, GC), since they are, structurally, very similar to TG. 1425 – 1447 cm^{-1}: CH_3-asymmetric bending.

Obviously, every section chosen is directly connected to the molecular vibration patterns of each species involved in the analysis. This means mainly FAME molecules, but also glycerol, MAG, DAG and TAG since the transesterification reaction imposes molecular modifications that influence the FTIR spectrum. The most important or mostly discussed in the literature are summarized in Table A9 (see Appendix A).

In this work, the FAME yield quantification was evaluated by using the spectrum range between 1410 cm^{-1} – 1480 cm^{-1}. The calculation methodology was based on the area ratio of a specific peak at 1436 cm^{-1} limited between 1427 – 1441 cm^{-1} – associated directly to TAG conversion to FAME – and the whole area of the IR range. To do this, Gaussian functions, defined by the Equation (XI), were used to fit the sole peak at 1436 cm^{-1} as well as to cover the whole 1410 – 1480 cm^{-1} FTIR spectrum at maximum to obtain a very precise area value when compared to the area calculated using integration techniques (Trapezoid rule) with experimental data existent.

$$f(x) = a \cdot e^{-(x-b)^2/(2c^2)} \qquad \textbf{(11)}$$

Where,

a: Arbitrary value associated to the height of the curve.

b: Arbitrary value associated to the center position of the curve (sometimes represented by μ).

c: Arbitrary value associated to the width of the curve (also named standard deviation, σ).

x: FTIR experimental data point.

Hence, the Gaussian functions need also to be placed in the spectrum in a way to reflect the variations of the spectrum, which means its peaks and valleys. This process is graphically presented in Figure 19.

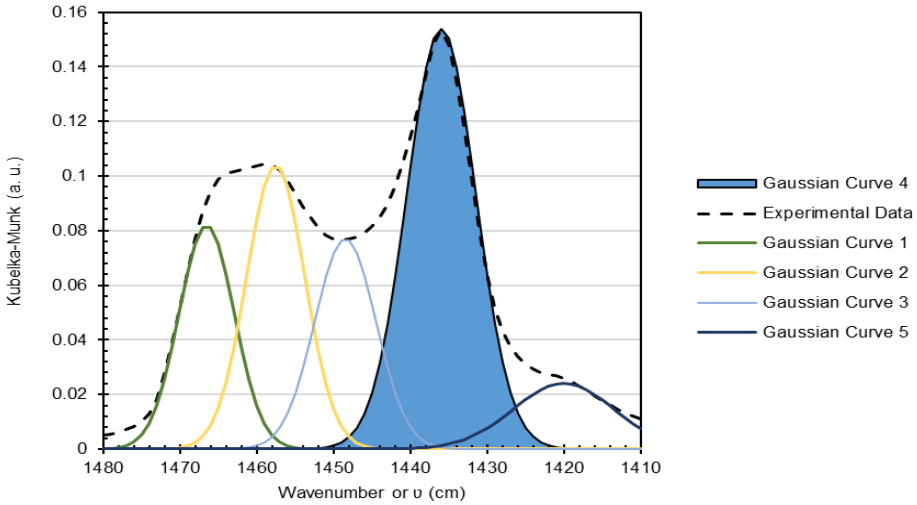

Figure 19 – Exemplification of FAME yield area calculation using Gaussian functions

Finally, the obtain the FAME yield result, the Equation (XII) was used, which is a line equation holding parameters obtained from a calibration curve for biodiesel FAME yield previously done by Catarino et al. (2020); Rosset & Perez-Lopez (2019); Soares Dias et al. (2019) using biodiesel patterns in different ratios (0 % up to 100 %) for FTIR and CG FAME yield measurements.

$$FAME\ Yield\ (\%) = AR \cdot x + B \qquad \textbf{(12)}$$

Where,

FAME Yield: Biodiesel FAME yield in the sample.

AR: Area ratio of 1436 cm^{-1} peak and 1410 – 1480 cm^{-1} spectrum predicted area.

x: Line equation angular coefficient derived from calibration curve (x ≈ 381.71).

B: Line equation linear coefficient derived from calibration curve (B ≈ -54.84).

6. RESULTS AND DISCUSSION

The data collected for this work is presented in separated sections, specifically, focused on the raw materials, the catalysts (pre and post transesterification), and biodiesel and glycerin characterizations. Among each section, proper discussion and argumentation is presented as to sustain the affirmations and support the experimental data collected.

6.1 Raw Materials Characterization

Throughout this work several raw materials were utilized and are, as follows, evaluated by certain characterization techniques.

6.1.1 Fly Ash

The two main raw materials utilized in the catalyst methodology proposed in this work are fly ash and chicken egg shells. The first material, according to the work of Policht-Latawiec (2013) done with FA from the same powerplant as this work and presented in Table 4, indicates that it is classified as fly ash class F (see section 4.2.1).

Table 4 – Skawina powerplant fly ash chemical composition (% wt.)

SiO_2	Al_2O_3	Fe_2O_3	CaO	MgO	K_2O
56.30 %	24.10 %	7.10 %	3.17 %	2.31 %	2.52 %

Source: Policht-Latawiec (2013)

Figures 20 and 21 present, respectively, a XRD diffractogram and a FTIR of a FA in natura (also referred in this work as raw fly ash) and a FA after the acid-leaching process with HCl 3M. In Figure 20 it is possible to observe that the XRD diffractogram is very similar to what it is expected from a typical coal fly ash sample, even with the natural variability of its major components.

When the standards for quartz, mullite, hematite and calcite (highlighted in the same figure) obtained from Lafuente et al. (2016) are compared with the sample data, it is possible to evidence the presence of these components. Furthermore, comparing the present XRD experimental data and the chart with the works of Asl et al. (2018); Kruse et al. (2012); Jain, Khatri & Rani (2011); Petkowicz et al. (2008); Ismail, Hussin & Idris (2007), a clear similarity between all the FA samples can be to observed.

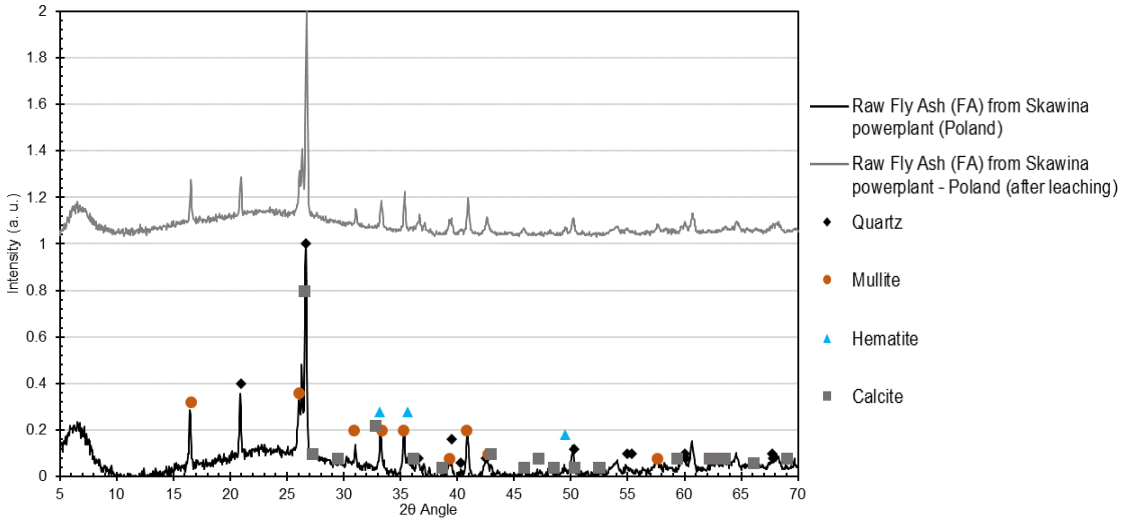

Figure 20 – Raw fly ash XRD diffractogram.

The FTIR chart presented in Figure 26 shows the raw FA and highlights certain standard materials – quartz, hematite (PDF 33-664), calcite (PDF 5-586) and brucite (PDF 7-239) – obtained from Lafuente et al. (2016). Associating this analysis with FTIR molecular vibrational patterns for silicon bonds (Si-O) present in quartz (SiO_2) it is possible to attest that this material is present in the studied FA sample.

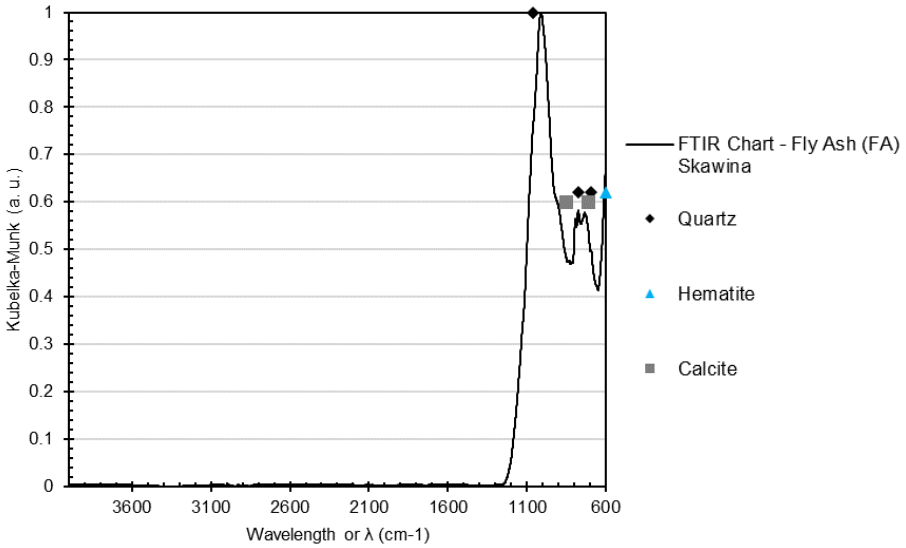

Figure 21 – Raw fly ash FTIR chart

Strong FTIR peaks for Si-O bonds, discussed by Silverstein, Webster & Kiemle (2005), are expected in the range of 830 – 1110 cm^{-1} (asymmetric stretching vibration). Furthermore, according to W. K. W. Lee & Van Deventer (2002), Si-O bond at 882 cm^{-1}, Si-O-Si bond at 798 cm^{-1} (symmetric stretching) and Si-O-Si/ Al-O-Si bonds at 727 cm^{-1} (symmetric stretching). Similar patterns for FA can be found in FTIR spectrum from Asl et al. (2018); R. Kumar, Kumar & Mehrotra (2007).

Following the FTIR analysis, Figure 22 presents the spectrum differences between raw FA pre and post acid-leaching process with HCl. It is visible that the FA maintain its essential structure and composition, which suggests that the acidic attack only promoted the leaching of species, such as Fe, Al, Ca, Mg and K as chloride salts.

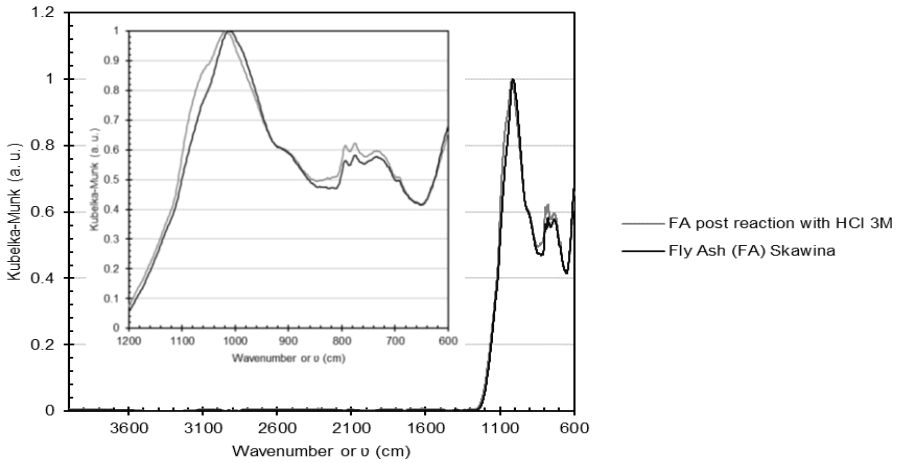

Figure 22 – Raw and post acid leaching process fly ash FTIR data. Note: The inset chart highlights the range 600 – 1200 cm^{-1}

To support this analysis, the SEM images for raw FA, before and after leaching, are presented in Figure 23. It is possible to observe that the superficial aspect of FA does not change much after the acid leaching process, the present spherical structures suggest. Focusing on the spherical particles, it is possible to observe a slight difference in terms of superficial aspect since the FA in natura presents, in general, very clean and plain spherical particles, while the acid-leached FA started to present mild changes in these spheres.

There exist several examples presenting less spherical shapes (see arrow in Figure 28) with flat regions and even deeper holes (or the beginning of their formation). This specific aspect is not ubiquitous in the sample, which means that there still exist preserved spherical particles, such as those found in FA in natura, and the reason for that of the conditions of acid treatment (the acid and the short reactional time) were not enough to remove chemical elements from the entire material. Another interesting aspect to highlight and perhaps the most discrepant aspect between the two images is the presence of more voids in between the particles in the leached FA in comparison to the FA in natura.

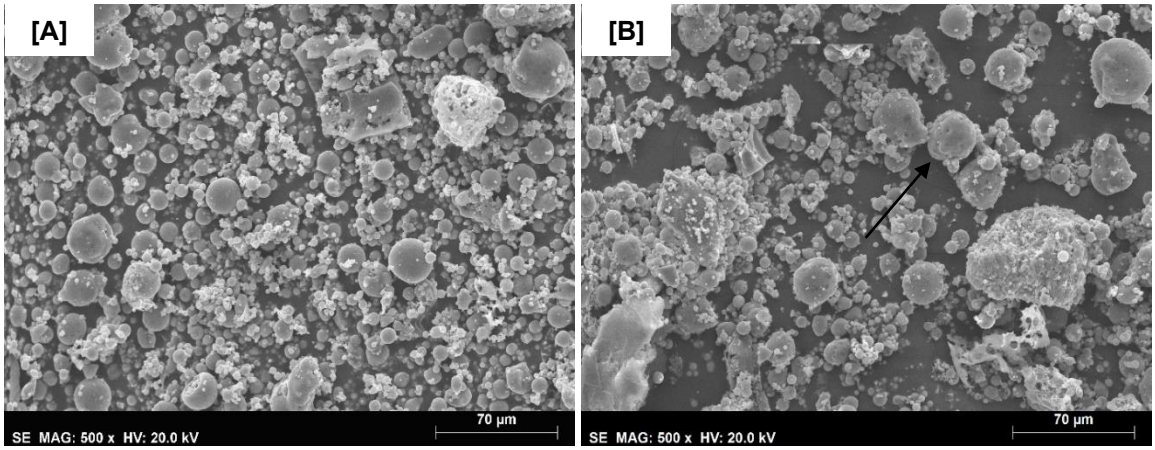

Figure 23 – SEM images of Raw FA [A] *in natura* and [B] after acid leaching

6.1.2 Chicken Egg Shells

The other raw material utilized in this work was chicken egg shells. Figure 24 presents a FTIR of $CaCO_3$ in natura and Figure 26 a FTIR of $CaCO_3$ calcined at 800 °C and 900 °C, becoming CaO . For $CaCO_3$, according to Lafuente et al. (2016); Rodriguez-Blanco, Shaw & Benning (2011) the peaks between 1100 – 1600 cm^{-1} and 873 cm^{-1} refer to asymmetric vibration of CO_3^{2-} species, and at 1805 cm^{-1}, 1090 cm^{-1} and 725 cm^{-1} to symmetric vibrations of CO_3^{2-}.

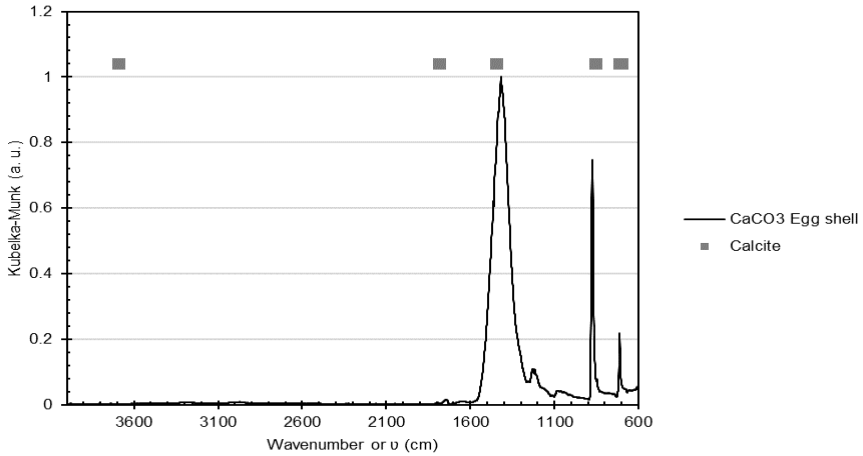

Figure 24 – FTIR spectrum of chicken egg shell *in natura*

The SEM image for $CaCO_3$ presented in Figure 25 shows the general aspect for a such material. The visible shape can be associated with a grained rock-like solid material, such as calcium carbonate. The particles are not uniform which may be the effect of the hand milling procedure which is not perfect.

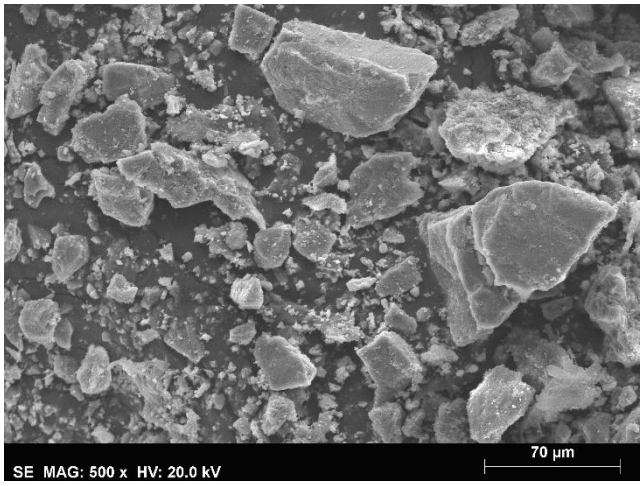

Figure 25 – SEM image of chicken egg shell *in natura*

The FTIR most relevant peaks, according to the literature and the works of Pandey & Sengupta (2014); Nasrazadani & Eureste (2008); Arnold, Rozario-Ranasinghe & Youtcheff (2006); Zaki et al. (2006) for lime are the one around 3608 – 3630 cm^{-1} (range usually between 3584 – 3700 cm^{-1}) which is related to free hydroxyl (OH) species adsorbed in lime's surface (i.e. hydrated lime), and others around 1399 – 1406 cm^{-1} and 873 cm^{-1}, which are associated to the remnants of uncalcined calcium carbonate (see Figure 24 for $CaCO_3$ FTIR standard peaks).

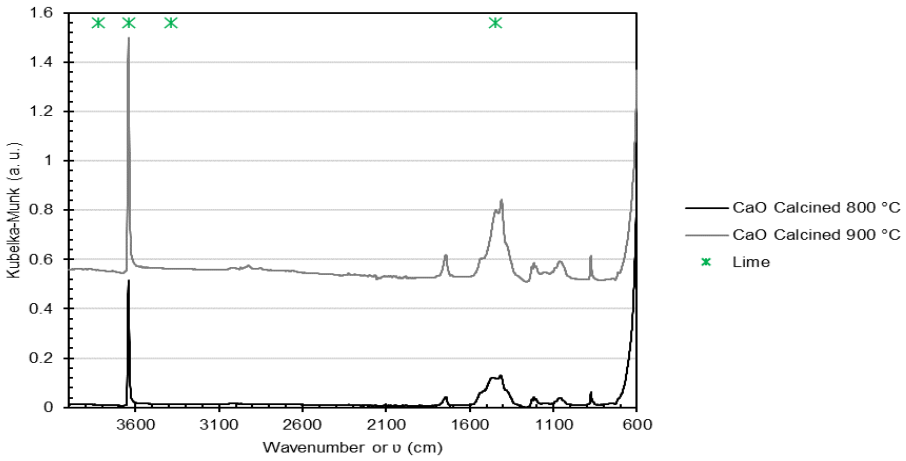

Figure 26 – FTIR spectra of CaO calcined at 800 °C and 900 °C

It is important to mention that the peak related to free hydroxyl species has a specific shape, strong and sharp, which distinguish it from the one related to bonded hydroxyl species existent in several materials. The latter is characterized, according to Silverstein, Webster & Kiemle (2005), as being strong and broad, covering a lower spectrum range, between 3200 – 3550 cm^{-1}.

Comparing Figures 24 and 26, it is possible to derive that the majority of $CaCO_3$ was successfully converted to CaO since the most prominent peak of $CaCO_3$, between 1100 – 1600 cm^{-1}, was drastically reduced as CaO was being formed. Also, the peak associated to free hydroxyl species in CaO appeared strongly in a spectrum's region without vibrations for $CaCO_3$. Finally, it is interesting

to discuss the shape of the hydroxyl peak, since, in terms of the two calcination temperatures for $CaCO_3$, it is clear that at 900 °C there was a more complete degradation of $CaCO_3$ when compared to 800 °C. Hence, this means the content of CaO is higher and thus the purity is somewhat higher. This, definitely, can influence in the following experiments in this work, since, as already discussed, CaO is an active alkaline heterogeneous catalyst for biodiesel transesterification.

The SEM image for calcined $CaCO_3$ at two temperatures, 800 °C and 900 °C, are shown in Figure 27. The two catalysts in terms of particle aspects and size seem to be similar. This indicates that the temperature change from 800 °C to 900 °C does not impact very much the catalyst superficial characteristics.

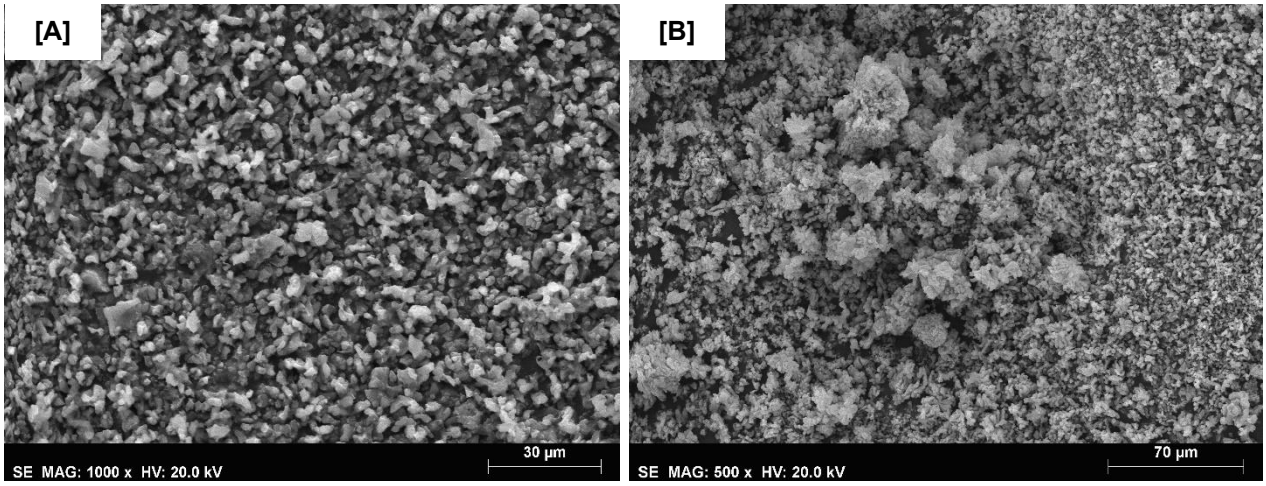

Figure 27 – SEM images of CaO calcined at [A] 800 °C and [B] 900 °C

6.1.3 Vegetable Oils

As explained in the previous chapter, two oleaginous raw materials were used in this work, a mixture of soybean and sunflower oils, and waste frying oil. Both materials were characterized in terms of FTIR and acidity.

Figure 28 presents an entire FTIR spectrum for both materials and, recalling the remarks in terms of TAG and FAME reference molecular vibrations summarized in Table A9 (see also section 5.4.10), it is possible to segment the a FTIR spectrum in at least four (4) areas of interest, as indicated in the figure.

A more detailed focus on the same chart, as presented in Figure 28, highlights the $-CH_3$ (from methanol) and TAG, DAG and MAG (C-O) segments, both of much importance for the further discussions in terms of Fame yield. The former is the FTIR range selected for FAME quantification in this work, while the latter refers to unreacted vegetable oil and partially transesterified TAG molecules (*i.e.* DAG and MAG).

It is possible to observe small differences between the two vegetable oils, mainly related to the water content in WFO, based on the wide band between 3100 and 3600 cm^{-1}. Also, there is a relevant variation between the soybean and the WFO in the range between 1000 – 1070 cm^{-1}, which is, according to Silverstein, Webster & Kiemle (2005), associated to C-O stretching vibrations in alcohols and can be connected to the presence of MAGs and DAGs molecules. They, in WFOs, can appear, for example, in consequence of TAG molecular degradations.

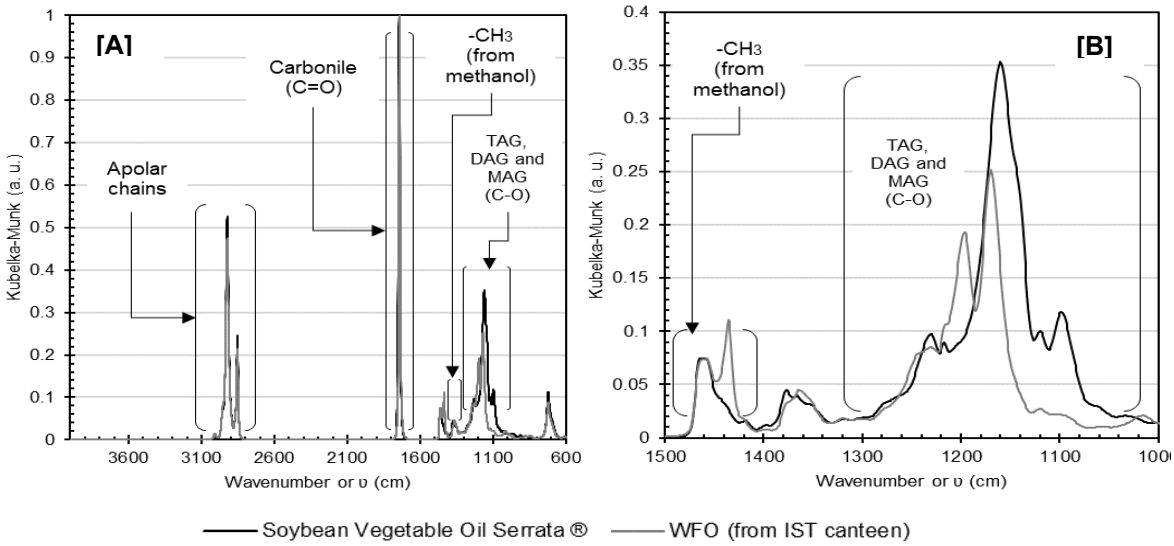

Figure 28 – Full [A] and detailed [B] soybean and WFO oils

Acidity index measurement was carried out for the two oleaginous materials to verify the level of FFA present in each, as well as to evaluate the possible occurrence of soap formation or emulsions during the transesterification. The obtained results for acidity in soybean-sunflower and WFO oils are presented in Table 5 as an average of the all 4 data. For all the analysis, it was considered a correction factor for the NaOH solutions of 0.99.

Table 5 – Acidity index of the oleaginous raw materials

	Soybean-Sunflower oil				WFO			
Acidity (mg KOH/ g)	0.09	0.09	0.09	0.09	1.22	1.32	1.22	1.27
IA (average)	0.09				1.24			

6.2 Fly Ash-Egg Shells (FAES) Catalysts

Following the established experimental procedures, the 8 synthetized FAES catalysts were characterized by XRD and FTIR both in natura and calcined at 800 °C for 3 hours (only FAES N° 1 and CaO were calcined also at 900 °C). Detailed data for each sample and the mineral species identified are summarized in Table 6.

Table 6 – Mineral species identified via XRD for FAES catalysts

	Andradite	Brownmillerite	Calcite	Gehlenite	Lime	Mayenite	Mullite	Periclase	Quartz	Wadalite
FAES N° 1	X		X	X	X		X	X	X	
FAES N° 2	X		X	X	X	X				X
FAES N° 3		X			X	X				
FAES N° 4		X			X					
FAES N° 5		X			X					
FAES N° 6	X	X			X	X		X		X
FAES N° 7	X	X			X	X		X		X
FAES N° 8	X				X	X	X	X	X	X

Figure 29 presents a XRD diffractogram for all the catalysts as synthesized (i.e. in natura). A more detailed perspective for each spectrum separately can be found in Appendix A.

It is possible to observe there exist interesting differences between all the studied catalysts, even more apparent when compared with the raw FA and the $CaCO_3$. The FA original structure for FAES N° 1 catalyst, which is based on using this material directly, is not present in the XRD anymore. Species of mullite (peaks ca. 16°, 33°, 35° and 41°), hematite (ca. 33° and 50°) and quartz (ca. 21°, 27°, 50° and 61°) appear only as very weak reflections.

Contrastingly, these peaks are still present in FAES N° 8, even though the preparation of this sample was very similar to that of FAES N° 1, as both used the raw FA directly instead of using the acid leachates (as all the others). One of the major differences between these catalysts was that $CaCO_3$ in natura (without being acid leached previously) was added directly to the synthesis in FAES N° 1, while only its leachate was used for FAES N° 8. The standard reflections for $CaCO_3$ are visible in the diffractogram of FAES N° 1, which could influence the performance of the material in transesterification (as $CaCO_3$ is a precursor of CaO).

The FAES N° 8 XRD pattern is quite similar to that of raw FA, which suggests there was not much structural change nor formation of new species, possibly due to the lack of sufficient ions to favor nucleation and precipitation of other species of interest (as happened in case of the other FAES catalysts).

As concerns the $CaCO_3$ presence in the catalysts (since $CaCO_3$ acidic leachate and/ or $Ca(OH)_2$ are part of the synthesis methodology), a reflection of high intensity *ca*. 29° and two others of lower intensity *ca*. 47° and 48° are present for the FAES catalysts and the $CaCO_3$. They are related to carbonate species in the materials, in good agreement with Lafuente et al. (2016).

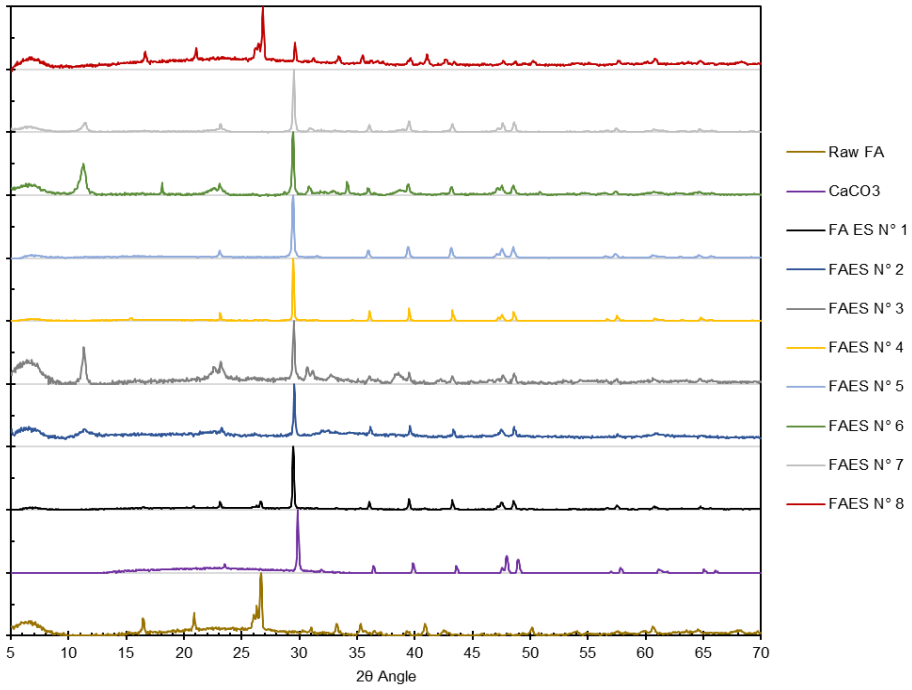

Figure 29 – XRD diffractograms for all the as synthesized FAES catalysts

Figure 30 depicts a XRD patterns for all FAES calcined catalysts. A more detailed perspective for each diffractogram separately can be found in Appendix A.

For all the catalysts there are some similarities. The $CaCO_3$ reflections at *ca*. 29°, 47° and 48°, clearly identified in the raw catalysts, almost completely disappeared (in samples FAES N° 2, 3, 4 and 5, the one *ca*. 29° is not existent at all), confirming the conversion to lime. Moreover, other group of reflections, directly associated to a lime XRD standard, as mentioned by Kumpala, Horpibulsuk & Suebsuk (2012); Mäkelä et al. (2011), *ca*. 18°, 33°, 38°, 47°, 54°, 62°, 64° and 67° are easily identifiable.

The reflection at *ca*. 38° is one of the strongest. When comparing these peaks with the spectrum of CaO calcined at 800 °C and 900 °C, it is observable the increase in reflections associated to the increase of temperature. Furthermore, for the CaO calcined at 800 °C XRD patterns still show the presence of characteristic reflections for $CaCO_3$ at *ca*. 29° and 47°. Both are better reduced for the CaO calcined at 900 °C.

Comparing the FAES N° 1 catalysts calcined at different temperatures, a difference in the intensity of the reflections of CaO can be seen. In the one calcined at 800 °C, they are much stronger (*e.g*. those at *ca*. 18°, 29°, 33°, 34° and 54°). The reflection at *ca*. 18° almost disappeared in FAES N° 1 calcined at 900 °C as compared to the same catalyst at 800 °C, similarly as the reflections at 33°, 34°, 37° and 54°. Furthermore, it is also possible to identify remnants from the raw materials utilized to synthesize the FAES N° 1 catalysts (*i.e.* the raw FA), since at *ca*. 26°, 27°, 39° and 40° reflections related to mullite and quartz appear. However, for FAES N° 1 calcined at 900 °C, they are much smaller.

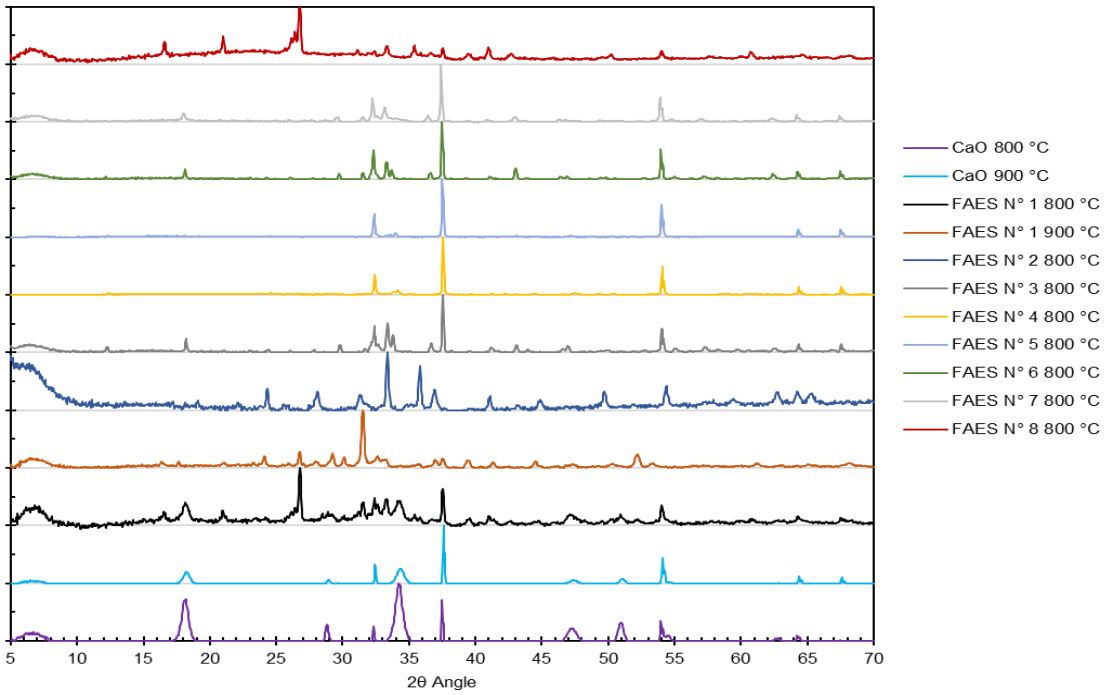

Figure 30 – XRD diffractogram for all the calcined FAES catalysts

Beyond that, there exists more species between 30° and 35° degrees in FAES N° 1 calcined at 800 °C rather than at 900 °C. This less complex region for the latter contains one reflection of high intensity at *ca*. 32°, associated to gehlenite (PDF 35-755), while, for the former catalyst, it is of much lower intensity. Other reference reflections for gehlenite, as presented by Lafuente et al. (2016), can be found at *ca*. 16°, 17°, 21°, 24°, 29°, 37°, 38°, 39°, 44°, 52° and 68°, all of them with a relatively low intensity.

The FAES N° 1 calcined at 800 °C presents a strong reflection at *ca*. 36°, which is directly associated to the presence of periclase (MgO), according to XRD reference PDF 45-0946 and (Gates-Rector & Blanton (2019). Another reflection for periclase can be noted in the structure of FAES N° 1calcined at 800 °C *ca*. 43° but with a very small intensity. Both reflections are still present in FAES N° 1 calcined at 900 °C, but of much lower intensity. The occurrence of MgO species in the catalysts is interesting since raw FA contains Mg (SEM-EDS measurements) it is recognized as a material capable of promoting basic catalysis transesterification, as evidenced by Boey, Maniam & Hamid (2009).

Furthermore, MgO is an oxide that can be also found in calcined LDH materials, which could be an alternative for biodiesel transesterification due to the formation of mixed oxides, rich in basic sites, as discussed by Othman et al. (2009); Tichit et al. (2006); Dutta, Auerbach & Carrado (2004); Tichit & Coq (2003).

The FAES N° 2, similarly as the other catalysts, shows reflections characteristic of lime, however, not in the same amount. In fact, it only has it *ca*. 54° and *ca*. 63° and 64°, all of which are of good intensity. An important peak for lime *ca*. 32° is almost undetectable in the XRD diffractogram but still existent. The strong reflection at *ca*. 36° is connected to the formation of wadalite ($Ca_6Al_5Si_2O_{16}Cl_3$,

PDF 81-1135), andradite ($Ca_2(Fe^{3+})_2(SiO_4)_3$, PDF 10-288) and mayenite ($Ca_{12}Al_{14}O_{33}$, PDF 9-413). Other reflections confirm the existence of wadalite at *ca*. 27°, 57°, 62° and 63°, even though in very low intensity. For andradite, reflections are identified at *ca*. 33° (the most intense one), 41°, 54° (should be present in the same positions as lime) and 55° (the second most intense). Lastly, for mayenite, the peaks *ca*. 18°, 27°, 41°, 55° and 57°, also with low intensities. For FAES N° 2, only the reflections at *ca*. 27° and 41° for wadalite and mayenite show a good intensity. Gehlenite could also be found as evidenced by reflections at *ca*. 24°, 37° and 44°, all of them with a relatively low intensity.

The phase composition of the FAES N° 3 FAES N° 4 and N° 5 is similar, however, it holds a more complex segment in the range between 29° and 37°, 40° and 50°, and 55° and 64°. This turns it more closely related to FAES N° 6 and N° 7. Lime is evidenced by the reflections at *ca*. 32°, 37°, 63° (even very small ones), 64° and 67°, all of them also identified in CaO and other catalysts (FAES N° 1, N° 4, N° 5, N° 6 and N° 7 calcined at 800 °C). Additionally, the presence of brownmillerite ($Ca_2(Al,Fe^{3+})_2O_5$, PDF 30-226) – an oxide of iron, calcium and aluminum, as stated by Anthony et al. (2003); "Mindat," (n.d.) – is confirmed by the reflections at *ca*. 12°, 23°, 24°, 26°, 32°, 33°, 37°, 44°, 47° and 50° according to standard XRD data of Lafuente et al. (2016), though in very low intensities. Mayenite in FAES N° 3 is easier to identify due to more intense reflections at *ca*. 18°, 28°, 30°, 33°, 35°, 37°, 41°, 47°, 55°, 57°, 61°, 62°, 63°, 67° and 69°.

The catalysts FAES N° 4 and N° 5 calcined at 800 °C have almost identical XRD diffractograms with very strong reflections of CaO at *ca*. 33°, 38°, 54°, 64° and 67°. Additionally according to the XRD data, there are also small amounts of brownmillerite. This material, according to Lafuente et al. (2016), shows XRD reflections at 12°, 33° (most intense), 23°, 24°, 25°, 30°, 34°, 36°, 44°, 47°, 51°, 59°, 60°, 61°, 62°, 63°, 67° and 69.

This resemblance of these two specific catalysts can be associated to the synthesis methodology itself, as in these cases both the FSS and the SSS were used. The only difference was the pH of alkaline solution and the crystallization duration (respectively, 6 hours and 168 hours). The similarity of XRD patterns suggests that crystallization time did not have high influence on the phase composition.

Also, it may suggest that the acid-leached species from FA did not participate in relevant amounts since only brownmillerite appeared. Thus, the sole presence of ionic species in the medium is not enough to promote the precipitation of different compounds, which means that the right choice of an alkaline solution and the crystallization and aging steps have more impact on the final catalyst synthesized.

Brownmillerite is a mixed metal oxide composed in majority of Al_2O_3, Fe_2O_3 and CaO but can be associated with titanium oxide (TiO_2) and chromium oxide (CrO_2), according to Lafuente et al. (2016); Anthony et al. (2003). It belongs to a group of perovskites and, as part of a catalyst, it possibly can influence positively the transesterification of oils, similar to periclase and to what discussed Lima-

Corrêa, Castro & Assaf (2018); Bennett, Wilson & Lee (2016); Wilson & Lee (2012); Fraile et al. (2010); Martino Di Serio et al. (2008).

The crystalline structure of FAES N° 6 and N° 7 is quite similar. It is mostly composed of lime, mayenite, brownmillerite, wadalite and andradite, with traces of periclase. This can be seen clearly in XRD diffractograms (see Appendix A). Only one more reflection, that associated to brownmillerite at *ca*. 33º, is not present in FAES N° 7in contrast to FAES N° 6.

Lime was identified by the same reflections as for the other catalysts (*ca*. 33°, 37°, 54°, 64° and 67°), as well as mayenite (18°, 28°, 30°, 33°, 36°, 41°, 47°, 55°, 57° and 67°). Brownmillerite (12°, 23°, 24°, 26°, 32°, 33°, 44°, 47° and 50°), wadalite (28°, 30°, 33°, 37, 38°, 53°, 54°, 55°, 57°, 62° and 63°), andradite (21°, 29°, 33°, 35°, 37°, 38°, 41°, 47°, 53°, 54°, 55°, 57° and 62°. Periclase was also registered, though in small amounts (43° and 62°).

XRD patterns of the FAES N° 8 calcined at 800 °C, as consequence of having raw FA in its synthesis, show several reflections associated with mullite (at *ca*. 12°, 25°, 30°, 33°, 39°, 41°, 43° and 57°) and quartz (at *ca*. 21°, 27°, 37°, 40°, 50°, 60° and 68°). Since CaO was also used in the synthesis, it is evidenced by certain reflections but not as many and as strong as for the other catalysts. They can be found mainly at *ca*. 33° (almost undetectable), 37°, 54° and 64°. Besides these compounds, wadalite, mayenite and andradite were also identified by weak reflections at *ca*. 34°, 37°, 41°, 57° and 62° (see the diffractogram in Appendix B). Also, periclase is evidenced by a relatively strong reflection at *ca*. 43°. Brownmillerite is not present in the material (at least in relevant amounts) since there is no reflections with an intensity similar to the other catalysts were registered at *ca*. 12°, 23°, 58° and 59°. This fact can be associated directly with the single difference between the synthesis procedure utilized for FAES N° 8 and for FAES N° 6 and N° 7, which is the direct use of FA, instead of only the acid-leached solution (FSS).

Therefore it may be concluded that the presence of cations in solution is favorable to promote the precipitation and growth of the compounds, such as wadalite, brownmillerite, andradite, mayenite and periclase in considerable quantities (as in FAES N° 6 and N° 7). Furthermore, with respect to the CaO reflections, present but with lower intensity (according to what it is expected for the standard XRDs), the SSS with calcium nitrates derived from chicken egg shells and the $Ca(OH)_2$ did not contribute enough to favor the formation of CaO as happened in case of FAES N° 3, N° 4, N° 5 N° 6 or N° 7.

All the catalysts developed in this work, as the proposed methodology indicates, do not have a strict control of stoichiometry to promote a foreseeable precipitation of minerals. This is mostly caused by the choice made to use only residues as raw materials in contrast to analytical grade chemicals. Specifically, a good example of the lack of stoichiometric control is the acid leaching of FA, which extract different species in different amounts in every batch (even though always done under the same reactional conditions). Hence, a direct consequence of this unbalance in terms of stoichiometry is evidenced in the precipitated compounds identified by XRD.

The studied catalysts preparation procedures had specific variations (e.g. pH, crystallization time and alkaline species added) though the main elements of synthesis methodology was kept fixed. This was done in order to find out if possible variations in precipitated species and the quality of the material influenced transesterification. The different catalysts have specific variations (e.g. pH, crystallization time and alkaline species added) in terms of their synthesis methodology even though the main core was kept fixed. This was done as to evidence possible variations in precipitated species and the quality of the material for transesterification, since the simpler and cheaper the whole process the better to save costs and materials. In relation to this, it should be stated that FAES N° 6 and FEAS N° 7 as strictly equal and, based on the XRD diffractograms of both, it is perceivable that the methodology is repeatable and presents very similar results.

It should be stated that FAES N° 6 and FAES N° 7 as strictly equal and, based on the XRD diffractograms of both, it is perceivable that the methodology is repeatable and presents very similar results. This fact is important since the catalyst produced needs to be continuously reproduced and with the same result all the time. Obviously, considering the nature of the chosen raw materials, slight differences can and, in reality, are expected to occur, as the two XRD patterns indicate. However, it should be stressed that, the exact same species are produced in both, which guarantees that the methodology can result in a material with the same characteristics as FAES N° 6 and N° 7. Figure 31 presents the FTIR spectra for all the as synthesized FAES catalysts. Evaluating the spectra it is possible to observe that all the FAES catalysts have a very similar structure as compared to the calcium carbonate, with a slight difference in the range between 900 – 1200 cm^{-1}. The other regions, specifically between 1100 – 1600 cm^{-1} and the very narrow and intense peak at 873 cm^{-1} refer to the asymmetric vibration of CO_3 species, as cited by Lafuente et al. (2016); Rodriguez-Blanco, Shaw & Benning (2011). The other peaks commonly observed in $CaCO_3$ related to the symmetric vibrations of CO_3 – at 725 cm^{-1}, 1090 cm^{-1} and 1805 cm^{-1} (very low intensity) – are not present in any of the catalysts, solely the first one.

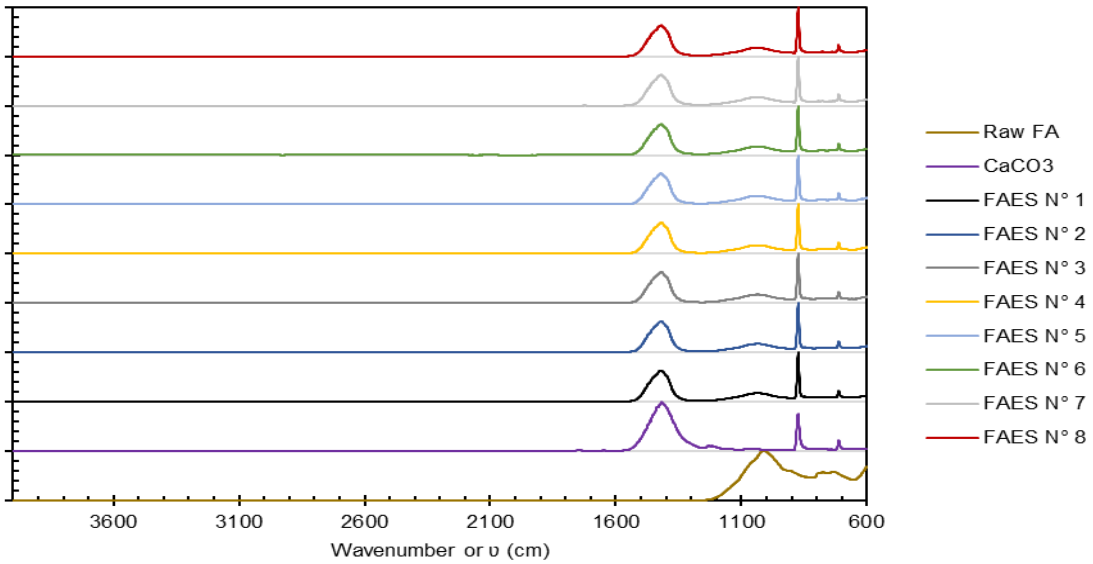

Figure 31 – FTIR spectra for all the as synthesized FAES catalysts

Comparing the raw FA FTIR spectrum with the synthesized catalysts, it is evidenced that different molecular bonds and interrelations were stablished for all, even for those that had in its preparation the direct use of FA instead of the acid-leached solution (FSS), like FAES N° 1 and FAES N° 8.

The Figure 32 presents all the FAES calcined catalysts, together with CaO, and raw FA and $CaCO_3$ as to favor the comparison in terms of changes among the materials. All that combined with the remarks already exposed.

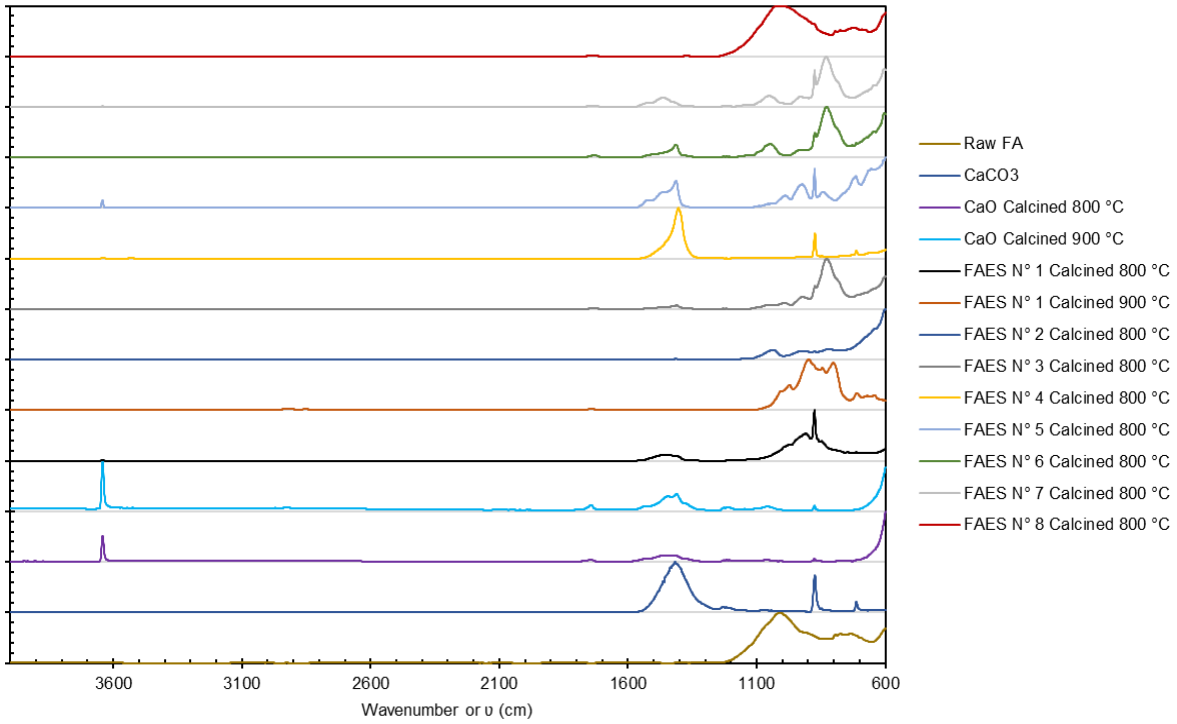

Figure 32 – FTIR of all FAES calcined catalysts

To support the discussion related to the FAES catalysts, the SEM-EDS images for all the calcined FAES catalysts are presented in Figure 33.

It is interesting to observe the superficial variation among the different synthesized catalysts, which are very connected to the precipitated species (e.g. lime, mayenite, brownmillerite, wadalite, andradite and periclase) based on the applied methodology variations. For instance, images for FAES N° 1/ 800 °C and FAES N° 1/ 900 °C clearly show that presence of the characteristic sphere-like particles of raw FA among the lime particles, which does not have a uniform aspect. This can be verified by the quartz peaks in the XRD diffractograms. Furthermore, it is interesting to see that some spherical particles are supported with lime particles on the surface, giving an aspect of small white-like dots around the darker FA particle.

For FAES N° 2, the superficial aspect of the particles are the most discrepant in relation to all the other catalysts since it has a more rock-like shaped particles among some smaller ones with an

agglomerated aspect, which are characteristic of calcite and lime. Besides, species like gehlenite, calcite, lime, mayenite and andradite are also existent. FAES N° 3, 4 and 5, according to their XRD data, have very similar structures, even though the N° 3 contains, besides CaO like the other FAES samples, brownmillerite and mayenite. The particles hold an agglomerated characteristic and a nonuniform aspect, as well as several regions containing lime aleatory mixed and combined with the other minerals.

Obviously, this is expected since the methodology allowed and stimulated a random formation of minerals, without much stoichiometric control in terms of ions or chemical elements. FAES N° 4 and N° 5, as already mentioned, are very similar in terms of mineral species present, mainly lime, even though their particles are slightly different in terms of particles, as for the former it is more agglomerated and bigger, while for the latter it is smaller and more spread, very much similar to a pure CaO catalyst (see Figure 26 for further analysis and comparisons).

It is interesting to observe the superficial variation among the different synthesized catalysts, which are very connected to the precipitated species (e.g. lime, mayenite, brownmillerite, wadalite, andradite and periclase) based on the applied methodology variations. For instance, images for FAES N° 1/ 800 °C and FAES N° 1/ 900 °C clearly show that some spherical particles are covered with lime particles on their surface. This is in agreement with XRD patterns showing quartz reflections. Furthermore, it is interesting to see that lime particles are supported on some spherical particles , visible as small whitish dots around the darker FA particle.

The FAES N° 2 sample differs the most from all the other catalysts since it has a more rock-shaped particles among some smaller ones (seeming to be agglomerated), which are characteristic of calcite and lime. Besides, species like gehlenite, calcite, lime, mayenite and andradite are also present. FAES N° 3, 4 and 5, according to their XRD data, have very similar structures, even though the N° 3 contains, besides CaO like the other FAES samples, also brownmillerite and mayenite. The particles are agglomerated and nonuniform, as well as several regions containing lime mixed and combined with other minerals.

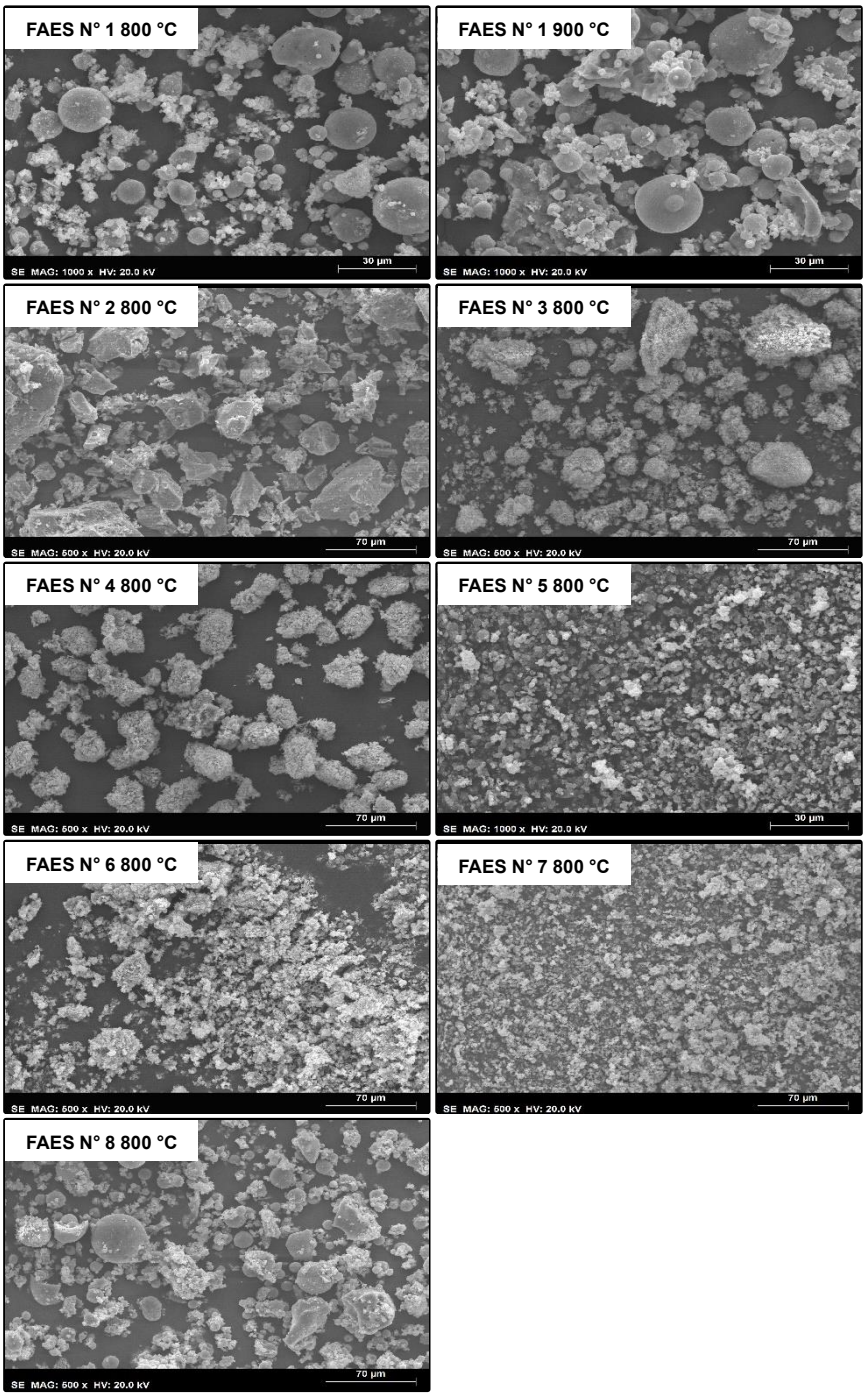

Figure 33 – SEM images for all the calcined FAES catalysts

This suggests that the used methodology allowed and stimulated a random formation of minerals, without much stoichiometric control in terms of ions or chemical elements. FAES N° 4 and N° 5 are quite similar where mineral species present, mainly lime, are concerned, though their particles are slightly different for the former the particles are more agglomerated and bigger, while for the latter they are smaller and more spread, similar to a pure CaO catalyst (see Figure 26).

FAES N° 6 and N° 7 had quite similar XRD diffractograms. From SEM images it can be seen that they have similar particles with agglomerated and nonuniform shape, showing sections of lime

among the other minerals. This variability can be of some impact in FAME conversion for biodiesel and will be further discussed. Lastly, SEM of FAES N° 8, which was produced using acid-leached FA, not only its leachate, presents sphere-like particles among other with an agglomerated and nonuniform shape, characteristic for lime and other minerals, such as wadalite, mayenite and andradite.

Another valuable information obtained from SEM analysis is the EDS, which can determine the chemical elements existent in the catalysts. This information is important as to confirm the formation of several of the minerals identified by XRD and FTIR. The respective data is summarized in Table 7.

It is possible to observe several aspects related to the raw materials (*i.e.* raw fly ash chicken egg shells) and the synthesized catalysts in terms of surface chemical composition. FA *in natura* and acid-leached FA show that rests of carbon were removed, similarly as calcium and iron, as an effect of HCl acid attack (additionally confirmed by the presence of chlorine in acid-leached FA structure). This process of leaching certain elements is attested by the ubiquitous presence of Fe in all FAES catalysts, carbon in FAES N° 3 to N° 7 and relevant amounts of Ca in FAES catalysts.

Table 7 – EDS chemical element content (%) data

	Raw FA	FA$^{\Delta}$	$CaCO_3$	CaO *	CaO †	FAES N° 1*	FAES N° 1†	FAES N° 2*	FAES N° 3*	FAES N° 4*	FAES N° 5*	FAES N° 6*	FAES N° 7*	FAES N° 8*
O	37.69	42.08	33.31	31.37	37.79	32.93	37.04	36.50	44.49	50.29	45.30	46.59	41.47	34.54
C	16.71	–	4.96	–	–	–	–	5.36	10.41	7.00	23.09	16.98	17.22	–
Si	14.38	27.70	–	–	–	21.16	25.01	3.46	1.51	1.04	0.68	0.51	0.34	36.85
Al	11.81	20.47	–	–	–	17.56	14.69	14.10	4.39	3.24	0.46	2.81	1.28	8.26
Mg	0.84	0.90	–	–	0.79	1.94	1.50	3.40	2.95	1.03	1.04	3.58	1.68	1.45
Fe	8.05	1.89	–	–	–	2.69	2.55	24.09	6.95	8.99	2.40	3.63	1.78	10.32
Ca	3.93	–	60.18	25.29	61.42	18.19	6.84	9.25	26.98	26.71	27.03	24.47	35.32	2.95
K	3.51	3.64	0.73	–	–	1.60	8.92	–	–	–	–	–	–	3.79
Na	1.20	0.90	–	–	–	1.86	1.97	–	–	–	–	–	–	–
Ti	1.89	1.23	–	–	–	0.98	1.48	0.68	–	0.43	–	–	–	1.83
Cl	–	1.18	–	–	–	–	–	–	1.31	0.12	–	1.43	0.91	–
P	–	–	0.81	–	–	1.09	–	2.80	0.99	0.65	–	–	–	–
Mn	–	–	–	–	–	–	–	0.36	–	–	–	–	–	–
Total	100	100	100	100	100	100	100	100	100	100	100	100	100	100

Remarks:

*****: Calcined at 800 °C. **†**: Calcined at 900 °C. **Δ**: Acid leached.

EDS measurements were done in different regions of each catalyst. One of it was selected to compose this table.

Interestingly, Ca is, theoretically, only existent in FA or $CaCO_3$ (and its direct derivatives) but even in catalysts which does not utilized $Ca(OH)_2$ to increase the pH, such as FAES N° 3, N° 4 and N° 5, the content is quite high. Hence, this also highlight the leaching effect of HCl within FA. Other elements in smaller amounts, such as Ti and Cl, became part of the precipitated minerals in some FAES

catalysts, suggesting that the variations in methodology impacts the elements precipitation. Silicon, for instance, even though present in high amounts in FA, is was registered in FAES catalysts in small amounts (*ca*. 1 % or less) for those using the acid leachate. Only in FAES N° 1, N° 2 and N° 8, which have, directly, incorporated FA in the preparation methodology show higher amounts (around 30 %).

Finally, Na and K, naturally present in raw FA and $CaCO_3$, were not registered in any FAES catalyst except those using directly FA in its preparation methodology (*i.e.* FAES N° 1 and N° 8). This is of importance since both elements can be of harm to biodiesel, because they can induce the formation of soap and therefore have maximum levels determined by the technical standards.

6.3 Biodiesel

All the catalysts developed in this work were evaluated in the transesterification reaction of soybean-sunflower oil and WFO (for selected catalysts based on the data from the previous oil). The Table 7 summarizes all the results for FAME yield – including an arithmetic average result made with the 4 reactions done for each sample – for each homogeneous and heterogeneous catalyst utilized.

The homogeneous catalyst utilized (*i.e.* NaOH) is recognized by the reference literature (see subsection 3.3.2) as an efficient material for biodiesel conversion via transesterification. FAME conversion levels near 100 % for a reactional time of approximately 1 hour were reached as quantified *e.g*. by GC. In this work, even considering the fact that FAME measurement is an alternative technique, it should be expected to find the same high levels for the homogeneous catalyst. Notwithstanding, the differences in methodology could impact the final result, which means conversions near 100 % could be not verified.

The experimental data, depicted in Figures 34 and 35, show that NaOH conversion for soybean-sunflower and WFO oils are always around the 80 % and were thus considered as a reference level in terms of quality and conversion to be reached by any catalyst evaluated under the same FAME conversion methodology used in this work.

Two major regions in both Figures can be recognized, one in the upper part, between 70 % and 90 %, and another in the bottom part, between 30 % and 0 %. All the heterogeneous catalysts, not containing FA in the synthesis methodology, but prepared only with the acid leachate are in the former group. In relation to the latter, FA is part of the synthesis methodology for FAES N° 1/ 900 °C and N° 8/ 800 °C. For FAES N° 2/ 800 °C, and even though it does not contain FA, the methodology was fixed at a pH of 5, which probably did not favor a good precipitation of chemical elements and a further formation of minerals.

Table 8 – FAME yield for all the catalysts in biodiesel production

	Reaction 1	Repetition 1	Repetition 2	Repetition 3	Average	Variance (σ^2)	SD (σ)
Soybean-Sunflower							
Homogeneous							
NaOH	79.2	78.0	78.3	75.0	77.6	3.3	1.8
Heterogeneous							
Raw FA	0.0	0.0	0.0	0.0	0	0	0
Cao 800 °C	83.2	80.2	77.6	81.4	80.6	5.5	2.3
CaO 900 °C	75.0	66.5	72.5	67.0	70.2	17.2	4.1
FAES N° 1 800 °C	73.1	83.0	81.3	66.1	75.9	61.1	7.8
FAES N° 1 900 °C	24.6	0.0	0.0	0.0	6.2	151.8	12.3
FAES N° 2 800 °C	13.4	19.5	29.0	12.6	18.6	57.5	7.6
FAES N° 3 800 °C	89.7	68.8	81.3	69.7	77.4	99.5	10.0
FAES N° 4 800 °C	81.9	85.0	84.7	63.3	78.7	108.4	10.4
FAES N° 5 800 °C	78.1	86.7	82.7	79.9	81.9	14.1	3.8
FAES N° 6 800 °C	84.5	85.1	78.9	73.8	80.6	28.2	5.3
FAES N° 7 800 °C	77.2	79.7	79.4	88.9	81.3	26.8	5.2
FAES N° 8 800 °C	3.8	0.3	5.4	4.6	3.5	5.0	2.2
WFO							
Homogeneous							
NaOH	70.2	79.0	80.0	86.9	79.0	47.0	6.9
Heterogeneous							
CaO 800 °C	81.2	84.0	82.4	84.5	83.0	2.2	1.5
FAES N° 1 800 °C	88.9	84.8	79.6	78.7	83.0	23.0	4.8
FAES N° 7 800 °C	79.6	73.9	80.5	74.1	77.0	12.5	3.5

This is corroborated by the data for FAES N° 6/ 800 °C and N°7/ 800 °C which had similar synthesis methodologies, only differing in terms of pH (10 in these two cases). Combining with data from FTIR, XRD and SEM-EDS, shows the variability in mineral precipitation between catalysts, highlight its differences and reinforces the impact in FAME conversion.

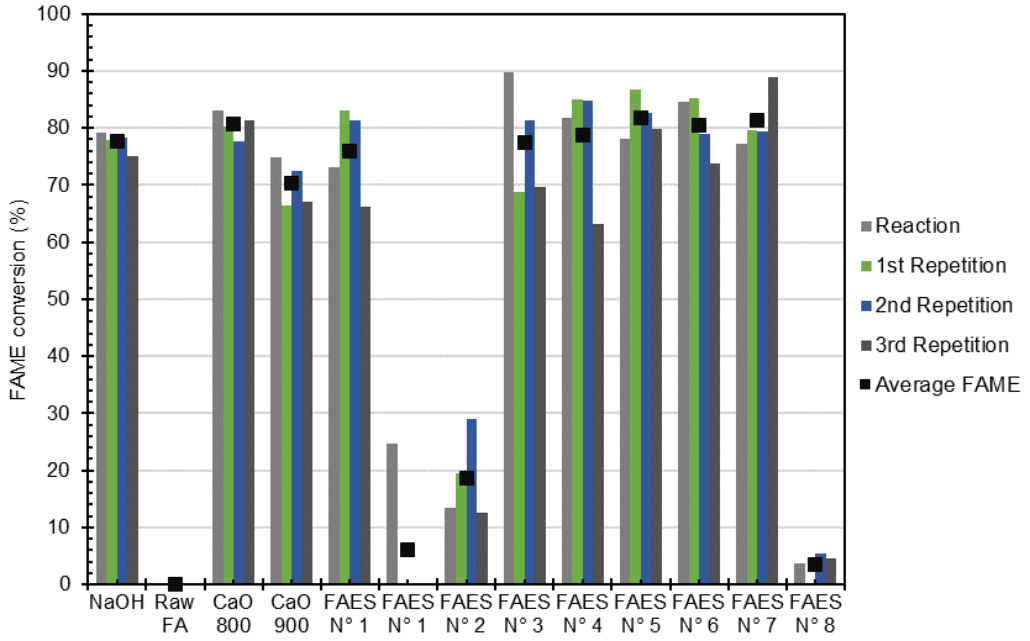

Figure 34 – Soybean-Sunflower oil FAME conversion for all catalysts

When comparing FAES N° 1 calcined at 900 °C and 800 °C, it may be seen that the latter at had conversion for FAME, always near 70 %. To justify the bad performance of FAES N° 1/ 900 °C it is needed to evaluate all the data collected. For instance, SEM-EDS chemical element content show very similar amounts for all elements but calcium, whose amount was reduced from 18.19 % in the sample calcined at 800 °C to 6.84 % in the one calcined at 900 °C. This variation in the Ca content is relevant since it is derived, directly, from chicken egg shells and, when being part of lime, it is a very efficient catalyst for biodiesel. In fact, the alkaline solution $(NH_4)_2CO_3$, does not contribute at all with the Ca content in the catalyst. The lime, as already discussed, is clearly identified by XRD and FTIR.

In relation to the upper part of Figures 34 and 35, it may be seen that the synthesized heterogeneous FAES catalysts have a very good performance for biodiesel conversion, similar or even superior to NaOH (77.60 %) and traditional and alternative materials CaO (80.60 %). On average, according to Table 7, FAES N° 5, N° 6 and N° 7, showed FAME conversion of, respectively, 81.87 %, 80.59 % and 81.30 %.

The biggest discrepancy between these three FAES catalysts is almost the sole presence of lime with traces of brownmillerite in FAES N° 5, in comparison to FAES N° 6 and N° 7. Hence, theoretically, the FAES N° 5 holds a potential to carry a biodiesel conversion reaction because lime is a well-known good heterogeneous catalyst. The FAES N° 6 and N° 7 have a much more complex mineral structure, very similar between them, and holding a much more complex mineral phase when compared to FAES N° 5. These two catalysts contain lime but also other minerals, such as mayenite, andradite, wadalite, brownmillerite and periclase, all of them being mixed oxides of different chemical elements.

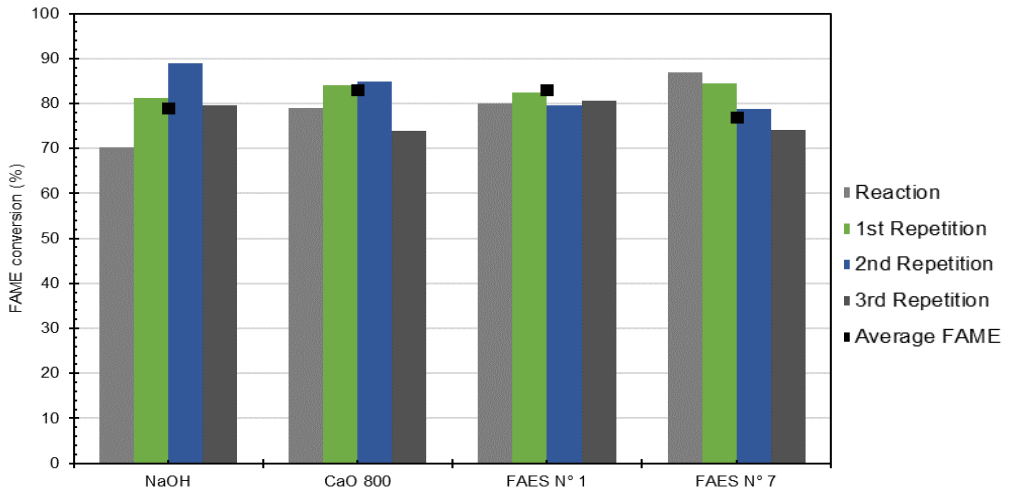

Figure 35 – WFO FAME conversion for selected catalysts

This argumentation can support the main driving force of this entire work, to develop an efficient, economical and environmentally-friendly, heterogeneous catalyst capable of producing biodiesel at a similar level as traditional catalysts, homogeneous or heterogeneous. The more complex structure of FAES N° 6 and N° 7, specifically, can contribute to the higher FAME conversion since the mixed oxides existent are also capable of catalyzing the transesterification and contain different types of active sites, acidic or basic, from Brønsted-Lowry and/ or Lewis.

This proves that FA can be used as a source material for synthesis of the discussed catalysts. The literature is rich in examples of valorization of FA for heterogeneous catalyst development even though with several differences in comparison to the methodology proposed in this work. Kuwahara et al. (2010) proposed a synthesis methodology based on coprecipitation and pH variation with NaOH using BFS as raw material, obtaining a HT-based and a zeolite-based catalyst completely different than the ones from this work but with a methodology not very discrepant (mostly in terms alkaline solution to increase the pH, and the crystallization and aging times and temperatures).

Besides, the raw material has a composition similar to FA (34.58 % of SiO_2, 14.78 % of Al_2O_3, 1.53 % of Fe_2O_3 and 40.09 % of CaO), only with a different content of CaO. Nevertheless, when calcined, the HT material produced a mixed oxide (dependent on the original composition) which holds much similarities to the FAES catalysts of the current work, mostly in terms of the oxides (*i.e.* brownmillerite, wadalite, andradite, mayenite and periclase). The SEM-EDS data presented indicated the existence of ions such as Ca, Al, Mg, Cl, Fe and Mn, many of those present in the calcined FAES catalysts.

It is important to highlight that Kuwahara et al. (2010) evaluated the HT catalysts developed for removal of phosphates in water but another work done by Kuwahara et al. (2012) and Kuwahara & Yamashita (2015) using the same methodology and catalysts (this time calcined) focused on biodiesel production via transesterification. They observed the positive effect in terms of surface basicity caused by chemical elements, such as Fe, Mg and Mn, many of them present in the FAES catalysts studied in

this work. The catalysts calcined at 800 °C reached FAME yields of above 95 % (analyzed using GC) in reactions using 1.42 % wt. of catalyst, values superior those using sole CaO as catalyst. This behavior, as already mentioned, was also observed with the FAES catalysts.

Other authors, also dedicated to valorize FA, are Manique et al. (2017); Muriithi et al. (2017); Volli & Purkait (2015). The first authors focused on developing a catalyst using FA together with solutions of Al and Mg nitrates, and Na carbonate. The final catalyst synthesized was a HT-like material used for mustard oil transesterification after calcination at 500 °C. The methodology proposed by these authors has similarities to the one used in this work, however, since they used analytical grade reagents, an certain impact in costs of production can exist.

This is even more relevant considering that the final catalysts used were composed of mixed metal oxides (with bifunctional characteristic) which, according to SEM-EDS data, contain many elements similar found in the presented thesis. Obviously, there exists a remarkable difference in terms of Al and Si since Volli & Purkait (2015) used FA directly in the methodology. Evaluating the Fe and Ca content, the FAES catalysts had higher content of it and did not have any trace of Na for some samples while the HT catalysts had around 6.20 % sodium oxide.

This presence of Na can be positive for TAG conversion but also be harmful as it can leach to the FAME phase, contaminating it. The FAME conversion reached by this catalyst was 67.1 % (estimated via spectroscopy) at 65 °C, methanol: oil ratio of 12:1 and 5 % wt. of catalyst for 6 hours. Comparing this FAME yield results from HT-derived catalysts with the ones from FAES N° 6 and N° 7 suggest that FAES catalysts perform better.

Muriithi et al. (2017) proposed probably the closest methodology for a FA-based catalyst in comparison to the methodology proposed in this work, even though the final catalyst was different. The authors used an acid leachate of FA combined with a 2M NaOH alkaline solution to increase the pH up to 11.5 with an aging step of 12 hours at 70 °C. The final catalyst was claimed to be a HT material which, theoretically, after calcination, can convert TAG into FAME.

Finally, Manique et al. (2017) proposed a zeolite derived from coal fly ashes using sodium aluminate ($NaAlO_2$) in a methodology more complex and time-consuming in comparison to the one proposed in this work. FAME conversion (measured by GC) reached 95.5 % at 65 °C, methanol: oil ratio of 12:1 and 4 % wt. of catalyst for 2 hours. The differences in methodology and reagents in comparison to the one for FAES catalysts may not prove viable since the preparation was more demanding (*i.e*. reagents, quality of raw materials and time) to obtain a catalyst with somewhat similar efficiency for FAME conversion.

7. CONCLUSIONS

The fundamental proposal of this work to synthesize an efficient and economical heterogeneous catalyst derived from residues – fly ash and chicken egg shell – for biodiesel production from soybean-sunflower oil and WFO was properly achieved. The methodology applied, based on simplicity and reduction of chemical reagents usage but with a small control of chemical elements stoichiometry, was capable to produce a series of FAES catalysts with different phase composition. These catalysts performed, accordingly to the existent minerals, differently for biodiesel production via transesterification.

The data collected via XRD, FTIR and SEM-EDS were capable of highlighting the differences and indicate the reasons why for the differences in FAME conversion performance. Specifically, the most prominent heterogeneous catalysts developed were FAES N° 6 and FAES N° 7, both following an equal methodology, and holding very equivalent crystalline structures. Beyond that, these catalysts achieved even higher conversion levels for FAME when compared to traditional catalysts, homogeneous (i.e. NaOH) or heterogeneous (i.e. CaO).

Several characteristics related to these catalysts differentiate them from others, such as the presence, among the CaO used in the methodology and well-known as an efficient biodiesel catalyst, of minerals like brownmillerite, andradite, periclase, wadalite and mayenite. These structures arise after a calcination process (at 800 °C in this case) and are all mixed metal oxides formed out of the chemical elements acid-leached form FA (*e.g.* Mg, Al, Si, Fe, Ti and Mn). This characteristic favors the material to be a good catalyst since it can present different active sites of acidic and alkaline origin.

Up to this point, after this entire discussion and debate, what is very interesting to note is the fact that energy, perceived in the genesis of the strong development of human species since the advent of fire, started to be faced as a global challenge to humanity as a whole. Alternatives are all around claiming sometimes support, courage and dedication of governments and people to turn it into reality. Definitely, there is still space for oil and gas, even with their known side effects, which can be extenuated at some level. Yet, there is also much space for waste valorization, biomass and biofuels, wind and solar energies, and any other creative idea that could cooperate to the main objective of caring for Earth and harnessing a brighter and beautiful future for the coming generations.

REFERENCES

AASHTO. (2019). *AASHTO M 295 - Standard Specification for Coal Fly Ash and Raw or Calcined Natural Pozzolan for Use in Concrete*. Retrieved from https://infostore.saiglobal.com/en-gb/Standards/AASHTO-M-295-2019-1182_SAIG_AASHTO_AASHTO_2720318/

Aatola, H., Larmi, M., Sarjovaara, T., & Mikkonen, S. (2008). Hydrotreated Vegetable Oil (HVO) as a Renewable Diesel Fuel: Trade-off between NOx, Particulate Emission, and Fuel Consumption of a Heavy Duty Engine. *SAE Int. J. Engines*, *1*(1), 1251–1262. https://doi.org/10.4271/2008-01-2500

Abdullah, S. H. Y. S., Hanapi, N. H. M., Azid, A., Umar, R., Juahir, H., Khatoon, H., & Endut, A. (2017). A review of biomass-derived heterogeneous catalyst for a sustainable biodiesel production. *Renewable and Sustainable Energy Reviews*, *70*(September 2015), 1040–1051. https://doi.org/10.1016/j.rser.2016.12.008

ACAA. (n.d.). American Coal Ash Association. Retrieved February 18, 2020, from https://www.acaa-usa.org/

Agarwal, A. K. (2007). Biofuels (alcohols and biodiesel) applications as fuels for internal combustion engines. *Progress in Energy and Combustion Science*, *33*(3), 233–271. https://doi.org/10.1016/j.pecs.2006.08.003

Ahmaruzzaman, M. (2010). A review on the utilization of fly ash. *Progress in Energy and Combustion Science*, *36*(3), 327–363. https://doi.org/10.1016/j.pecs.2009.11.003

Al-Alawi, A., Van de Voort, F. R., & Sedman, J. (2004). New FTIR method for the determination of FFA in oils. *JAOCS, Journal of the American Oil Chemists' Society*, *81*(5), 441–446. https://doi.org/10.1007/s11746-004-0920-9

Aliske, M. A., Zagonel, G. F., Costa, B. J., Veiga, W., & Saul, C. K. (2007). Measurement of biodiesel concentration in a diesel oil mixture. *Fuel*, *86*(10–11), 1461–1464. https://doi.org/10.1016/j.fuel.2006.11.008

Amani, H., Ahmad, Z., Asif, M., & Hameed, B. H. (2014). Transesterification of waste cooking palm oil by MnZr with supported alumina as a potential heterogeneous catalyst. *Journal of Industrial and Engineering Chemistry*, *20*(6), 4437–4442. https://doi.org/10.1016/j.jiec.2014.02.012

Ambat, I., Srivastava, V., & Sillanpää, M. (2018). Recent advancement in biodiesel production

methodologies using various feedstock: A review. *Renewable and Sustainable Energy Reviews*, *90*(February 2017), 356–369. https://doi.org/10.1016/j.rser.2018.03.069

ANP. *Portaria ANP N° 255*. , (2003).

ANP. (2014). *Resolução N° 45*. Retrieved from http://legislacao.anp.gov.br/?path=legislacao-anp/resol-anp/2014/agosto&item=ranp-45-2014

ANP. (2018). *Oil, Natural Gas and Biofuels Statistical Yearbook 2018*. https://doi.org/ISSN 1983-5884

Anthony, J. W., Bideaux, R. A., Bladh, K. W., & Nichols, C. M. (2003). *Handbook of Mineralogy*. Retrieved from http://www.handbookofmineralogy.org/.

Antón, S. C., & Josh Snodgrass, J. (2012). Origins and evolution of genus Homo: New perspectives. *Current Anthropology*, *53*(SUPPL. 6). https://doi.org/10.1086/667692

Aranda, D. A. G., & Machado, G. D. (2016). *Biodiesel Production by Hydroesterification: Simulation Studies BT - Green Fuels Technology: Biofuels* (C. R. Soccol, S. K. Brar, C. Faulds & L. P. Ramos, Eds.). https://doi.org/10.1007/978-3-319-30205-8_13

Aransiola, E. F., Ikhu-Omoregbe, D. I. O., Madzimbamuto, T. F., Ojumu, T. V., & Oyekola, O. O. (2013). A review of current technology for biodiesel production: State of the art. *Biomass and Bioenergy*, *61*, 276–297. https://doi.org/10.1016/j.biombioe.2013.11.014

Arent, D. J., Wise, A., & Gelman, R. (2011). The status and prospects of renewable energy for combating global warming. *Energy Economics*, *33*(4), 584–593. https://doi.org/10.1016/j.eneco.2010.11.003

Arnold, T. S., Rozario-Ranasinghe, M., & Youtcheff, J. (2006). Determination of lime in hot-mix asphalt. *Transportation Research Record*, (1962), 113–120. https://doi.org/10.3141/1962-13

Arzamendi, G., Campo, I., Arguiñarena, E., Sánchez, M., Montes, M., & Gandía, L. M. (2007). Synthesis of biodiesel with heterogeneous NaOH/ alumina catalysts: Comparison with homogeneous NaOH. *Chemical Engineering Journal*, *134*(1–3), 123–130. https://doi.org/10.1016/j.cej.2007.03.049

Asl, S. M. H., Ghadi, A., Baei, M. S., Javadian, H., Maghsudi, M., & Kazemian, H. (2018). Porous catalysts fabricated from coal fly ash as cost-effective alternatives for industrial applications: A review. *Fuel*, *217*(December 2017), 320–342. https://doi.org/10.1016/j.fuel.2017.12.111

ASTM International. (2014). *ASTM D7371-14, Standard Test Method for Determination of Biodiesel (Fatty Acid Methyl Esters) Content in Diesel Fuel Oil Using Mid Infrared Spectroscopy (FTIR-ATR-PLS Method)*. https://doi.org/10.1520/D7371-14

ASTM International. (2019a). *ASTM C618 - 19 - Standard Specification for Coal Fly Ash and Raw or Calcined Natural Pozzolan for Use in Concrete* (p. 3). p. 3. https://doi.org/10.1520/C0618-19

ASTM International. (2019b). *ASTM D6751-19 - Standard Specification for Biodiesel Fuel Blend Stock (B100) for Middle Distillate Fuels*. https://doi.org/10.1520/D6751-19

Atadashi, I. M., Aroua, M. K., Abdul Aziz, A. R., & Sulaiman, N. M. N. (2013). The effects of catalysts in biodiesel production: A review. *Journal of Industrial and Engineering Chemistry*, *19*(1), 14–26. https://doi.org/10.1016/j.jiec.2012.07.009

Atadashi, I. M., Aroua, M. K., & Aziz, A. A. (2011). Biodiesel separation and purification: A review. *Renewable Energy*, *36*(2), 437–443. https://doi.org/10.1016/j.renene.2010.07.019

Atadashi, I. M., Aroua, M. K., Aziz, A. R. A., & Sulaiman, N. M. N. (2011). Refining technologies for the purification of crude biodiesel. *Applied Energy*, *88*(12), 4239–4251. https://doi.org/10.1016/j.apenergy.2011.05.029

Augustyn, A., Bauer, P., Duignan, B., Eldridge, A., Gregersen, E., McKenna, E., Petruzzello, M., Rafferty, J. P., Ray, M., Rogers, K., Tikkanen, A., Wallenfeldt, J., Zeidan, A., & Zelazko, A. (2016). Bragg law. In *Encyclopædia Britannica*. Retrieved from https://www.britannica.com/science/Bragg-law

Avhad, M. R., & Marchetti, J. M. (2015). A review on recent advancement in catalytic materials for biodiesel production. *Renewable and Sustainable Energy Reviews*, *50*, 696–718. https://doi.org/10.1016/j.rser.2015.05.038

Azevedo, F. A. C., Carvalho, L. R. B., Grinberg, L. T., Farfel, J. M., Ferretti, R. E. L., Leite, R. E. P., Filho, W. J., Lent, R., & Herculano-Houzel, S. (2009). Equal numbers of neuronal and nonneuronal cells make the human brain an isometrically scaled-up primate brain. *Journal of Comparative Neurology*, *513*(5), 532–541. https://doi.org/10.1002/cne.21974

Baileys, S. D. (2005). Bailey's Industrial Oil and Fat Products. In F. Shahidi (Ed.), *Wiley Interscience* (Vol. 5). https://doi.org/10.1002/047167849X

Banerji, R., Chowdhury, A. R., Misra, G., Sudarsanan, G., Verma, S. C., & Srivastava, G. S. (1985). Jatropha seed oils for energy. *Biomass*, *8*(4), 277–282. https://doi.org/10.1016/0144-

4565(85)90060-5

Banković-Ilić, I. B., Stamenković, O. S., & Veljković, V. B. (2012). Biodiesel production from non-edible plant oils. *Renewable and Sustainable Energy Reviews*, *16*(6), 3621–3647. https://doi.org/10.1016/j.rser.2012.03.002

Barnwal, B. K., & Sharma, M. P. (2005). Prospects of biodiesel production from vegetable oils in India. *Renewable and Sustainable Energy Reviews*, *9*(4), 363–378. https://doi.org/10.1016/j.rser.2004.05.007

Basu, M., Pande, M., Bhadoria, P. B. S., & Mahapatra, S. C. (2009). Potential fly-ash utilization in agriculture: A global review. *Progress in Natural Science*, *19*(10), 1173–1186. https://doi.org/10.1016/j.pnsc.2008.12.006

Belviso, C. (2018). State-of-the-art applications of fly ash from coal and biomass: A focus on zeolite synthesis processes and issues. *Progress in Energy and Combustion Science*, *65*, 109–135. https://doi.org/10.1016/j.pecs.2017.10.004

Bennett, J. A., Wilson, K., & Lee, A. F. (2016). Catalytic applications of waste derived materials. *Journal of Materials Chemistry A*, *4*(10), 3617–3637. https://doi.org/10.1039/c5ta09613h

Berrios, M., & Skelton, R. L. (2008). Comparison of purification methods for biodiesel. *Chemical Engineering Journal*, *144*(3), 459–465. https://doi.org/10.1016/j.cej.2008.07.019

Bhandari, R., Volli, V., & Purkait, M. K. (2015). Preparation and characterization of fly ash based mesoporous catalyst for transesterification of soybean oil. *Journal of Environmental Chemical Engineering*, *3*(2), 906–914. https://doi.org/10.1016/j.jece.2015.04.008

Bhatt, A., Priyadarshini, S., Acharath Mohanakrishnan, A., Abri, A., Sattler, M., & Techapaphawit, S. (2019). Physical, chemical, and geotechnical properties of coal fly ash: A global review. *Case Studies in Construction Materials*, *11*, 1–11. https://doi.org/10.1016/j.cscm.2019.e00263

Binal, A., Bas, B., & Karamut, O. R. (2016). Improvement of the Strength of Ankara Clay with Self-cementing High Alkaline Fly Ash. *Procedia Engineering*, *161*, 374–379. https://doi.org/10.1016/j.proeng.2016.08.577

Blissett, R. S., & Rowson, N. A. (2012). A review of the multi-component utilisation of coal fly ash. *Fuel*, *97*, 1–23. https://doi.org/10.1016/j.fuel.2012.03.024

Bockisch, M. B. T. (1998). *Fats and Oils Handbook* (M. B. T.-F. and O. H. Bockisch, Ed.).

https://doi.org/https://doi.org/10.1016/B978-0-9818936-0-0.50007-X

Boey, P. L., Maniam, G. P., & Hamid, S. A. (2009). Utilization of waste crab shell (Scylla serrata) as a catalyst in palm olein transesterification. *Journal of Oleo Science*, *58*(10), 499–502. https://doi.org/10.5650/jos.58.499

Borges, M. E., & Díaz, L. (2012). Recent developments on heterogeneous catalysts for biodiesel production by oil esterification and transesterification reactions: A review. *Renewable and Sustainable Energy Reviews*, *16*(5), 2839–2849. https://doi.org/10.1016/j.rser.2012.01.071

BP. (2019). *BP Statistical Review of World Energy* (68th ed.). Retrieved from https://www.bp.com/en/global/corporate/energy-economics/statistical-review-of-world-energy.html

Canakci, M., & Van Gerpen, J. (1999a). *B p a c*. *42*(1984), 1203–1210.

Canakci, M., & Van Gerpen, J. (1999b). Biodiesel production via acid catalysis. *Transactions of the ASAE*, *42*(5), 1203–1210.

Cao, X., Sun, S., & Sun, R. (2017). Application of biochar-based catalysts in biomass upgrading: A review. *RSC Advances*, *7*(77), 48793–48805. https://doi.org/10.1039/c7ra09307a

Catarino, M., Ferreira, E., Soares Dias, A. P., & Gomes, J. (2020). Dry washing biodiesel purification using fumed silica sorbent. *Chemical Engineering Journal*, *386*(November 2019), 123930. https://doi.org/10.1016/j.cej.2019.123930

Cavani, F., Trifirò, F., & Vaccari, A. (1991). Hydrotalcite-type anionic clays: preparation, properties and applications. *Catalysis Today*, *11*(2), 173–301. https://doi.org/https://doi.org/10.1016/0920-5861(91)80068-K

CEN. (2018). *CEN EN 14214 - Liquid petroleum products - Fatty acid methyl esters (FAME) for use in diesel engines and heating applications - Requirements and test methods* (p. 32). p. 32. Retrieved from http://cen.eu

Chakraborty, R., Bepari, S., & Banerjee, A. (2010). Transesterification of soybean oil catalyzed by fly ash and egg shell derived solid catalysts. *Chemical Engineering Journal*, *165*(3), 798–805. https://doi.org/10.1016/j.cej.2010.10.019

Chauhan, B. S., Kumar, N., Du Jun, Y., & Lee, K. B. (2010). Performance and emission study of preheated Jatropha oil on medium capacity diesel engine. *Energy*, *35*(6), 2484–2492.

https://doi.org/10.1016/j.energy.2010.02.043

Chindaprasirt, P., De Silva, P., Sagoe-Crentsil, K., & Hanjitsuwan, S. (2012). Effect of SiO2 and Al2O3 on the setting and hardening of high calcium fly ash-based geopolymer systems. *Journal of Materials Science*, *47*(12), 4876–4883. https://doi.org/10.1007/s10853-012-6353-y

Chouhan, A. P. S., & Sarma, A. K. (2011). Modern heterogeneous catalysts for biodiesel production: A comprehensive review. *Renewable and Sustainable Energy Reviews*, *15*(9), 4378–4399. https://doi.org/10.1016/j.rser.2011.07.112

Cleveland, C. J., & Morris, C. (2014). Handbook of Energy. Volume II - Chronologies, Top Ten Lists, and Word Clouds. In *Handbook of Energy*. https://doi.org/10.1016/B978-0-12-397219-4.00009-6

CNPE. (2018). *Resolução N° 16*. Retrieved from http://www.mme.gov.br/web/guest/cnpe-2018

Colthup, N. B., Daly, L. H., & Wiberley, S. E. (1990). *Introduction to Infrared and Raman Spectroscopy* (3rd ed.). https://doi.org/https://doi.org/10.1016/C2009-0-21628-X

Cruz, M., Almeida, M. F., Alvim-Ferraz, M. da C., & Dias, J. M. (2019). Monitoring Enzymatic Hydroesterification of Low-Cost Feedstocks by Fourier Transform Infrared Spectroscopy. *Catalysts*, *9*(5), 535. https://doi.org/https://doi.org/10.3390/catal9060535

Dai, Y. M., Chen, K. T., Wang, P. H., & Chen, C. C. (2016). Solid-base catalysts for biodiesel production by using silica in agricultural wastes and lithium carbonate. *Advanced Powder Technology*, *27*(6), 2432–2438. https://doi.org/10.1016/j.apt.2016.08.021

Davini, P. (1996). Investigation of the SO2 adsorption properties of Ca(OH)2 - fly ash systems. *Fuel*, *75*(6), 713–716. https://doi.org/10.1016/0016-2361(95)00303-7

Dawodu, F. A., Ayodele, O., Xin, J., Zhang, S., & Yan, D. (2014). Effective conversion of non-edible oil with high free fatty acid into biodiesel by sulphonated carbon catalyst. *Applied Energy*, *114*, 819–826. https://doi.org/10.1016/j.apenergy.2013.10.004

de Almeida, R. M., Noda, L. K., Gonçalves, N. S., Meneghetti, S. M. P., & Meneghetti, M. R. (2008). Transesterification reaction of vegetable oils, using superacid sulfated TiO2-base catalysts. *Applied Catalysis A: General*, *347*(1), 100–105. https://doi.org/10.1016/j.apcata.2008.06.006

Demirbaş, A. (2002). Biodiesel from vegetable oils via transesterification in supercritical methanol. *Energy Conversion and Management*, *43*, 2349–2356.

Demirbaş, A. (2008). Comparison of transesterification methods for production of biodiesel from vegetable oils and fats. *Energy Conversion and Management*, *49*(1), 125–130. https://doi.org/10.1016/j.enconman.2007.05.002

Demirbaş, A. (2009). Progress and recent trends in biodiesel fuels. *Energy Conversion and Management*, *50*(1), 14–34. https://doi.org/10.1016/j.enconman.2008.09.001

Demirbaş, A. (2010). Biorefineries: For biomass upgrading facilities. *Green Energy and Technology*. https://doi.org/10.1007/978-1-84882-721-9

Demirbaş, A., Bafail, A., Ahmad, W., & Sheikh, M. (2016). Biodiesel production from non-edible plant oils. *Energy Exploration and Exploitation*, *34*(2), 290–318. https://doi.org/10.1177/0144598716630166

Di Serio, M., Ledda, M., Cozzolino, M., Minutillo, G., Tesser, R., & Santacesaria, E. (2006). Transesterification of soybean oil to biodiesel by using heterogeneous basic catalysts. *Industrial and Engineering Chemistry Research*, *45*(9), 3009–3014. https://doi.org/10.1021/ie051402o

Di Serio, M., Tesser, R., Dimiccoli, M., Cammarota, F., Nastasi, M., & Santacesaria, E. (2005). Synthesis of biodiesel via homogeneous Lewis acid catalyst. *Journal of Molecular Catalysis A: Chemical*, *239*(1–2), 111–115. https://doi.org/10.1016/j.molcata.2005.05.041

Di Serio, Martino, Tesser, R., Pengmei, L., & Santacesaria, E. (2008). Heterogeneous Catalysts for Biodiesel Production. *Energy & Fuels*, *22*(9), 207–217. https://doi.org/10.1002/bmc

DIN. (2014). *DIN EN 14078 - Liquid petroleum products - Determination of the content of fatty acid methyl ester (FAME) in middle distillates - Infrared spectrometric method*. https://doi.org/https://dx.doi.org/10.31030/2232694

Dong, X., Li, Q., Sun, D., Chen, X., & Yu, X. (2015). Direct FTIR Analysis of Free Fatty Acids in Edible Oils Using Disposable Polyethylene Films. *Food Analytical Methods*, *8*(4), 857–863. https://doi.org/10.1007/s12161-014-9963-y

Dos Santos, L. K., Calera, G. C., Stringaci, J. C. T., Vilaça, S. M., Viviani, V. E., & Flumignan, D. L. (2015). Estado da arte da aplicação do processo de hidroesterificação na produção de biodiesel a partir de matérias-primas de baixa qualidade. *Revista Principia - Divulgação Científica e Tecnológica Do IFPB*, *1*(28), 178. https://doi.org/10.18265/1517-03062015v1n28p178-190

Downs, R. T., & Hall-Wallace, M. (2003). The American Mineralogist crystal structure database. *American Mineralogist*, *88*, 247–250. Retrieved from

http://www.minsocam.org/msa/AmMin/AmMineral.html

Dubé, M. A., Zheng, S., McLean, D. D., & Kates, M. (2004). A comparison of attenuated total reflectance-FTIR spectroscopy and GPC for monitoring biodiesel production. *JAOCS, Journal of the American Oil Chemists' Society*, *81*(6), 599–603. https://doi.org/10.1007/s11746-006-0948-x

Dubois, V., Breton, S., Linder, M., Fanni, J., & Parmentier, M. (2007). Fatty acid profiles of 80 vegetable oils with regard to their nutritional potential. *European Journal of Lipid Science and Technology*, *109*(7), 710–732. https://doi.org/10.1002/ejlt.200700040

Dutta, P. K., Auerbach, S. M., & Carrado, K. A. (Eds.). (2004). *Handbook of layered materials*. New York, USA: Marcel Dekker Inc.

ECOBA. (2016). European Coal Combustion Products Association. Retrieved February 20, 2020, from Production and Utilisation of CCPs in 2016 in Europe (EU 15) website: http://www.ecoba.org/ecobaccpprod.html;jsessionid=AB36291DB752E9594BF74813EEE72FE7

EIA. (2019a). Biofuels Explained. Retrieved from https://www.eia.gov/energyexplained/biofuels/

EIA. (2019b). Monthly Energy Review - July. In *Monthly Energy Review*. Retrieved from http://www.eia.gov/totalenergy/data/monthly no

El-Rahman, F. A., Mahmoud, N. S., El-Khair Badawy, A., & Youns, S. M. (2018). Extraction of fish oil from fish viscera. *Egyptian Journal of Chemistry*, *61*(2), 201–211. https://doi.org/10.21608/ejchem.2018.2798.1230

Encarnação, A. P. G. (2007). *Production of biodiesel by transesterication and hidroesterificacion processes – an economic evaluation*. Federal University of Rio de Janeiro (UFRJ).

Endalew, A. K., Kiros, Y., & Zanzi, R. (2011a). Heterogeneous catalysis for biodiesel production from Jatropha curcas oil (JCO). *Energy*, *36*(5), 2693–2700. https://doi.org/10.1016/j.energy.2011.02.010

Endalew, A. K., Kiros, Y., & Zanzi, R. (2011b). Inorganic heterogeneous catalysts for biodiesel production from vegetable oils. *Biomass and Bioenergy*, *35*(9), 3787–3809. https://doi.org/10.1016/j.biombioe.2011.06.011

Engel, J. J., Smith, J. W., Unruh, J. A., Goodband, R. D., O'Quinn, P. R., Tokach, M. D., & Nelssen, J. L. (2001). Effects of choice white grease or poultry fat on growth performance, carcass leanness, and meat quality characteristics of growing-finishing pigs. *Journal of Animal Science*,

79(6), 1491–1501. https://doi.org/10.2527/2001.7961491x

EU. (n.d.). Statistics Explained. Retrieved February 16, 2020, from https://ec.europa.eu/eurostat/statistics-explained/index.php/Main_Page

EU. Directive 2003/30/EC of the European Parliament and of the Council of 8 May 2003 on the promotion of the use of biofuels or other renewable fuels for transport. , 4 Official Journal of the European Union § (2003).

EU. (2009). Directive 2009/28/EC of the European Parliament and of the Council of 23 April 2009. *Official Journal of the European Union*, *140*(16), 16–62. https://doi.org/10.3000/17252555.L_2009.140.eng

EU. (2018). Directive EU 2018/ 2001 of the European Parliament and of the Council of 11 December 2018 on the promotion of the use of energy from renewable sources. *Official Journal of the European Union*, 128. Retrieved from https://eur-lex.europa.eu/legal-content/EN/TXT/?uri=uriserv:OJ.L_.2018.328.01.0082.01.ENG&toc=OJ:L:2018:328:TOC

Faccini, C. S. (2008). *Uso de Adsorventes na Purificação de Biodiesel*. Federal University of Rio Grande do Sul (UFRS).

FAO. (2015). *World Programme for the Census of Agriculture 2020* (Vol. 1). Retrieved from http://www.fao.org/fileadmin/templates/ess/documents/world_census_of_agriculture/appendix3_r7.pdf

Farooq, M., Ramli, A., & Subbarao, D. (2013). Biodiesel production from waste cooking oil using bifunctional heterogeneous solid catalysts. *Journal of Cleaner Production*, *59*, 131–140. https://doi.org/10.1016/j.jclepro.2013.06.015

Feofilova, E. P., Sergeeva, Y. E., & Ivashechkin, A. A. (2010). Biodiesel-fuel: Content, production, producers, contemporary biotechnology (Review). *Applied Biochemistry and Microbiology*, *46*(4), 369–378. https://doi.org/10.1134/s0003683810040010

Fernandez Pales, A., Levi, P., & Vass, T. (2019). *Tracking Industry*. Retrieved from https://www.iea.org/reports/tracking-industry-2019

Ferreira, A. B., Lemos Cardoso, A., & da Silva, M. J. (2012). Tin-Catalyzed Esterification and Transesterification Reactions: A Review. *ISRN Renewable Energy*, *2012*, 1–13. https://doi.org/10.5402/2012/142857

Fischer, E., & Speier, A. (1895). Darstellung der Ester. *Berichte Der Deutschen Chemischen Gesellschaft*, *28*(3), 3252–3258. https://doi.org/10.1002/cber.189502803176

Fisher, G. L., Prentice, B. A., Sllberman, D., Ondov, J. M., Biermann, A. H., Ragainl, R. C., & McFarl, A. R. (1978). Physical and Morphological Studies of Size-Classified Coal Fly Ash. *Environmental Science and Technology*, *12*(4), 447–451. https://doi.org/10.1021/es60140a008

Foidl, N., Foidl, G., Sanchez, M., Mittelbach, M., & Hackel, S. (1996). Jatropha curcas L. as a source for the production of biofuel in Nicaragua. *Bioresource Technology*, *58*, 77–82.

Fonseca, J. M., Teleken, J. G., de Cinque Almeida, V., & da Silva, C. (2019). Biodiesel from waste frying oils: Methods of production and purification. *Energy Conversion and Management*, *184*(January), 205–218. https://doi.org/10.1016/j.enconman.2019.01.061

Formo, M. W. (1954). Ester reactions of fatty materials. *Journal of the American Oil Chemists Society*, *31*(11), 548–559. https://doi.org/10.1007/BF02638571

Fraile, J. M., García, N., Mayoral, J. A., Pires, E., & Roldán, L. (2010). The basicity of mixed oxides and the influence of alkaline metals: The case of transesterification reactions. *Applied Catalysis A: General*, *387*(1–2), 67–74. https://doi.org/10.1016/j.apcata.2010.08.002

Freedman, B., Pryde, E. H., & Mounts, T. L. (1984). Variables affecting the yields of fatty esters from transesterified vegetable oils. *JAOCS, Journal of the American Oil Chemists' Society*, *61*(10), 1638–1643. https://doi.org/10.1007/BF02541649

Fukuda, H., Kondo, A., & Noda, H. (2001). Biodiesel fuel production by transesterification of oils. *Journal of Bioscience and Bioengineering*, *92*(5), 405–416. https://doi.org/https://doi.org/10.1016/S1389-1723(01)80288-7

Galadima, A., & Muraza, O. (2020). Waste materials for production of biodiesel catalysts: Technological status and prospects. *Journal of Cleaner Production*, *263*, 121–358. https://doi.org/10.1016/j.jclepro.2020.121358

Gates-Rector, S. D., & Blanton, T. N. (2019). The Powder Diffraction File: A Quality Materials Characterization Database. *Powder Diffraction Journal*, *34*(4), 352–360. https://doi.org/10.1017/S0885715619000812

Ghazani, S. M., & Marangoni, A. G. (2015). Healthy Fats and Oils. In *Encyclopedia of Food Grains: Second Edition* (2nd ed., Vol. 2–4). https://doi.org/10.1016/B978-0-12-394437-5.00100-5

Ghosh, A., & Subbarao, C. (1998). Hydraulic conductivity and leachate characteristics of stabilized fly ash. *Journal of Environmental Engineering*, *124*(9), 812–820. https://doi.org/10.1061/(asce)0733-9372(1998)124:9(812)

Goering, C. E., Schwab, A. W., Daugherty, M. J., Pryde, E. H., & Heakin, A. J. (1982). Fuel Properties of Eleven Vegetable Oils. *Transactions of the ASAE*, *25*(6), 1472–1477. https://doi.org/https://doi.org/10.13031/2013.33748

Gupta, R. B., & Demirbaş, A. (2010). *Gasoline, Diesel and Ethanol Biofuels from Grasses and Plants* (1st ed.). New York: Cambridge University Press: 1.

Hammond, E. W. (2003). Vegetable Oils. In B. Caballero, L. Trugo & P. M. Finglas (Eds.), *Encyclopedia of Food Sciences and Nutrition* (2nd ed., pp. 5899–5904). Academic Press: 2nd.

Hardy, A., & Finch, P. (2017). A chemical study of the contents of an Early Dynastic Egyptian storage jar. *Pharmaceutical Historian*, *47*(1), 1–7.

Hattori, H. (2004). Solid base catalysts: Generation, characterization and catalytic behavior of basic sites. *Journal of the Japan Petroleum Institute*, *47*(2), 67–81. https://doi.org/https://doi.org/10.1627/jpi.47.67

He, J., Wei, M., Li, B., Kang, Y., Evans, D. G., & Duan, X. (2005). Preparation of Layered Double Hydroxides. In D. G. Evans & X. Duan (Eds.), *Layered Double Hydroxides* (1st ed., Vol. 1, pp. 89–119). https://doi.org/10.1007/b100426

Helwani, Z., Othman, M. R., Aziz, N., Fernando, W. J. N., & Kim, J. (2009a). Technologies for production of biodiesel focusing on green catalytic techniques: A review. *Fuel Processing Technology*, *90*(12), 1502–1514. https://doi.org/10.1016/j.fuproc.2009.07.016

Helwani, Z., Othman, M. R., Aziz, N., Kim, J., & Fernando, W. J. N. (2009b). Solid heterogeneous catalysts for transesterification of triglycerides with methanol: A review. *Applied Catalysis A: General*, *363*(1–2), 1–10. https://doi.org/10.1016/j.apcata.2009.05.021

Herculano-Houzel, S. (2012). The remarkable, yet not extraordinary, human brain as a scaled-up primate brain and its associated cost. *Proceedings of the National Academy of Sciences*, *109*(Supplement_1), 10661–10668. https://doi.org/10.1073/pnas.1201895109

Herculano-Houzel, S. (2016). *The Human Advantage: How Our Brains Became Remarkable*. MIT Press.

Ho, W. W. S., Ng, H. K., Gan, S., & Tan, S. H. (2014). Evaluation of palm oil mill fly ash supported calcium oxide as a heterogeneous base catalyst in biodiesel synthesis from crude palm oil. *Energy Conversion and Management*, *88*, 1167–1178. https://doi.org/10.1016/j.enconman.2014.03.061

Hower, J. C., Robertson, J. D., Thomas, G. A., Wong, A. S., Schram, W. H., Graham, U. M., Rathbone, R. F., & Robl, T. L. (1996). Characterization of fly ash from Kentucky power plants. *Fuel*, *75*(4), 403–411. https://doi.org/10.1016/0016-2361(95)00278-2

Huerlimann, R., de Nys, R., & Heimann, K. (2010). Growth, lipid content, productivity, and fatty acid composition of tropical microalgae for scale-up production. *Biotechnology and Bioengineering*, *107*(2), 245–257. https://doi.org/10.1002/bit.22809

Human Origins Initiative. (n.d.). Retrieved December 10, 2018, from Smithsonian National Museum of Natural History website: http://humanorigins.si.edu/

IAL. (2008). *Métodos físicos-quimicos para análise de Alimentos* (4th ed., Vol. 1; O. Zenebon, N. S. Pascuet & P. Tiglea, Eds.). São Paulo, SP, Brasil: Instituto Adolfo Lutz: 4th.

IEA. (2018a). *Coal 2018*. https://doi.org/https://doi.org/https://doi.org/10.1787/coal_mar-2018-en

IEA. (2018b). Renewables Information 2018: Overview. *IEA Statistics*, 497. https://doi.org/10.1787/renew-2018-en

IEA. (2019). *Electricity Information 2019*. https://doi.org/https://doi.org/https://doi.org/10.1787/e0ebb7e9-en

Ismail, K. N., Hussin, K., & Idris, M. S. (2007). Pysical , Chemical & Mineralogical Properties of Fly-ash. *Journal of Nuclear and Related Technology*, *4*(January), 47–51.

Issariyakul, T., & Dalai, A. K. (2014). Biodiesel from vegetable oils. *Renewable and Sustainable Energy Reviews*, *31*, 446–471. https://doi.org/10.1016/j.rser.2013.11.001

Iyer, R. S., & Scott, J. A. (2001). Power station fly ash - A review of value-added utilization outside of the construction industry. *Resources, Conservation and Recycling*, *31*(3), 217–228. https://doi.org/10.1016/S0921-3449(00)00084-7

Jachuck, R., Pherwani, G., & Gorton, S. M. (2009). Green engineering: Continuous production of biodiesel using an alkaline catalyst in an intensified narrow channel reactor. *Journal of Environmental Monitoring*, *11*(3), 642–647. https://doi.org/10.1039/b807390m

Jain, D., Khatri, C., & Rani, A. (2011). Synthesis and characterization of novel solid base catalyst from fly ash. *Fuel*, *90*(6), 2083–2088. https://doi.org/10.1016/j.fuel.2010.09.025

Jalani, B. S., Cheah, S. C., Rajanaidu, N., & Darus, A. (1997). Improvement of palm oil through breeding and biotechnology. *JAOCS, Journal of the American Oil Chemists' Society*, *74*(11), 1451–1455. https://doi.org/10.1007/s11746-997-0253-3

Joo, H., & Kumar, A. (2019). *World Biodiesel Policies and Production* (1st ed.). https://doi.org/https://doi.org/10.1201/9780429282881

Joshi, R. C., & Lothia, R. P. (1997). Fly ash in concrete: production, properties and uses. In *Advances in concrete technology* (1st ed.). Amsterdam, Netherlands: Gordon and Breach Science Publishers: 1st.

Kamal-Eldin, A., & Andersson, R. (1997). A multivariate study of the correlation between tocopherol content and fatty acid composition in vegetable oils. *JAOCS, Journal of the American Oil Chemists' Society*, *74*(4), 375–380. https://doi.org/10.1007/s11746-997-0093-1

Kapil, A., Wilson, K., Lee, A. F., & Sadhukhan, J. (2011). Kinetic modeling studies of heterogeneously catalyzed biodiesel synthesis reactions. *Industrial and Engineering Chemistry Research*, *50*(9), 4818–4830. https://doi.org/10.1021/ie101403f

Kaur, M., & Ali, A. (2011). Lithium ion impregnated calcium oxide as nano catalyst for the biodiesel production from karanja and jatropha oils. *Renewable Energy*, *36*(11), 2866–2871. https://doi.org/10.1016/j.renene.2011.04.014

Kesić, Ž., Lukić, I., Zdujić, M., Mojović, L., & Skala, D. (2016). Calcium oxide based catalysts for biodiesel production: A review. *Chemical Industry and Chemical Engineering Quarterly*, *22*(4), 391–408. https://doi.org/10.2298/ciceq160203010k

Kincs, F. R. (1985). Meat fat formulation. *Journal of the American Oil Chemists' Society*, *62*(4), 815–818. https://doi.org/10.1007/BF03028759

Kiss, A. A., Dimian, A. C., & Rothenberg, G. (2006). Solid acid catalysts for biodiesel production - Towards sustainable energy. *Advanced Synthesis and Catalysis*, *348*(1–2), 75–81. https://doi.org/10.1002/adsc.200505160

Knothe, G. (1999). Rapid monitoring of transesterification and assessing biodiesel fuel quality by near-infrared spectroscopy using a fiber-optic probe. *JAOCS, Journal of the American Oil Chemists' Society*, *76*(7), 795–800. https://doi.org/10.1007/s11746-999-0068-5

Knothe, G. (2001). Historical perspectives on vegetable oil-based fuels. *INFORM - International News on Fats, Oils and Related Materials*.

Knothe, G., & Steidley, K. R. (2009). A comparison of used cooking oils: A very heterogeneous feedstock for biodiesel. *Bioresource Technology*, *100*(23), 5796–5801. https://doi.org/10.1016/j.biortech.2008.11.064

Knothe, G., Van Gerpen, J., & Krahl, J. (2005). The Biodiesel Handbook. In *The Biodiesel Handbook* (1st ed.). https://doi.org/10.1016/c2015-0-02453-4

Kollar, S. R. M., Novotny, E. H., Do Nascimento, C. J., & Suarez, P. A. Z. (2017). Nuclear magnetic resonance (1.40 T) and mid infrared (FTIR-ATR) associated with chemometrics as analytical methods for the analysis of methyl ester yield obtained by esterification reaction. *Journal of the Brazilian Chemical Society*, *28*(10), 1917–1925. https://doi.org/10.21577/0103-5053.20170031

Kotwal, M. S., Niphadkar, P. S., Deshpande, S. S., Bokade, V. V., & Joshi, P. N. (2009). Transesterification of sunflower oil catalyzed by flyash-based solid catalysts. *Fuel*, *88*(9), 1773–1778. https://doi.org/10.1016/j.fuel.2009.04.004

Krawczyk, T. (1996). Biodiesel - Alternative fuel makes inroads but hurdles remain. *INFORM - International News on Fats, Oils and Related Materials*, *7*, 801–829.

Kruse, K., Jasso, A., Folliard, K., Ferron, R., Juenger, M., & Drimalas, T. (2012). *Characterizing Fly Ash* (Vol. 7, p. 172). Vol. 7, p. 172. Austin: Center for Transportation Research - The University of Texas at Austin.

Kumar, D., Singh, B., Banerjee, A., & Chatterjee, S. (2018). Cement wastes as transesterification catalysts for the production of biodiesel from Karanja oil. *Journal of Cleaner Production*, *183*, 26–34. https://doi.org/10.1016/j.jclepro.2018.02.122

Kumar, P., Aslam, M., Singh, N., Mittal, S., Bansal, A., Jha, M. K., & Sarma, A. K. (2015). Characterization, activity and process optimization with a biomass-based thermal power plant's fly ash as a potential catalyst for biodiesel production. *RSC Advances*, *5*(13), 9946–9954. https://doi.org/10.1039/c4ra13475c

Kumar, R., Kumar, S., & Mehrotra, S. P. (2007). Towards sustainable solutions for fly ash through mechanical activation. *Resources, Conservation and Recycling*, *52*(2), 157–179. https://doi.org/10.1016/j.resconrec.2007.06.007

Kumpala, A., Horpibulsuk, S., & Suebsuk, J. (2012). Improvement of swelling-collapsible

behaviors of silty clay by calcium carbide residue. *Advances in Transportation Geotechnics II - Proceedings of the 2nd International Conference on Transportation Geotechnics, ICTG 2012*, (April 2020), 326–333. https://doi.org/10.1201/b12754-46

Kuwahara, Y., Ohmichi, T., Kamegawa, T., Mori, K., & Yamashita, H. (2009). A novel synthetic route to hydroxyapatite-zeolite composite material from steel slag: Investigation of synthesis mechanism and evaluation of physicochemical properties. *Journal of Materials Chemistry*, *19*(39), 7263–7272. https://doi.org/10.1039/b911177h

Kuwahara, Y., Ohmichi, T., Kamegawa, T., Mori, K., & Yamashita, H. (2010). A novel conversion process for waste slag: Synthesis of a hydrotalcite-like compound and zeolite from blast furnace slag and evaluation of adsorption capacities. *Journal of Materials Chemistry*, *20*(24), 5052–5062. https://doi.org/10.1039/c0jm00518e

Kuwahara, Y., Tamagawa, S., Fujitani, T., & Yamashita, H. (2013). A novel conversion process for waste slag: Synthesis of calcium silicate hydrate from blast furnace slag and its application as a versatile adsorbent for water purification. *Journal of Materials Chemistry A*, *1*(24), 7199–7210. https://doi.org/10.1039/c3ta11064h

Kuwahara, Y., Tsuji, K., Ohmichi, T., Kamegawa, T., Mori, K., & Yamashita, H. (2012). Transesterifications using a hydrocalumite synthesized from waste slag: An economical and ecological route for biofuel production. *Catalysis Science and Technology*, *2*(9), 1842–1851. https://doi.org/10.1039/c2cy20113e

Kuwahara, Y., & Yamashita, H. (2015). Synthesis of Ca-based Layered Double Hydroxide from Blast Furnace Slag and Its Catalytic Applications. *ISIJ International*, *55*(7), 1531–1537. https://doi.org/10.2355/isijinternational.55.1531

Kuwahara, Y., & Yamashita, H. (2017). Phosphate Removal from Aqueous Solutions Using Calcium Silicate Hydrate Prepared from Blast Furnace Slag. *ISIJ International*, *57*(9), 1657–1664. https://doi.org/10.2355/isijinternational.isijint-2017-123

Lafuente, B., Downs, R. T., Yang, H., & Stone, N. (2016). The power of databases: The RRUFF project. *Highlights in Mineralogical Crystallography*, 1–29. https://doi.org/10.1515/9783110417104-003

Lam, M. K., Lee, K. T., & Mohamed, A. R. (2009). Sulfated tin oxide as solid superacid catalyst for transesterification of waste cooking oil: An optimization study. *Applied Catalysis B: Environmental*, *93*(1–2), 134–139. https://doi.org/10.1016/j.apcatb.2009.09.022

Larkin, P. J. (2011). *IR and Raman spectroscopy Principles and spectral interpretation* (1st ed.). https://doi.org/10.3390/rel9100297

Lee, A. F., Bennett, J. A., Manayil, J. C., & Wilson, K. (2014). Heterogeneous catalysis for sustainable biodiesel production via esterification and transesterification. *Chemical Society Reviews*, *43*(22), 7887–7916. https://doi.org/10.1039/c4cs00189c

Lee, D. W., Park, Y. M., & Lee, K. Y. (2009). Heterogeneous base catalysts for transesterification in biodiesel synthesis. *Catalysis Surveys from Asia*, *13*(2), 63–77. https://doi.org/10.1007/s10563-009-9068-6

Lee, S. H., Kim, H. J., Sakai, E., & Daimon, M. (2003). Effect of particle size distribution of fly ash-cement system on the fluidity of cement pastes. *Cement and Concrete Research*, *33*(5), 763–768. https://doi.org/10.1016/S0008-8846(02)01054-2

Lee, H. V., Juan, J. C., & Taufiq-Yap, Y. H. (2015). Preparation and application of binary acid-base CaO-La2O3 catalyst for biodiesel production. *Renewable Energy*, *74*, 124–132. https://doi.org/10.1016/j.renene.2014.07.017

Lee, W. K. W., & Van Deventer, J. S. J. (2002). Structural reorganisation of class F fly ash in alkaline silicate solutions. *Colloids and Surfaces A: Physicochemical and Engineering Aspects*, *211*(1), 49–66. https://doi.org/10.1016/S0927-7757(02)00237-6

Leung, D. Y. C., Wu, X., & Leung, M. K. H. (2010). A review on biodiesel production using catalyzed transesterification. *Applied Energy*, *87*(4), 1083–1095. https://doi.org/10.1016/j.apenergy.2009.10.006

Li, M., Zheng, Y., Chen, Y., & Zhu, X. (2014). Biodiesel production from waste cooking oil using a heterogeneous catalyst from pyrolyzed rice husk. *Bioresource Technology*, *154*, 345–348. https://doi.org/10.1016/j.biortech.2013.12.070

Lima-Corrêa, R. A. B., Castro, C. S., & Assaf, J. M. (2018). Lithium containing MgAl mixed oxides obtained from sol-gel hydrotalcite for transesterification. *Brazilian Journal of Chemical Engineering*, *35*(1), 189–195. https://doi.org/10.1590/0104-6632.20180351s20160146

Lin, L., Cunshan, Z., Vittayapadung, S., Xiangqian, S., & Mingdong, D. (2011). Opportunities and challenges for biodiesel fuel. *Applied Energy*, *88*(4), 1020–1031. https://doi.org/10.1016/j.apenergy.2010.09.029

Lotero, E., Liu, Y., Lopez, D. E., Suwannakarn, K., Bruce, D. A., & Goodwin, J. G. (2005). Synthesis

of biodiesel via acid catalysis. *Industrial and Engineering Chemistry Research*, *44*(14), 5353–5363. https://doi.org/10.1021/ie049157g

Lourinho, G., & Brito, P. (2014). Advanced biodiesel production technologies: novel developments. *Reviews in Environmental Science and Biotechnology*, *53*(4), 1387–1408. https://doi.org/10.1016/j.rser.2015.12.007

Lu, G. Q., & Do, D. D. (1991). Adsorption properties of fly ash particles for NOx removal from flue gases. *Fuel Processing Technology*, *27*(1), 95–107. https://doi.org/10.1016/0378-3820(91)90011-Z

Ma, F., Clements, L. D., & Hanna, M. (1998). the Effects of Catalyst, Free Fatty Acids, and Water on Transesterification of Beef Tallow. *Transactions of the ASAE*, *41*(5), 1261–1264. https://doi.org/10.13031/2013.17292

Ma, F., & Hanna, M. A. (1999). Biodiesel production : a review. *Bioresour Technol*, *70*(1), 1–15. https://doi.org/10.1016/S0960-8524(99)00025-5

Mahamuni, N. N., & Adewuyi, Y. G. (2009). Fourier transform infrared spectroscopy (FTIR) method to monitor soy biodiesel and soybean oil in transesterification reactions, petrodiesel- biodiesel blends, and blend adulteration with soy oil. *Energy and Fuels*, *23*(7), 3773–3782. https://doi.org/10.1021/ef900130m

Mahesar, S. A., Kandhro, A. A., Khaskheli, A. R., Talpur, M. Y., & Sherazi, S. T. H. (2014). SB-ATR FTIR spectroscopic monitoring of free fatty acids in commercially available Nigella sativa (Kalonji) oil. *Journal of Spectroscopy*, *2014*, 1–5. https://doi.org/10.1155/2014/510890

Mahesar, S. A., Shah, S. N., Mahesar, A. W., Kandhro, A. A., Khaskheli, A. R., Menghwar, P., & Sherazi, S. T. H. (2017). A chemometric approach for the quantification of free fatty acids in cottonseed oil by Fourier transform infrared spectroscopy. *International Journal of Food Properties*, *20*(8), 1913–1920. https://doi.org/10.1080/10942912.2016.1223129

Mäkelä, M., Paananen, T., Kokkonen, T., Makkonen, H., Heino, J., & Dahl, O. (2011). Preliminary evaluation of fly ash and lime for use as supplementary cementing materials in cold-agglomerated blast furnace briquetting. *ISIJ International*, *51*(5), 776–781. https://doi.org/10.2355/isijinternational.51.776

Makhlouf, A. S. H., & Aliofkhazraei, M. (Eds.). (2016). *Handbook of Materials Failure Analysis with Case Studies from the Oil and Gas Industry* (1st ed.). https://doi.org/https://doi.org/10.1016/C2014-0-01712-1

Manayil, J. C., Lee, A. F., & Wilson, K. (2019). Functionalized periodic mesoporous organosilicas: Tunable hydrophobic solid acids for biomass conversion. *Molecules*, *24*(239), 1–25. https://doi.org/10.3390/molecules24020239

Maneerung, T., Kawi, S., & Wang, C. H. (2015). Biomass gasification bottom ash as a source of CaO catalyst for biodiesel production via transesterification of palm oil. *Energy Conversion and Management*, *92*, 234–243. https://doi.org/10.1016/j.enconman.2014.12.057

Manique, M. C., Lacerda, L. V., Alves, A. K., & Bergmann, C. P. (2017). Biodiesel production using coal fly ash-derived sodalite as a heterogeneous catalyst. *Fuel*, *190*, 268–273. https://doi.org/10.1016/j.fuel.2016.11.016

Mansir, N., Rashid, U., Teo, S. H., Taufiq-Yap, Y. H., Alsultan, G. A., Tan, Y. P., & Saiman, M. I. (2018). Modified waste egg shell derived bifunctional catalyst for biodiesel production from high FFA waste cooking oil. A review. *Renewable and Sustainable Energy Reviews*, *82*(February 2018), 3645–3655. https://doi.org/https://doi.org/10.1016/j.rser.2017.10.098

Mansir, N., Taufiq-Yap, Y. H., Rashid, U., & Lokman, I. M. (2017). Investigation of heterogeneous solid acid catalyst performance on low grade feedstocks for biodiesel production: A review. *Energy Conversion and Management*, *141*, 171–182. https://doi.org/10.1016/j.enconman.2016.07.037

Mardhiah, H. H., Ong, H. C., Masjuki, H. H., Lim, S., & Lee, H. V. (2017). A review on latest developments and future prospects of heterogeneous catalyst in biodiesel production from non-edible oils. *Renewable and Sustainable Energy Reviews*, *67*, 1225–1236. https://doi.org/10.1016/j.rser.2016.09.036

Marinković, D. M., Stanković, M. V., Veličković, A. V., Avramović, J. M., Miladinović, M. R., Stamenković, O. O., Veljković, V. B., & Jovanović, D. M. (2016). Calcium oxide as a promising heterogeneous catalyst for biodiesel production: Current state and perspectives. *Renewable and Sustainable Energy Reviews*, *56*(January), 1387–1408. https://doi.org/10.1016/j.rser.2015.12.007

Marinković, M. M., Stojković, N. I., Vasić, M. B., Ljupković, R. B., Rancić, S. M., Spalović, B. R., & Zarubica, A. R. (2016). Sinteza biodizela iz suncokretovog ulja korišćenjem heterogenog katalizatora na bazi kalijum-jodida na alumini: Uticaj procesnih parametara. *Hemijska Industrija*, *70*(6), 639–648. https://doi.org/10.2298/HEMIND150807001M

Marwaha, A., Rosha, P., Mohapatra, S. K., Mahla, S. K., & Dhir, A. (2018). Waste materials as potential catalysts for biodiesel production: Current state and future scope. *Fuel Processing Technology*, *181*(September), 175–186. https://doi.org/10.1016/j.fuproc.2018.09.011

Mattigod, S. V., Rai, D., Eary, L. E., & Ainsworth, C. C. (1990). Geochemical Factors Controlling the Mobilization of Inorganic Constituents from Fossil Fuel Combustion Residues: II. Review of the Minor Elements. *Journal of Environmental Quality*, *19*(2), 202–214. https://doi.org/10.2134/jeq1990.00472425001900020005x

Matwijczuk, A., Zając, G., Kowalski, R., Kachel-Jakubowska, M., & Gagoś, M. (2017). Spectroscopic studies of the quality of fatty acid methyl esters derived from waste cooking oil. *Polish Journal of Environmental Studies*, *26*(6), 2643–2650. https://doi.org/10.15244/pjoes/70431

Meher, L. C., Vidya Sagar, D., & Naik, S. N. (2006). Technical aspects of biodiesel production by transesterification - A review. *Renewable and Sustainable Energy Reviews*, *10*(3), 248–268. https://doi.org/10.1016/j.rser.2004.09.002

Mendonça, I. M., Paes, O. A. R. L., Maia, P. J. S., Souza, M. P., Almeida, R. A., Silva, C. C., Duvoisin, S., & de Freitas, F. A. (2019). New heterogeneous catalyst for biodiesel production from waste tucumã peels (Astrocaryum aculeatum Meyer): Parameters optimization study. *Renewable Energy*, *130*, 103–110. https://doi.org/10.1016/j.renene.2018.06.059

Mindat. (n.d.). Retrieved from https://www.mindat.org/

Mofijur, M., Atabani, A. E., Masjuki, H. H., Kalam, M. A., & Masum, B. M. (2013). A study on the effects of promising edible and non-edible biodiesel feedstocks on engine performance and emissions production: A comparative evaluation. *Renewable and Sustainable Energy Reviews*, *23*, 391–404. https://doi.org/10.1016/j.rser.2013.03.009

Monteiro, M. R., Ambrozin, A. R. P., Lião, L. M., & Ferreira, A. G. (2008). Critical review on analytical methods for biodiesel characterization. *Talanta*, *77*(2), 593–605. https://doi.org/10.1016/j.talanta.2008.07.001

Moreno, N., Querol, X., Andrés, J. M., Stanton, K., Towler, M., Nugteren, H., Janssen-Jurkovicová, M., & Jones, R. (2005). Physico-chemical characteristics of European pulverized coal combustion fly ashes. *Fuel*, *84*(11), 1351–1363. https://doi.org/10.1016/j.fuel.2004.06.038

Moss, G. P., Smith, P. A. S., & Tavernier, D. (1995). Glossary of class names of organic compounds and reactivity intermediates based on structure (IUPAC Recommendations 1995). *Pure and Applied Chemistry*, Vol. 67, p. 1307. https://doi.org/10.1351/pac199567081307

Mukherjee, A. B., Zevenhoven, R., Bhattacharya, P., Sajwan, K. S., & Kikuchi, R. (2008). Mercury flow via coal and coal utilization by-products: A global perspective. *Resources, Conservation and Recycling*, *52*(4), 571–591. https://doi.org/10.1016/j.resconrec.2007.09.002

Muriithi, G. N., Petrik, L. F., Gitari, W. M., & Doucet, F. J. (2017). Synthesis and characterization of hydrotalcite from South African Coal fly ash. *Powder Technology*, *312*, 299–309. https://doi.org/10.1016/j.powtec.2017.02.018

Murtha, M. J., Burnet, G., & Harnby, N. (1983). Power plant fly ash - Disposal and utilization. *Environmental Progress*, *2*(3), 193–198.

Nanakoudis, A. (2019). *SEM: Types of Electrons and the Information They Provide*. Retrieved from https://www.thermofisher.com/blog/microscopy/sem-types-electrons-and-the-information-they-provide/

Narasimha, C., Rajesh, M., Rice, K., & Nitrate, E. H. (2013). Performance and emissions characteristics of diesel engine fuelled with rice bran oil. *International Journal of Engineering Trends and Technology*, *4*(10), 4574–4578.

Narasimharao, K., Lee, A., & Wilson, K. (2007). Catalysis in production of biodiesel: A review. *Journal of Biobased Materials and Bioenergy*, *1*, 1–12. https://doi.org/10.1166/jbmb.2007.002

Nasrazadani, S., & Eureste, E. (2008). Application of FTIR for Quantitative Lime Analysis. *University of North Texas*, *1*(1), 60.

Natalello, A., Sasso, F., & Secundo, F. (2013). Enzymatic transesterification monitored by an easy-to-use Fourier transform infrared spectroscopy method. *Biotechnology Journal*, *8*(1), 133–138. https://doi.org/10.1002/biot.201200173

OECD. (1997). Glossary of Environment Statistics. In *Studies in Methods Series F*. New York, USA: United Nations Publications.

Olfs, H. W., Torres-Dorante, L. O., Eckelt, R., & Kosslick, H. (2009). Comparison of different synthesis routes for Mg-Al layered double hydroxides (LDH): Characterization of the structural phases and anion exchange properties. *Applied Clay Science*, *43*(3–4), 459–464. https://doi.org/10.1016/j.clay.2008.10.009

Othman, M. R., Helwani, Z., Martunus, & Fernando, W. J. N. (2009). Synthetic hydrotalcites from different routes and their application as catalysts and gas adsorbents: A review. *Applied Organometallic Chemistry*, *23*(9), 235–246. https://doi.org/10.1002/aoc.1517

Ozcanli, M., Gungor, C., & Aydin, K. (2013). Biodiesel fuel specifications: A review. *Energy Sources, Part A: Recovery, Utilization and Environmental Effects*, *35*(7), 635–647. https://doi.org/10.1080/15567036.2010.503229

Pandey, S., & Sengupta, J. B. (2014). Fourier Transform Infrared Spectroscopy: A tool for detection of lime content in hot mix asphalt. *26th ARRB Conference – Research Driving Efficiency*, 1–11.

Pandian, N. S. (2004). Fly ash characterization with reference to geotechnical applications. *Journal of the Indian Institute of Science*, *84*(6), 189–216.

Parr, S. W. (1922). The Classification of Coal. *Journal of Industrial & Engineering Chemistry*, *14*(10), 919–922. https://doi.org/10.1021/ie50154a019

Pavlović, S. M., Marinković, D. M., Kostić, M. D., Janković-Častvan, I. M., Mojović, L. V., Stanković, M. V., & Veljković, V. B. (2020). A CaO/zeolite-based catalyst obtained from waste chicken eggshell and coal fly ash for biodiesel production. *Fuel*, *267*(September 2019), 117171. https://doi.org/10.1016/j.fuel.2020.117171

Petkowicz, D. I., Radtke, C., dos Santos, J. H. Z., Pergher, S. B., & Rigo, R. T. (2008). Zeolite NaA from Brazilian chrysotile and rice husk. *Microporous and Mesoporous Materials*, *116*(1–3), 548–554. https://doi.org/10.1016/j.micromeso.2008.05.014

Pighinelli, A. L. M. T. (2007). *Extração mecânica de óleos de amendoim e de girassol para produçao de biodiesel via catálise básica* (Universidade Estadual de Campinas (Unicamp)). Retrieved from http://repositorio.unicamp.br/jspui/handle/REPOSIP/257085

Policht-Latawiec, A. (2013). Selected physicochemical properties of tested wastes from combined heat and power plants with regards to their potential applications. *Teka Komisji Ochrony i Kształtowania Środowiska Przyrodniczego*, (10), 143–152.

Pradana, Y. S., Fauzi, A., Pratama, S. H., & Sudibyo, H. (2018). Simulation of biodiesel production using hydro-esterification process from wet microalgae. *MATEC Web of Conferences*, *154*. https://doi.org/10.1051/matecconf/201815401007

Prankl, H., Körbitz, W., Mittelbach, M., & Wörgetter, M. (2004). Review on biodiesel standardization world-wide. *IEA Bioenergy Task*, *39*(May), 38–46. Retrieved from http://task39.sites.olt.ubc.ca/files/2013/05/Review-on-Biodiesel-Standardization.pdf

Rabelo, S. N., Ferraz, V. P., Oliveira, L. S., & Franca, A. S. (2015). FTIR Analysis for Quantification of Fatty Acid Methyl Esters in Biodiesel Produced by Microwave-Assisted Transesterification. *International Journal of Environmental Science and Development*, *6*(12), 964–969. https://doi.org/10.7763/ijesd.2015.v6.730

Rabiah Nizah, M. F., Taufiq-Yap, Y. H., Rashid, U., Teo, S. H., Shajaratun Nur, Z. A., & Islam, A.

(2014). Production of biodiesel from non-edible Jatropha curcas oil via transesterification using Bi2O3-La2O3 catalyst. *Energy Conversion and Management*, *88*, 1257–1262. https://doi.org/10.1016/j.enconman.2014.02.072

Ram, L. C., & Masto, R. E. (2014). Fly ash for soil amelioration: A review on the influence of ash blending with inorganic and organic amendments. *Earth-Science Reviews*, *128*, 52–74. https://doi.org/10.1016/j.earscirev.2013.10.003

Ramadhas, A. S., Muraleedharan, C., & Jayaraj, S. (2005). Performance and emission evaluation of a diesel engine fueled with methyl esters of rubber seed oil. *Renewable Energy*, *30*(12), 1789–1800. https://doi.org/10.1016/j.renene.2005.01.009

Ramezanianpour, A. A. (2014). *Cement Replacement Materials* (1st ed.). https://doi.org/https://doi.org/10.1007/978-3-642-36721-2

Ramli, A., Farooq, M., Naeem, A., Khan, S., Hummayun, M., Iqbal, A., Ahmed, S., & Shah, L. A. (2017). Bifunctional Heterogeneous Catalysts for Biodiesel Production using Low Cost Feedstocks: A Future Perspective. *Frontiers in Bioenergy and Biofuels*. https://doi.org/10.5772/65553

Ranjbar, N., & Kuenzel, C. (2017). Cenospheres: A review. *Fuel*, *207*, 1–12. https://doi.org/10.1016/j.fuel.2017.06.059

Reid, E. E. (1911). No Title. *Journal of the American Oil Chemists Society*, *45*(506).

Reyes, Y., Chenard, G., Aranda, D., Mesquita, C., Fortes, M., João, R., & Bacellar, L. (2012). Biodiesel production by hydroesterification of microalgal biomass using heterogeneous catalyst. *Natural Science*, *04*(10), 778–783. https://doi.org/10.4236/ns.2012.410102

Rigaudy, J., & Klesney, S. P. (1979). *Nomenclature of Organic Chemistry - Internatinal Union of Pure and Applied Chemistry (IUPAC)*. Oxford; New York: Pergamon Press.

Rochleder, F. (1847). Observations on glycerine. In W. Francis (Ed.), *Chemical Gazette or Journal of Practical Chemistry* (Vol. 5, p. 508).

Rodriguez-Blanco, J. D., Shaw, S., & Benning, L. G. (2011). The kinetics and mechanisms of amorphous calcium carbonate (ACC) crystallization to calcite, via vaterite. *Nanoscale*, *3*(1), 265–271. https://doi.org/10.1039/c0nr00589d

Rodríguez-Fernández, J., Hernández, J. J., Calle-Asensio, A., Ramos, Á., & Barba, J. (2019).

Selection of blends of diesel fuel and advanced biofuels based on their physical and thermochemical properties. *Energies*, *12*(11), 1–13. https://doi.org/10.3390/en12112034

Roschat, W., Siritanon, T., Yoosuk, B., & Promarak, V. (2016a). Biodiesel production from palm oil using hydrated lime-derived CaO as a low-cost basic heterogeneous catalyst. *Energy Conversion and Management*, *108*, 459–467. https://doi.org/10.1016/j.enconman.2015.11.036

Roschat, W., Siritanon, T., Yoosuk, B., & Promarak, V. (2016b). Rice husk-derived sodium silicate as a highly efficient and low-cost basic heterogeneous catalyst for biodiesel production. *Energy Conversion and Management*, *119*, 453–462. https://doi.org/10.1016/j.enconman.2016.04.071

Rosset, M., & Perez-Lopez, O. W. (2019). FTIR spectroscopy analysis for monitoring biodiesel production by heterogeneous catalyst. *Vibrational Spectroscopy*, *105*(September), 102990. https://doi.org/10.1016/j.vibspec.2019.102990

RSC. (n.d.). Chemspider. Retrieved November 5, 2019, from https://www.chemspider.com/

Rubel, A., Andrews, R., Gonzalez, R., Groppo, J., & Robl, T. (2005). Adsorption of Hg and NOX on coal by-products. *Fuel*, *84*(7–8), 911–916. https://doi.org/10.1016/j.fuel.2005.01.006

Ruhul, A. M., Kalam, M. A., Masjuki, H. H., Fattah, I. M. R., Reham, S. S., & Rashed, M. M. (2015). State of the art of biodiesel production processes: A review of the heterogeneous catalyst. *RSC Advances*, *5*(122), 101023–101044. https://doi.org/10.1039/c5ra09862a

Sahoo, P. K., Das, L. M., Babu, M. K. G., Arora, P., Singh, V. P., Kumar, N. R., & Varyani, T. S. (2009). Comparative evaluation of performance and emission characteristics of jatropha, karanja and polanga based biodiesel as fuel in a tractor engine. *Fuel*, *88*(9), 1698–1707. https://doi.org/10.1016/j.fuel.2009.02.015

Sanchez-Valente, J., Lopez-Salinas, E., & Sanchez-Cantu, M. (2008). *Patent No. US000007807128B220101005*.

Sanchez-Valente, J., Lopez-Salinas, E., & Sanchez-Cantu, M. (2010). *Patent No. US000007740828B220100622*.

Schwab, A. W., Bagby, M., & Freedman, B. (1987). Preparation and properties from vegetable oils. *Fuel*, *66*, 1372–1378.

Scott, A. C. (2018). *Burning Planet – The history of fire through the time* (1st ed.). Oxford, UK: Oxford University Press: 1st.

Shan, R., Lu, L., Shi, Y., Yuan, H., & Shi, J. (2018). Catalysts from renewable resources for biodiesel production. *Energy Conversion and Management*, *178*(July), 277–289. https://doi.org/10.1016/j.enconman.2018.10.032

Sharma, M., Khan, A. A., Puri, S. K., & Tuli, D. K. (2012). Wood ash as a potential heterogeneous catalyst for biodiesel synthesis. *Biomass and Bioenergy*, *41*, 94–106. https://doi.org/10.1016/j.biombioe.2012.02.017

Sharma, Y. C., Singh, B., & Korstad, J. (2010). Application of an efficient nonconventional heterogeneous catalyst for biodiesel synthesis from pongamia pinnata oil. *Energy and Fuels*, *24*(5), 3223–3231. https://doi.org/10.1021/ef901514a

Sharma, Yogesh C., Singh, B., & Korstad, J. (2011a). Advancements in solid acid catalysts for ecofriendly and economically viable synthesis of biodiesel. *Biofuels, Bioproducts and Biorefining*, *5*(1), 69–92. https://doi.org/https://doi.org/10.1002/bbb.253

Sharma, Yogesh C., Singh, B., & Korstad, J. (2011b). Latest developments on application of heterogenous basic catalysts for an efficient and eco friendly synthesis of biodiesel: A review. *Fuel*, *90*(4), 1309–1324. https://doi.org/10.1016/j.fuel.2010.10.015

Shu, Q., Yang, B., Yuan, H., Qing, S., & Zhu, G. (2007). Synthesis of biodiesel from soybean oil and methanol catalyzed by zeolite beta modified with La3+. *Catalysis Communications*, *8*(12), 2159–2165. https://doi.org/10.1016/j.catcom.2007.04.028

Siatis, N. G., Kimbaris, A. C., Pappas, C. S., Tarantilis, P. A., & Polissiou, M. G. (2006). Improvement of biodiesel production based on the application of ultrasound: Monitoring of the procedure by FTIR spectroscopy. *JAOCS, Journal of the American Oil Chemists' Society*, *83*(1), 53–57. https://doi.org/10.1007/s11746-006-1175-1

Silva, C. C. C. M., Ribeiro, N. F. P., Souza, M. M. V. M., & Aranda, D. A. G. (2010). Biodiesel production from soybean oil and methanol using hydrotalcites as catalyst. *Fuel Processing Technology*, *91*(2), 205–210. https://doi.org/10.1016/j.fuproc.2009.09.019

Silverstein, R. M., Webster, F. X., & Kiemle, D. (2005). *Spectrometric Identification of Organic Compounds* (7th ed.). Hoboken, New Jersey, USA: John Wiley & Sons, Ltd: 7th.

Singh, A., & Gaurav, K. (2018). Advancement in Catalysts for Transesterification in the Production of Biodiesel : A Review. *Journal of Biochemical Technology*, *7*, 1148–1158.

Sivasamy, A., Cheah, K. Y., Fornasiero, P., Kemausuor, F., Zinoviev, S., & Miertus, S. (2009).

Catalytic applications in the production of biodiesel from vegetable oils. *ChemSusChem*, *2*(4), 278–300. https://doi.org/10.1002/cssc.200800253

Snellings, R., Mertens, G., & Elsen, J. (2012). Supplementary cementitious materials. *Reviews in Mineralogy and Geochemistry*, *74*, 211–278. https://doi.org/10.2138/rmg.2012.74.6

Soares Dias, A. P., Bernardo, J., Felizardo, P., & Neiva Correia, M. J. (2012). Biodiesel production over thermal activated cerium modified Mg-Al hydrotalcites. *Energy*, *41*(1), 344–353. https://doi.org/10.1016/j.energy.2012.03.005

Soares Dias, A. P., Puna, J., Gomes, J., Neiva Correia, M. J., & Bordado, J. (2016). Biodiesel production over lime. Catalytic contributions of bulk phases and surface Ca species formed during reaction. *Renewable Energy*, *99*, 622–630. https://doi.org/10.1016/j.renene.2016.07.033

Soares Dias, A. P., Puna, J., Neiva Correia, M. J., Nogueira, I., Gomes, J., & Bordado, J. (2013). Effect of the oil acidity on the methanolysis performances of lime catalyst biodiesel from waste frying oils (WFO). *Fuel Processing Technology*, *116*, 94–100. https://doi.org/10.1016/j.fuproc.2013.05.002

Soares Dias, A. P., Ramos, M., Catarino, M., Puna, J., & Gomes, J. (2019). Solvent Assisted Biodiesel Production by Co-processing Beef Tallow and Soybean Oil Over Calcium Catalysts. *Waste and Biomass Valorization*. https://doi.org/10.1007/s12649-019-00903-7

Soares, I. P., Rezende, T. F., Silva, R. C., Castro, E. V. R., & Fortes, I. C. P. (2008). Multivariate calibration by variable selection for blends of raw soybean oil/biodiesel from different sources using Fourier transform infrared spectroscopy (FTIR) spectra data. *Energy and Fuels*, *22*(3), 2079–2083. https://doi.org/10.1021/ef700531n

Soriano, N. U., Venditti, R., & Argyropoulos, D. S. (2009). Biodiesel synthesis via homogeneous Lewis acid-catalyzed transesterification. *Fuel*, *88*(3), 560–565. https://doi.org/10.1016/j.fuel.2008.10.013

Sotelo-Boyás, R., Trejo-Zárraga, F., & Hernández-Loyo, F. de J. (2012). Hydroconversion of triglycerides into green liquid fuels. In I. Karamé (Ed.), *Hydrogenation* (1st ed., pp. 187–216). https://doi.org/10.5772/3208

Srivastava, A., & Prasad, R. (2000). Triglycerides-based diesel fuels. *Renewable & Sustainable Energy Reviews*, *4*(2), 111–133. https://doi.org/10.1016/S1364-0321(99)00013-1

Strezov, V., & Evans, T. J. (2014). Biomass processing technologies. In *Biomass Processing*

Technologies. https://doi.org/10.1201/b17093

Stumborg, M., Wong, A., & Hogan, E. (1996). Hydroprocessed vegetable oils for diesel fuel improvement. *Bioresource Technology*, *56*(1), 13–18. https://doi.org/10.1016/0960-8524(95)00181-6

Summers, K., Rupp, G. L., & Gherini, S. (1983). *Physical-chemical characteristics of utility solid wastes EPRI EA-3236*. Palo Alto, USA: Electric Power Research Institute.

Tanabe, K., & Fukuda, Y. (1974). Basic properties of alkaline earth metal oxides and their catalytic activity in the decomposition of diacetone alcohol. *Reaction Kinetics and Catalysis Letters*, *1*(1), 21–24. https://doi.org/10.1007/BF02075116

Tang, Z. E., Lim, S., Pang, Y. L., Ong, H. C., & Lee, K. T. (2018). Synthesis of biomass as heterogeneous catalyst for application in biodiesel production: State of the art and fundamental review. *Renewable and Sustainable Energy Reviews*, *92*(May), 235–253. https://doi.org/10.1016/j.rser.2018.04.056

Thanh, L. T., Okitsu, K., Boi, L. Van, & Maeda, Y. (2012). Catalytic Technologies for Biodiesel Fuel Production and Utilization of Glycerol: A Review. *Catalysts*, *2*(1), 191–222. https://doi.org/10.3390/catal2010191

Tichit, D., & Coq, B. (2003). Catalysis by Hydrotalcites and Related Materials. *CATTECH*, *7*(6), 206–217. https://doi.org/10.1023/B:CATT.0000007166.65577.34

Tichit, D., Gérardin, C., Durand, R., & Coq, B. (2006). Layered double hydroxides: Precursors for multifunctional catalysts. *Topics in Catalysis*, *39*(1–2), 89–96. https://doi.org/10.1007/s11244-006-0041-6

Tomasevic, A. V., & Siler-Marinkovic, S. S. (2003). Methanolysis of used frying oil. *Fuel Processing Technology*, *81*(1), 1–6. https://doi.org/10.1016/S0378-3820(02)00096-6

Torres, A., Fuentes, B., Rodríguez, K. E., Brito, A., & Díaz, L. (2020). Analysis of the Content of Fatty Acid Methyl Esters in Biodiesel by Fourier-Transform Infrared Spectroscopy: Method and Comparison with Gas Chromatography. *JAOCS, Journal of the American Oil Chemists' Society*, *97*(6), 651–661. https://doi.org/10.1002/aocs.12350

Valente, J. S., Sánchez-Cantú, M., & Figueras, F. (2008). A simple environmentally friendly method to prepare versatile hydrotalcite-like compounds. *Chemistry of Materials*, *20*(4), 1230–1232. https://doi.org/10.1021/cm7031306

Valente, J. S., Sánchez-Cantú, M., Lima, E., & Figueras, F. (2009). Method for large-scale production of multimetallic layered double hydroxides: Formation mechanism discernment. *Chemistry of Materials*, *21*(24), 5809–5818. https://doi.org/10.1021/cm902377p

Van Gerpen, J. H., Hammond, E. G., Johnson, L. A., Marley, S. J., Yu, L., Lee, I., & Monyem, A. (2010). Determining the Influence of Contaminants on Biodiesel Properties. *SAE Technical Paper Series*, *1*. https://doi.org/10.4271/971685

Vargas, E. M., Neves, M. C., Tarelho, L. A. C., & Nunes, M. I. (2019). Solid catalysts obtained from wastes for FAME production using mixtures of refined palm oil and waste cooking oils. *Renewable Energy*, *136*, 873–883. https://doi.org/10.1016/j.renene.2019.01.048

Vassilev, S. V., & Vassileva, C. G. (1996a). Mineralogy of combustion wastes from coal-fired power stations. *Fuel Processing Technology*, *47*(3), 261–280. https://doi.org/10.1016/0378-3820(96)01016-8

Vassilev, S. V., & Vassileva, C. G. (1996b). Occurrence, abundance and origin of minerals in coals and coal ashes. *Fuel Processing Technology*, *48*(2), 85–106. https://doi.org/10.1016/S0378-3820(96)01021-1

Vassilev, S. V., & Vassileva, C. G. (2005). Methods for characterization of composition of fly ashes from coal-fired power stations: A critical overview. *Energy and Fuels*, *19*(3), 1084–1098. https://doi.org/10.1021/ef049694d

Vichaphund, S., Aht-Ong, D., Sricharoenchaikul, V., & Atong, D. (2014). Characteristic of fly ash derived-zeolite and its catalytic performance for fast pyrolysis of Jatropha waste. *Environmental Technology (United Kingdom)*, *35*(17), 2254–2261. https://doi.org/10.1080/09593330.2014.900118

Volli, V., & Purkait, M. K. (2015). Preparation and characterization of hydrotalcite-like materials from flyash for transesterification. *Clean Technologies and Environmental Policy*, *18*(2), 529–540. https://doi.org/10.1007/s10098-015-1036-4

Wang, S., & Wu, H. (2006). Environmental-benign utilisation of fly ash as low-cost adsorbents. *Journal of Hazardous Materials*, *136*(3), 482–501. https://doi.org/10.1016/j.jhazmat.2006.01.067

Wdowin, M., Franus, M., Panek, R., Badura, L., & Franus, W. (2014). The conversion technology of fly ash into zeolites. *Clean Technologies and Environmental Policy*, *16*(6), 1217–1223. https://doi.org/10.1007/s10098-014-0719-6

Wilson, K., Hardacre, C., Lee, A. F., Montero, J. M., & Shellard, L. (2008). The application of calcined natural dolomitic rock as a solid base catalyst in triglyceride transesterification for biodiesel synthesis. *Green Chemistry*, *10*(6), 654–659. https://doi.org/10.1039/b800455b

Wilson, K., & Lee, A. F. (2012). Rational design of heterogeneous catalysts for biodiesel synthesis. *Catalysis Science and Technology*, *2*(5), 884–897. https://doi.org/10.1039/c2cy20038d

Wrangham, R. (2009). *Catching Fire How cooking made us human*. New York: Basic Books (Perseus Books Group).

Xiang, Y., Wang, L., & Jiao, Y. (2016). Ultrasound strengthened biodiesel production from waste cooking oil using modified coal fly ash as catalyst. *Journal of Environmental Chemical Engineering*, *4*(1), 818–824. https://doi.org/10.1016/j.jece.2015.12.031

Xie, W., & Li, H. (2006). Alumina-supported potassium iodide as a heterogeneous catalyst for biodiesel production from soybean oil. *Journal of Molecular Catalysis A: Chemical*, *255*(1–2), 1–9. https://doi.org/10.1016/j.molcata.2006.03.061

Yao, Z. T., Ji, X. S., Sarker, P. K., Tang, J. H., Ge, L. Q., Xia, M. S., & Xi, Y. Q. (2015). A comprehensive review on the applications of coal fly ash. *Earth-Science Reviews*, *141*, 105–121. https://doi.org/10.1016/j.earscirev.2014.11.016

Yergin, D. (2008). *The prize: The epic quest for oil, money, and power*. New York: Simon & Schuster.

Yusuf, N. N. A. N., Kamarudin, S. K., & Yaakub, Z. (2011). Overview on the current trends in biodiesel production. *Energy Conversion and Management*, *52*(7), 2741–2751. https://doi.org/10.1016/j.enconman.2010.12.004

Zabeti, M., Wan Daud, W. M. A., & Aroua, M. K. (2009). Activity of solid catalysts for biodiesel production: A review. *Fuel Processing Technology*, *90*(6), 770–777. https://doi.org/10.1016/j.fuproc.2009.03.010

Zaki, M. I., Knözinger, H., Tesche, B., & Mekhemer, G. A. H. (2006). Influence of phosphonation and phosphation on surface acid-base and morphological properties of CaO as investigated by in situ FTIR spectroscopy and electron microscopy. *Journal of Colloid and Interface Science*, *303*(1), 9–17. https://doi.org/10.1016/j.jcis.2006.07.011

Zeng, D., Liu, S., Gong, W., Wang, G., Qiu, J., & Chen, H. (2014). Synthesis, characterization and acid catalysis of solid acid from peanut shell. *Applied Catalysis A: General*, *469*, 284–289.

https://doi.org/10.1016/j.apcata.2013.09.038

Zhang, W. B. (2012). Review on analysis of biodiesel with infrared spectroscopy. *Renewable and Sustainable Energy Reviews*, *16*(8), 6048–6058. https://doi.org/10.1016/j.rser.2012.07.003

Zhang, Z., Xiao, Y., Wang, B., Sun, Q., & Liu, H. (2017). Waste is a Misplayed Resource: Synthesis of Zeolites from Fly Ash for CO2 Capture. *Energy Procedia*, *114*(November 2016), 2537–2544. https://doi.org/10.1016/j.egypro.2017.08.036

Żyrkowski, M. J. (2014). *Characterisation of fly-ash cenospheres from coal-fired power plant unit* (University of Lisbon - Instituto Superior Técnico). Retrieved from https://fenix.tecnico.ulisboa.pt/cursos/mege/dissertacao/565303595499581

APPENDIX A

Esterification reaction:

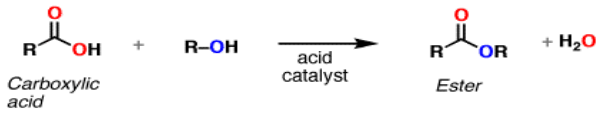

Esterification reaction detailed mechanism:

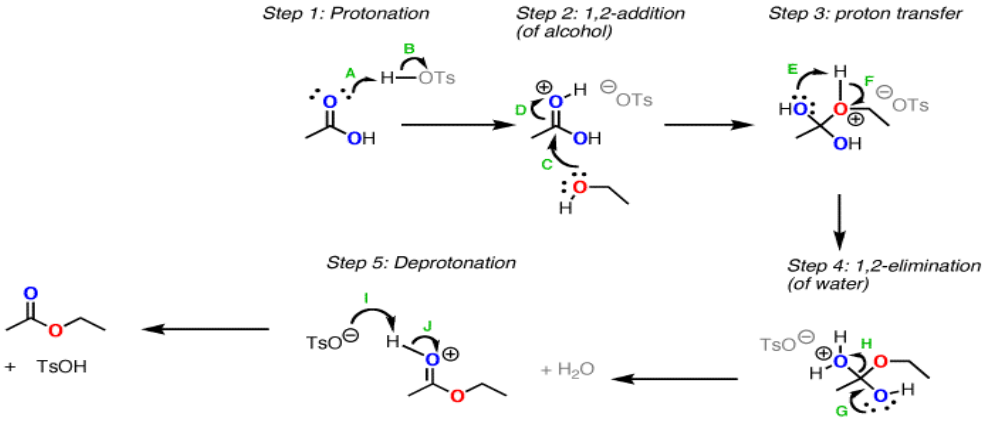

Alternative proton transfer mechanism (via water molecule):

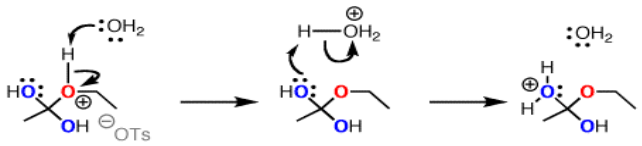

Figure A1 – Representation of the Fischer-Speier esterification mechanism. Adapted from: Master Organic Chemistry LLC

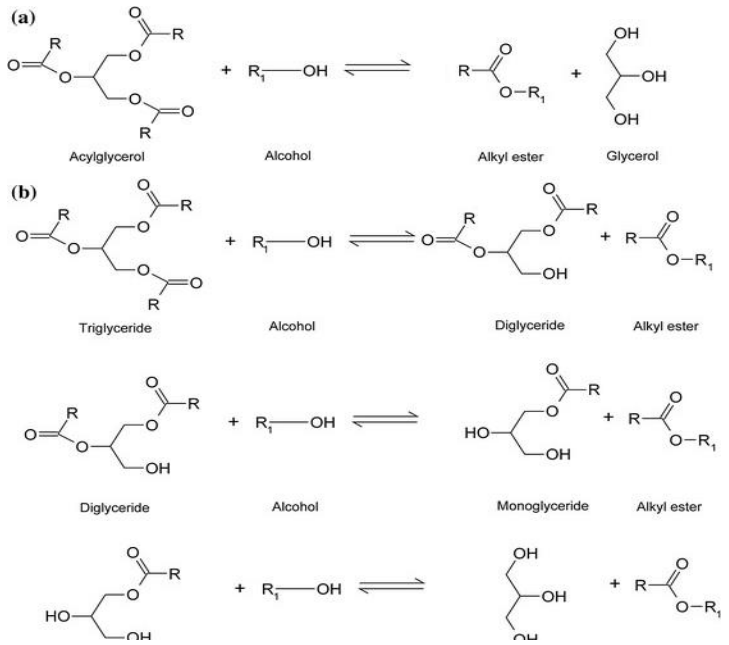

Figure A2 – Transesterification reaction mechanism. Adapted from: Lourinho & Brito (2014)

Table A1 – Classification of major fatty acids

SATURATED		
Trivial Name	**IUPAC's Official Name**	**Lipid No.**
Propionic	Propanoic	C3:0
Butyric	Butanoic	C4:0
Valeric	Pentanoic	C5:0
Caproic	Hexanoic	C6:0
Enanthic	Heptanoic	C7:0
Caprylic	Octanoic	C8:0
Capric	Decanoic	C10:0
Lauric	Dodecanoic	C12:0
Myristic	Tetradecanoic	C14:0
Palmitic	Hexadecanoic	C16:0
Stearic	Octadecanoic	C18:0
Arachidic	Eicosanoic	C20:0
Behenic	Docosanoic	C22:0
Lignoceric	Tetracosanoic	C24:0
Cerotic	Hexacosanoic	C26:0

INSATURATED				
Trivial Name	**IUPAC's Official Name**	**Δ^x**	**n-x/ ω-x**	**Lipid No.**
Palmitoleic	9 -hexadecaenoic (cis)	Δ^9	n-7 (or ω-7)	C16:1
Ricinoleic	12 - hydroxyoctadeca-9-enoic (cis)	Δ^9	n-9/ ω-9	C18:1
Oleic	9 - octadecaenoic (cis)	Δ^9	n-9/ ω-9	C18:1
Elaidic	9 - octadecaenoic (trans)	Δ^9	n-9/ ω-9	C18:1
Vaccenic	11 - octadecaenoic (trans)	Δ^{11}	n-7/ ω-7	C18:1
Linoleic	9, 12 - octadecadienoic (cis)	$\Delta^{9, 12}$	n-6/ ω-6	C18:2
Linolelaidic	9, 12 - octadecadienoic (trans)	$\Delta^{9, 12}$	n-6/ ω-6	C18:2
γ - Linolenic	6, 9, 12 - octadecatrienoic (cis)	$\Delta^{6, 9, 12}$	n-6/ ω-6	C18:3
α – Linolenic	6, 9, 15 - octadecatrienoic (cis)	$\Delta^{6, 9, 15}$	n-3/ ω-3	C18:3
Gondoic	11 - eicosaenoic (cis)	Δ^{11}	n-9/ ω-9	C20:1
Paullinic	13 - eicosaenoic (cis)	Δ^{13}	n-7/ ω-7	C20:1
Arachidonic	5, 8, 11, 14 - eicosatetraenoic (cis)	$\Delta^{5, 8, 11, 14}$	n-6/ ω-6	C20:4
Timnodonic	5,8,11,14,17 - eicosapentaenoic (cis)	$\Delta^{5, 8, 11, 14, 17}$	n-3/ ω-3	C20:5
Erucic	13 - docosenoic (cis)	Δ^{13}	n-9/ ω-9	C22:1
Cervonic	4, 7, 10 13, 16, 19 – docosahexaenoic (cis)	$\Delta^{4, 7, 10, 13, 16, 19}$	n-3/ ω-3	C22:6
Nervonic	15 - tetracosenoic (cis)	Δ^{15}	n-9/ ω-9	C24:1

Remarks:

The nomenclature n-x (or ω-x) indicates, by definition, the location of the double bond in the carbon chain (carbon-carbon) considering as referential the last methyl (CH_3), which means, the last carbon of the whole chain.

The nomenclature Lipid Number indicates the quantity of carbons (number followed by C) and the quantity of double bonds (after the ":" punctuation).

The Δ^X nomenclature precisely indicates the positions, considering the carbon chain (carbon-carbon) of the double bonds starting from the carboxyle.

Source: Moss, Smith & Tavernier (1995b); Rigaudy & Klesney (1979)

Table A2 – Fatty acid composition of major raw materials for biodiesel production

Vegetable Oil	Fatty Acid Description																	Ref.
	12:0	14:0	16:0	16:1	18:0	18:1	18:1 OH	18:2	18:3	20:0	20:1	20:4	20:5	22:0	22:1	24:0	24:1	
Soybean	0.1	0.1	10.2	–	3.7	22.8	–	53.7	8.6	–	–	–	–	–	–	–	–	[A]
Corn	–	<0.1	8 - 13	<1.0	1 - 4	24 - 32	–	55 - 62	<2.0	<1.0	–	–	–	<0.5	–	–	–	[B]
Palm	0.3	1.2	44.3	–	4.3	39.3	–	10.0	–	–	–	–	–	–	–	–	–	[C]
Palm Kernel	50.1	15.4	7.3	–	1.8	14.5	–	2.4	–	–	–	–	–	–	–	–	–	[C]
Castor	–	–	1-1.5	–	0.5-1.5	2.5-4	86-92	2.8-6	0.2-0.8	–	–	–	–	–	–	–	–	[D]
Sunflower	–	–	5.2	0.1	3.7	33.7	–	56.5	–	–	–	–	–	–	–	–	–	[E]
Rapeseed	–	0.1	4.2	0.3	2.1	62.8	–	19.2	9.0	0.7	1.2	–	–	0.3	–	0.2	0.1	[F]
Physic Nut	–	–	18.5	–	2.3	49.0	–	29.7	–	–	–	–	–	–	–	–	–	[G]
WFO[1]	–	0.394	10.42	4.69		24.03	–	53.65	6.81	–	–	–	–	–	–	–	–	[H]
Beef Tallow	0.1	2.8	23.3	–	19.4	42.4	–	2.9	0.9	–	–	–	–	–	–	–	–	[A]
Pork Lard	0.1	1.4	23.6	–	14.2	44.2	–	10.7	0.4	–	–	–	–	–	–	–	–	[A]
Poultry Fat	–	–	22.2	8.4	5.1	42.3	–	19.3	–	2.7	–	–	–	–	–	–	–	[K]
Fish Oil[2]	–	3.58	24.1	6.87	0.0	41.54	–	19.86	1.44	–	1.70	–	–	–	–	–	–	[I]
Algae[3]	5.0	–	37.5	23.3	0.9	11.9	–	1.5	–	0.1	–	3.3	15.3	0.4	–	–	–	[J]

Remarks:

[1]WFO composition varies a lot among samples. It is presented just for comparison reasons.
*[2]Fish oil refers to Tilapia (*Oreochromis niloticus*).*
[3]Algae oil refers to Nannochloropsis salina*.*

References:

[A] Kincs (1985); [B] Ghazani & Marangoni (2015); [C] Jalani et al. (1997); [D] Bockisch (1998); [E] Kamal-Eldin & Andersson (1997); [F] Soares Dias et al. (2016); [G] Banerji et al. (1985); [H] Knothe & Steidley (2009); [I] El-Rahman et al. (2018); [J] Huerlimann, de Nys & Heimann (2010); [K] Engel et al. (2001).

111

Table A3 – Biodiesel technical standards and requirements

Property	Unit	Limits		Test Method	
		ASTM D6751	EN 14214	ASTM D6751	EN 14214
Flash Point	°C	130.0 (min)	130.0 (min)	D93	ISO CD3679e
Kinematic Viscosity at 40 °C	mm²/ s	1.9 – 6.0	3.5 – 5.0	D445	EN ISO 3104
Cetane Number	–	47 (min.)	51 (min.)	D613	EN ISO 5165
Sulphated Ash content	% (m/ m)	0.020 (max.)	–	D874	ISO 3987
Copper Strip Corrosion	–	No. 3 (max.)	Class 1	D130	EN ISO 2160
Acid Value	mg KOH/ g	0.80 (max.)	0.5 (max.)	D664	EN 14104
Free Glycerol	% (m/ m)	0.020 (max.)	–	D6584	EN 14105m EN 14016
Total Glycerol	% (m/ m)	0.240 (max.)	0.25 (max.)	D6584	EN 14105m
Phosphorous content	% (m/ m)	0.001 (max.)	0.01 (max.)	D4951	EN 14107 EN 16294
Carbon Residue	% (m/ m)	0.050 (max. for 100 % sample)	0.3 (max. for 10 % bottoms)	D4530	EN ISO 10370
Cloud Point	°C	Report customer	–	D2500	–
Density at 15 °C	kg/ m³	–	860 - 900	–	EN ISO 3675 EN ISO 12185
Distillation T90 AET	°C	360 (max.)	–	D1160	–
Sulfur (S15 grade)	ppm	0.0015 (max.)	–	D5453	–
Sulfur (S500 grade)	ppm	0.05 (max.)	–	D5453	–
Sulfur content	mg/ kg	–	10 (max.)	–	–
Water and Sediment	% vol.	0.050 (max.)	–	D2709	–
Water content	mg/ kg	–	500 (max.)	–	EN ISO 12937
Total Contamination	mg/ kg	–	24 (max.)	–	EN 12662
Oxidation Stability at 110 °C	h	–	6 (min.)	–	EN 14112
Iodine Value	–	–	120 (max.)	–	EN 14111
Linolenic Acid Methyl Ester	% (m/ m)	–	12 (max.)	–	EN 14103d
Polyunsaturated Methyl Esters (≥4 double bonds)	% (m/ m)	–	1 (max.)	–	EN 14103
Ester content	% (m/ m)	–	96.5 (min.)	–	EN 14103d
Methanol content	% m/ m)	–	0.2 (max.)	–	EN 14110
Monoglyceride content	% (m/ m)	–	0.8 (max.)	–	EN 14105m
Diglyceride content	% (m/ m)	–	0.2 (max.)	–	EN 14105m
Triglyceride content	% (m/ m)	–	0.2 (max.)	–	EN 14105m
Alkaline Metals (Na + K)	mg/ kg	–	5 (max.)	–	EN 14108 EN 14109

Adapted from: **ASTM International (2019b); CEN (2018)**

Table A4 – Properties of fossil diesel, biodiesel, HVO and its blends

Properties		Flash Point (°C)	Pour Point (°C)	Specific Gravity	Calorific Value	Kinematic Viscosity at 40 °C	Cetane Number	Ref.
Unit		°C	°C	kg/ m³	MJ/ kg	mm²/ s	N/ A	–
ASTM D795		70	-17	830	42.2	2.5	40 (min.)	[A, B]
ASTM D6751		130	–	–	–	1.9 - 6.0	47 (min.)	[A]
Edible oil-derived biodiesel	**Palm**	160	13	880	38.69	3.94	50 - 62	[B]
	Rice Bran	165	3	874	37.9	4.63	56.2	[C]
	Canola	107	-8	875	–	3.32	61.5	[D]
Non-edible oil-derived biodiesel	**Jatropha curcas**	163 - 238	-3	864 - 880	38.5 - 42	3.7 - 5.8	46 - 55	[E]
	Karanja	163 - 187	-5.1	876 - 890	36 - 38	4.37 - 9.60	52 - 58	[F]
	Rubber Seed	130-140	-8	860 - 881	36.5 - 41.1	5.81 - 5.96	37 - 49	[G]
Biodiesel + Diesel Blends	**5 %**	–	–	831	42.6*	2.68	60.47*	[H]
	10 %	–	–	833	42.4*	2.82	61.75*	[H]
	15 %	–	–	837	42.1*	2.87	62.56*	[H]
HVO + Diesel Blends	**5 %**	–	–	828	43.1*	2.65	62.53*	[H]
	10 %	–	–	825	43.2*	2.71	63.36*	[H]
	15 %	–	–	823	43.2*	2.64	64.33*	[H]

Remarks:

*: Lower Heating Value (LHV)
*: Derived Cetane Number

References:

[A]: Yusuf, Kamarudin & Yaakub (2011); [B]: Mofijur et al. (2013); [C]: Narasimha et al. (2013); [D]: Ozcanli, Gungor & Aydin (2013); [E]: Chauhan et al. (2010); [F]: Sahoo et al. (2009); [G]: Ramadhas, Muraleedharan & Jayaraj (2005); [H]: Rodríguez-Fernández et al. (2019).

Adapted from : Rodríguez-Fernández et al. (2019) and Mardhiah et al. (2017)

Table A5 – Usual fly ash composition in terms of coal ranks

Component (% wt.) / Coal Rank	Anthracite[1]	Bituminous	Sub-bituminous	Lignite
SiO_2	28-57	20-60	40-60	15-45
Al_2O_3	18-36	5-35	20-30	10-25
Fe_2O_3	3-16	10-40	4-10	4-15
CaO	1-27	1-12	5-30	15-40
MgO	1-4	0-5	1-6	3-10
SO_3	0-9	0-4	0-2	0-10
Na_2O	0-1	0-4	0-2	0-6
K_2O	0-4	0-3	0-4	0-4
LOI*	1-8	0-15	0-3	0-5

Remarks:

*: Loss of Ignition (LOI).
[1]: Data from (Arent, Wise & Gelman, 2011) and treated by (Belviso, 2018).

Source: Ahmaruzzaman (2010)

Table A6 – Example studies of acidic, basic and bifunctional solid catalysts

Reaction[A]	Raw Material	Catalyst	Type of Catalyst	Reactional Conditions				Conversion (%)	Ref.
				Temp. (°C)	Time (h)	Alcohol: Oil Ratio	Catalyst Content (% wt.)		
T	Castor and soybean	TiO_2/ SO_4	Acidic	120	1	6:1	1	25 and 40	[A]
T	WFO	SnO_2/ SO_4 sup. on silica	Acidic	150	3	15:1	3	92.3	[B]
T	Soybean	zeolite β sup. with La	Acidic	60	4	14.5:1	0.011	48.9	[C]
T	WFO	Mn-Zr sup. on alumina	Acidic	150	5	14:1	2.5	>93	[D]
T	Soybean	KI, KBr, KCl, KF, KOH sup. on alumina	Basic	67	8	15:1	2.0	96 (KI sample)	[E]
T	Sunflower	Ki sup. on γ-alumina	Basic	67	3	12:1	2.5	99.99	[F]
T	Rapeseed and WFO	CaO	Basic	60	4	12:1	5.0	86 and 98	[G]
T	Palm	CaO	Basic	65	2	15:1	6.0	97	[H]
T	Soybean	Ce-doped HT	Basic	67	3	9:1	5.0	>90	[I]
T	Sunflower	NaOH sup. on alumina	Basic	50	4	12:1	0.9	>99	[J]
T	Soybean	MgO and calcined Mg-Al HT	Basic	180	1	0.88 g of methanol 2.0 g of oil	5.0	>98 and >95	[K]
T	*Jatropha curcas* and karanja[B]	Li doped CaO	Basic	65	2	12:1	5.0	>99	[L]
T	Karanja[B]	CaO*	Basic	65	2.5	8:1	2.5	>97.4	[M]
T & E	*Jatropha curcas*	Bi_2O_3 sup. on La_2O_3	Bifunc.	150	4	15:1	2.0	93	[N]
T & E	*Jatropha curcas* and rapeseed	La_2O_3 sup. on ZnO and alumina	Bifunc.	60	3	6:1	5.0	30 and >10[D]	[O]
		Li and iron sulfate sup. on CaO						>60 and 100/ >95	
		Li and iron sulfate[C] sup. on CaO						>95	
T & E	WFO	Mo-Mn sup. on γ-alumina and MgO	Bifunc.	100	4	27:1	5.0	91.4	[P]

Remarks:

Sup.: Means supported.; *: From chicken egg shells.; [A]: Transesterification (T) or Esterification (E).; [B]: *Pongamia pinnata*.; [C]: $(Fe_2(SO_4)_3)$.; D: Only for *Jatropha curcas* oil.

References:

[A] : de Almeida et al. (2008); [B] : Lam, Lee & Mohamed (2009); [C] : Shu et al. (2007); [D]: Amani et al. (2014); [E]: Xie & Li (2006); [F]: M. M. Marinković et al. (2016); [G]: Roschat et al. (2016a); [H]: Soares Dias et al. (2013); [I]: Soares Dias et al. (2012); [J]: Arzamendi et al. (2007); [K]: M. Di Serio et al. (2006); [L]: Kaur & Ali (2011); [M]: Y. C. Sharma, Singh & Korstad (2010); [N]: Rabiah Nizah et al. (2014), [O]: Endalew, Kiros & Zanzi (2011a); [P]: Farooq, Ramli & Subbarao (2013).

Table A7 – Worldwide coal fly ash compositions

Country	Chemical Composition (%)												Ref.
	SiO_2	Al_2O_3	Fe_2O_3	CaO	K_2O	MgO	SO_3	TiO_2	Na_2O	P_2O_5	MnO	LOI	
Australia	31.1 - 68.6	17 - 33	1 - 27.1	0.1 - 5.3	0.1 - 2.9	0 - 2	0 - 0.6	1.2 - 3.7	0 - 1.5	0 - 3.9	ND	NA	[A] [B]
Canada	35.5 - 62.1	12.5 - 23.2	3 - 44.7	1.2 - 13.3	0.5 - 3.2	0.4 - 3.1	0.2 - 7.8	0.4 - 1	0.1 - 7.3	0.1 - 1.5	NA	0.3 - 9.7	[C] [D]
China	35.6 - 57.2	18.8 - 55	2.3 - 19.3	1.1 - 7	0.8 - 0.9	0.7 - 4.8	1 - 2.9	0.2 - 0.7	0.6 - 1.3	1.1 - 1.5	ND	ND	[A]
Europe	28.5 - 59.7	12.5 - 35.6	2.6 - 21.2	0.5 - 28.9	0.4 - 4	0.6 - 3.8	0.1 - 12.7	0.5 - 2.6	0.1 - 1.9	0.1 - 1.7	0 - 0.2	0.8 - 32.8	[A]
Poland	32.2 - 53.3	4 - 32.2	4.5 - 8.9	1.2 - 29.9	0.2 - 3.3	1.2 - 5.9	NA	0.6 - 2.2	0.2 - 1.5	0.1 - 0.9	0 - 0.3	0.5 - 28	[E]
Germany	20 - 80	1 - 19	1 - 22	2 - 52	0 - 2	0.5 - 11	1 - 15	0.1 - 1	0 - 2	NA	NA	0 - 5	[F]
India	50.2 - 59.7	14 - 32.4	2.7 - 16.6	0.6 - 9	0.2 - 4.7	0.1 - 2.3	NA	0.3 - 2.7	0.2 - 1.2	NA	NA	0.5 - 7.2	[A] [G] [H]
USA	34.9 - 58.5	19.1 - 28.6	3.2 - 25.5	0.7 - 22.4	0.9 - 2.9	0.5 - 4.8	0.1 - 2.1	1 - 1.6	0.2 - 1.8	0.1 - 1.3	NA	0.2 - 20.5	[A] [I]
Russia	40.5 - 48.6	23.2 - 25.9	NA	6.9 - 13.2	1.9 - 2.6	2.6 - 4	NA	0.5 - 0.6	1.2 - 1.5	0.3 - 0.4	0.2 - 0.4	NA	[J]
South Africa	46.3 - 67	21.3 - 27	2.4 - 4.7	6.4 - 9.8	0.5 - 1	1.9 - 2.7	NA	1.2 - 1.6	0 - 1.3	0.3 - 0.9	0 - 0.5	NA	[K] [L] [M]

Remarks:
ND: Not Detected.
NA: Not Available.

References:

[A]: Blissett & Rowson (2012), [B]: Lu & Do (1991), [C]: Ram & Masto (2014), [D]: Ramezanianpour (2014), [E]: Moreno et al. (2005), [F]: Vichaphund et al. (2014), [G]: Pandian (2004), [H]: Ghosh & Subbarao (1998), [I]: Binal, Bas & Karamut (2016), [J]: Chindaprasirt et al. (2012), [K]: Mukherjee et al. (2008), [L]: ASTM International (2019a), [M]: S. H. Lee et al. (2003).

Adapted from: Bhatt et al. (2019)

Table A8 – Vegetable oil mean molar mass data

Fatty Acid Characteristics			Soybean				Sunflower			
Reference			[A]	[B]	[C]	[D]	[B]	[C]	[D]	[E]
Type	Carbon : Double Bond	MM (g/ mol)	% cont.	% cont.	% cont.	% cont.	% cont.	% cont.	% cont.	% cont.
Lauric	12:0	200.32	0.10	–	–	–	0.5	0.10	–	–
Myristic	14:0	228.37	0.10	0.10	–	–	0.10	0.20	–	0.10
Palmitic	16:0	256.42	10.20	10.80	10.00	11.75	6.40	6.80	6.08	6.40
Stearic	18:0	284.48	3.70	3.90	3.50	3.15	4.50	4.70	3.26	2.90
Arachidic	20:0	312.53	–	–	0.50	–	0.30	0.40	–	–
Behenic	22:0	340.58	–	–	0.30	–	0.80	–	–	–
Lignoceric	24:0	368.64	–	–	–	–	0.20	–	–	–
Palmitoleic	16:1 (n-7)	254.41	–	0.20	0.20	–	0.10	0.10	–	0.10
Oleic	18:1 (n-9)	282.46	22.80	23.90	21.00	23.26	22.10	18.60	16.93	17.70
Linoleic (ω-6)	18:2 (n-6, n-12)	280.45	53.70	52.10	55.30	55.53	65.60	68.60	73.73	72.80
Linolenic (ω-3)	18:3 (n-3, n-6, n-9)	278.43	8.60	7.80	9.20	6.31	0.50	0.50	–	–
Gondoic	20:1 (n-9)	310.51	–	0.10	–	–	0.20	–	–	–
Erucic	22:1 (n-9)	338.57	–	–	–	–	0.10	–	–	–
Mean Molar Mass (MMM)			866.21	863.57	874.18	872.32	889.58	875.90	876.42	875.96

References:

[A]: Kincs (1985), [B]: Dubois et al. (2007), [C]: Hammond (2003), [D]: Goering et al. (1982), [E]: Demirbaş (2002)

Table A9 – Molecular vibrational patterns in IR focused in biodiesel

Vegetable Oil and Biodiesel	
1000 - 1260 cm^{-1}	C-O stretching vibrations in alcohols, according to Silverstein, Webster & Kiemle (2005), varying in the range depending on the type of alcohol (primary, secondary, tertiary). The authors say that the C-O stretching and O-H bending modes are not independent vibrational modes because they couple with the vibrations of adjacent groups.
1170 cm^{-1}	C-O stretching vibrations composed of 2 asymmetrical coupled vibrations, C-C(=O)-C and O-C-C, being the former the most important.
1163 – 1210 cm^{-1}	For saturated esters (except for acetates) shows strongly in the region of 1210 - 1163 cm^{-1}, being usually broader and stronger than the C=O stretching absorption.
1175, 1205 and 1250 cm^{-1}	For methyl esters of long chain FAs present a three-band pattern near 1175, 1205 and 1250 cm^{-1}, being the last one the strongest. C-O-C symmetric stretch and C-C stretch at 1700 cm^{-1}, according to Siatis et al. (2006).
1150 - 1350 cm^{-1}	Methylene (CH_2) twisting and wagging vibrations, according to Silverstein, Webster & Kiemle (2005).
1209 cm^{-1}	O-H bending according to Silverstein, Webster & Kiemle (2005).
1238 - 1248 cm^{-1}	O-H deformation according to Siatis et al. (2006).
1378 cm^{-1}	Related to terminal CH_3 groups in TAG, DAG, MAG, FFA and FAME and to O-CH_2 groups in the glycerol moiety in TAG, DAG and MAG, according to Dubé et al. (2004).
1465 cm^{-1}	CH_2 scissoring ($\delta_s CH_2$), a very constant position in the spectrum, according to Silverstein, Webster & Kiemle (2005).
2840 - 3000 cm^{-1}	C-H stretching in alkanes. It has one of the most stable positions in the spectrum, according to Silverstein, Webster & Kiemle (2005).
2853 - 2926 cm^{-1}	CH_2 asymmetric stretching ($\upsilon_{AS} CH_2$) and symmetrical stretching ($\upsilon_S CH_2$). These bands does not vary more than ± 10 cm^{-1}, according to Silverstein, Webster & Kiemle (2005).
Only Vegetable Oil	
850 - 1000 cm^{-1}	Related to the out-of-plane OH deformation as mentioned by Kollar et al. (2017) and "strong and broad" when it is a bonded OH, as Silverstein, Webster & Kiemle (2005).
1075 - 1111 cm^{-1}	O-CH_2-C asymmetric axial stretching.
1100 cm^{-1}	O-CH_2-C asymmetric and/ or CH_2-OH vibration (typical glycerol peak).
1370 - 1400 cm^{-1}	CH_3 groups symmetrical bending in TAG, DAG, MAG, FFA and FAME and O-CH_2 groups in glycerol moiety of TAG, DAG and MAG, as highlighted by (Dubé et al., 2004) .The authors mention that the height of this peak should decrease by the time the transesterification reaction progresses (as glycerol moiety is lost).
1570 cm^{-1}	It refers to the carboxylate (COO-) molecule, the soap formed derived from a FFA, after a saponification reaction, as mentioned by Dong et al. (2015); Al-Alawi, Van de Voort & Sedman (2004).
1711 cm^{-1}	Cruz et al. (2019); Mahesar et al. (2017, 2014) indicate that this range refers to a C=O bond associated to a FFA molecule.
Only Biodiesel	
1060 - 1300 cm^{-1}	C-O vibration. This absorption range is related to the presence of esters and, specifically, glycerol esters (DAG and MAG) and methyl esters.
1188 - 1200 cm^{-1}	O-CH_3 stretching (added methyl group). It is the most characteristic peak, according to Rabelo et al. (2015); Siatis et al. (2006)
1735 - 1750 cm^{-1}	C=O stretching in methyl esters (R-C=O-O-CH_3), according to Larkin (2011).
1200 cm^{-1}	O-CH_3 stretching, according to Siatis et al. (2006).
1425 - 1447 cm^{-1}	CH3- asymmetric bending, according to Siatis et al. (2006).
1748 cm^{-1}	Cruz et al. (2019); Mahesar et al. (2014, 2017) indicate that this range refers to a C=O bond associated to a FAME molecule.

APPENDIX B

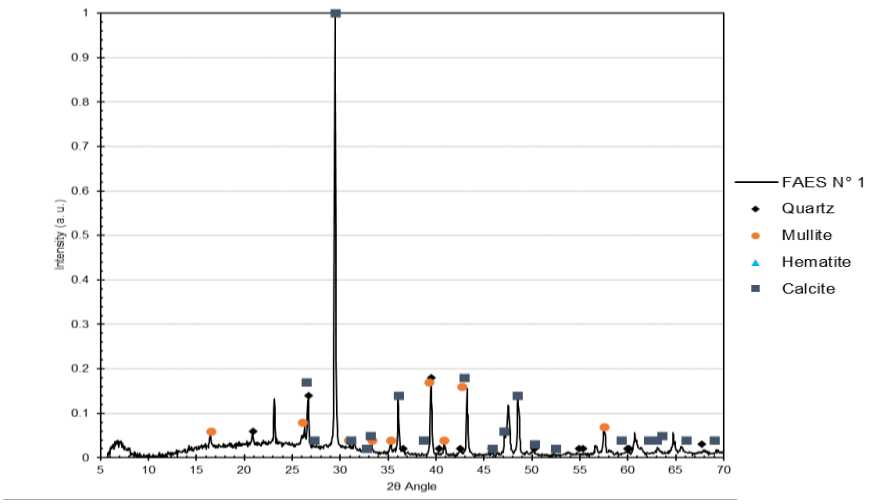

Figure B1 – XRD diffractogram for FAES N° 1 catalyst

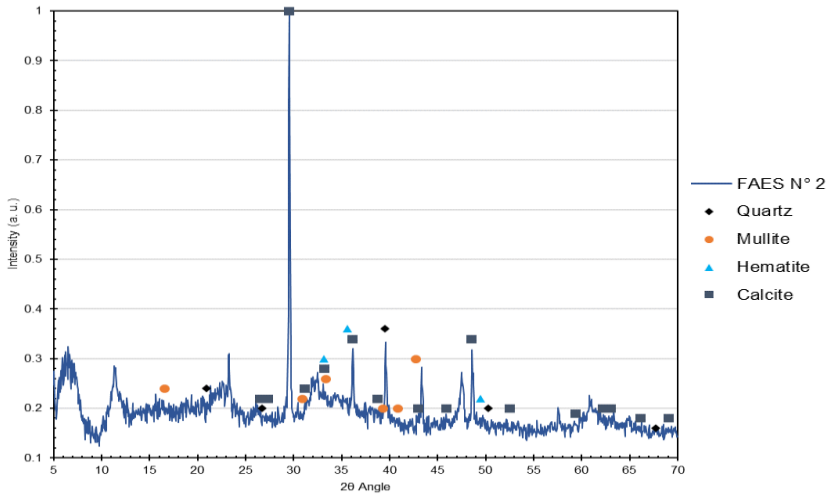

Figure B2 – XRD diffractogram for FAES N° 2 catalyst

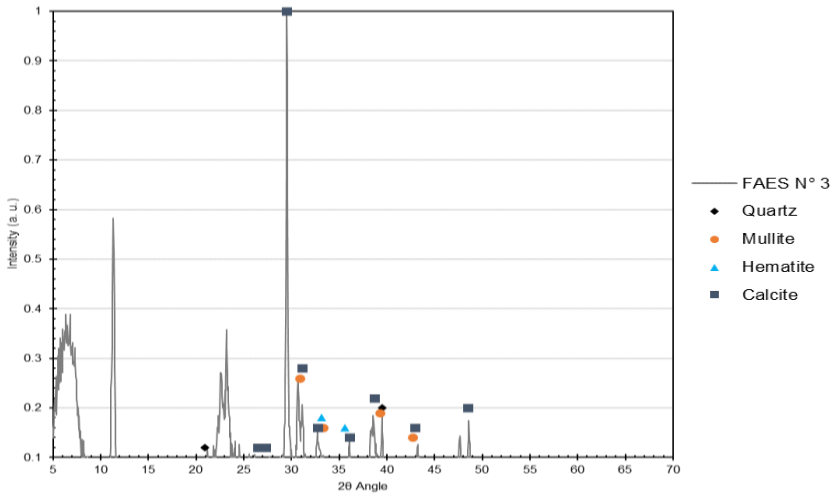

Figure B3 – XRD diffractogram for FAES N° 3 catalyst

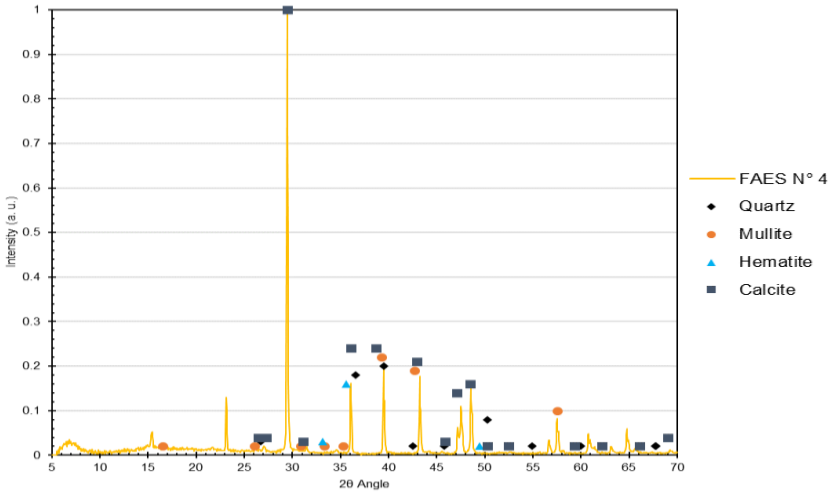

Figure B4 – XRD diffractogram for FAES N° 4 catalyst

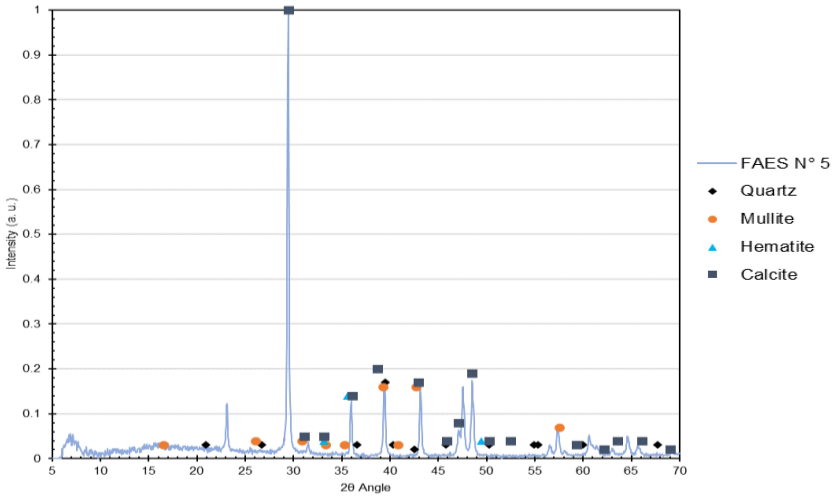

Figure B5 – XRD diffractogram for FAES N° 5 catalyst

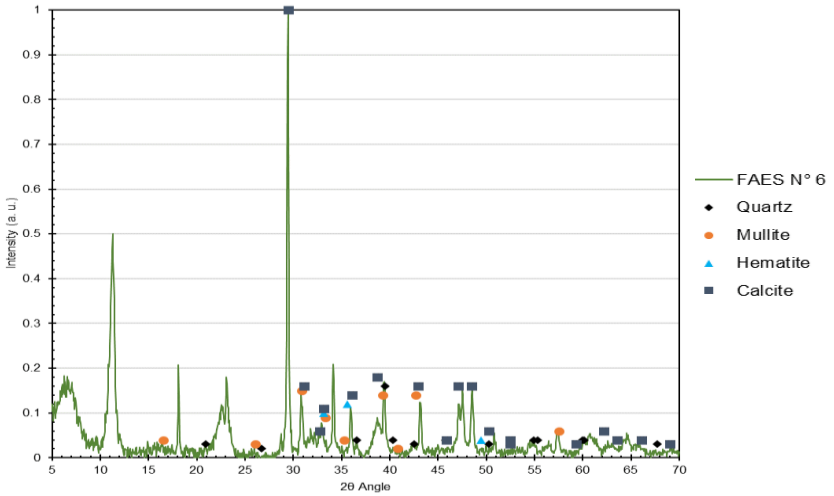

Figure B6 – XRD diffractogram for FAES N° 6 catalyst

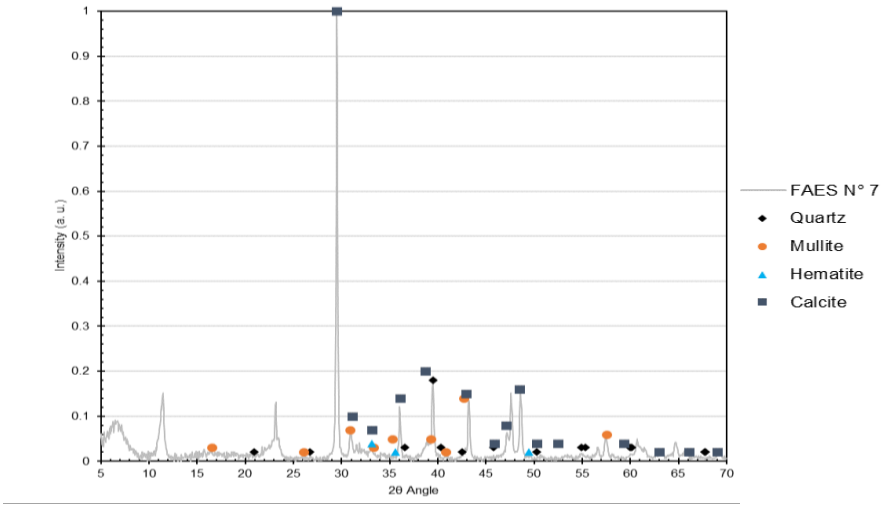

Figure B7 – XRD diffractogram for FAES N° 7 catalyst

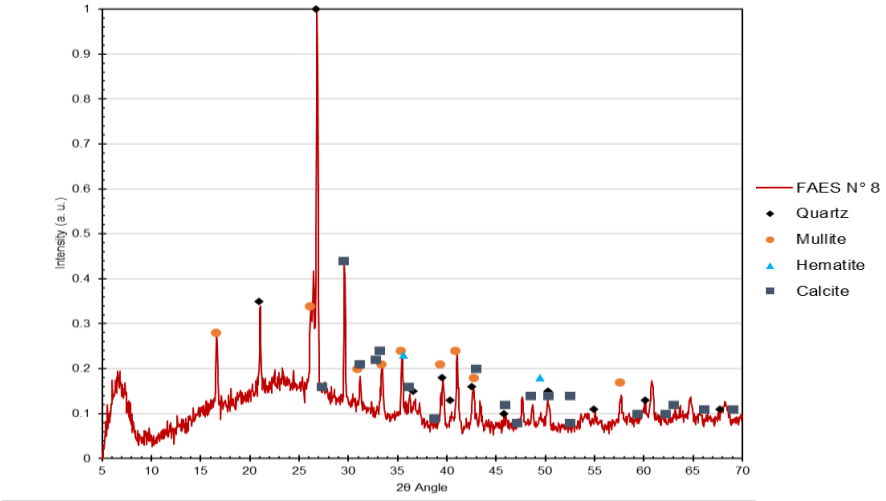

Figure B8 – XRD diffractogram for FAES N° 8 catalyst

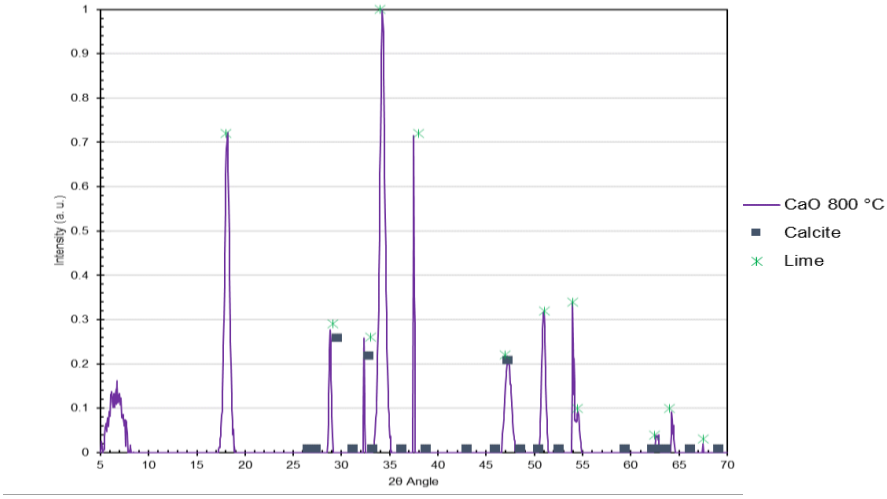

Figure B9 – XRD diffractogram for CaO catalyst calcined at 800 °C

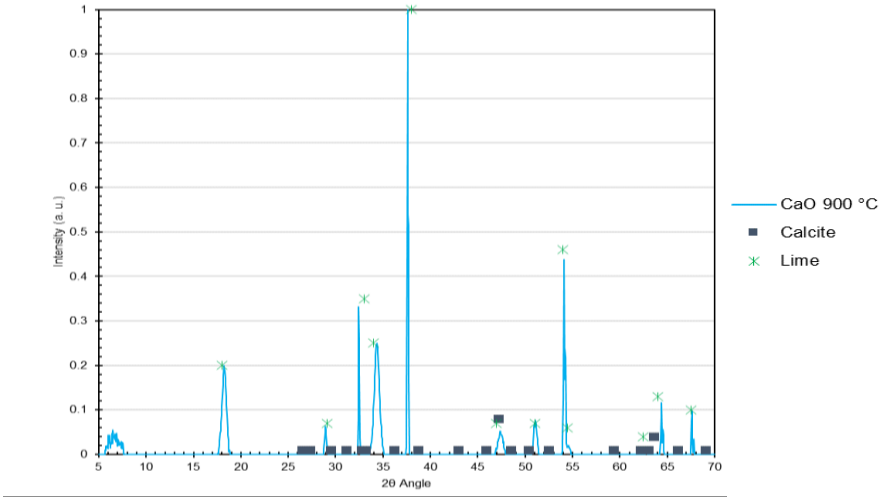

Figure B10 – XRD diffractogram for CaO catalyst calcined at 900 °C

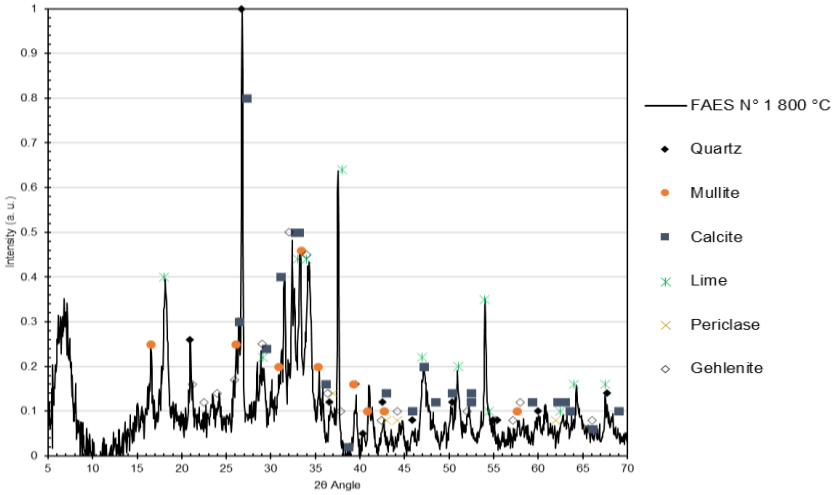

Figure B11 – XRD diffractogram for FAES N° 1 catalyst calcined at 800 °C

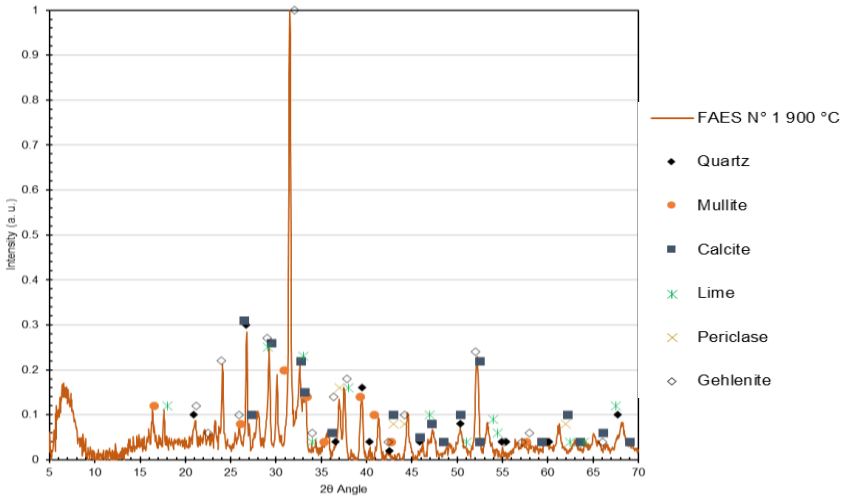

Figure B12 – XRD diffractogram for FAES N° 1 catalyst calcined at 900 °C

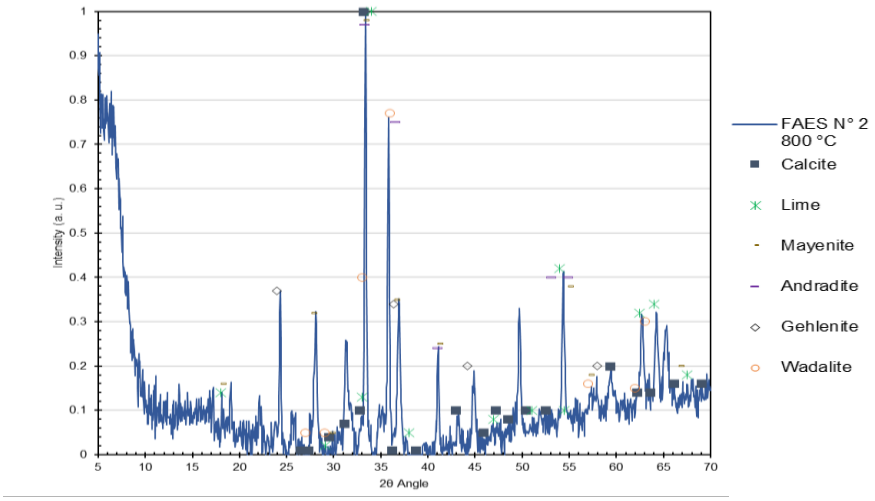

Figure B13 – XRD diffractogram for FAES N° 2 catalyst calcined at 800 °C

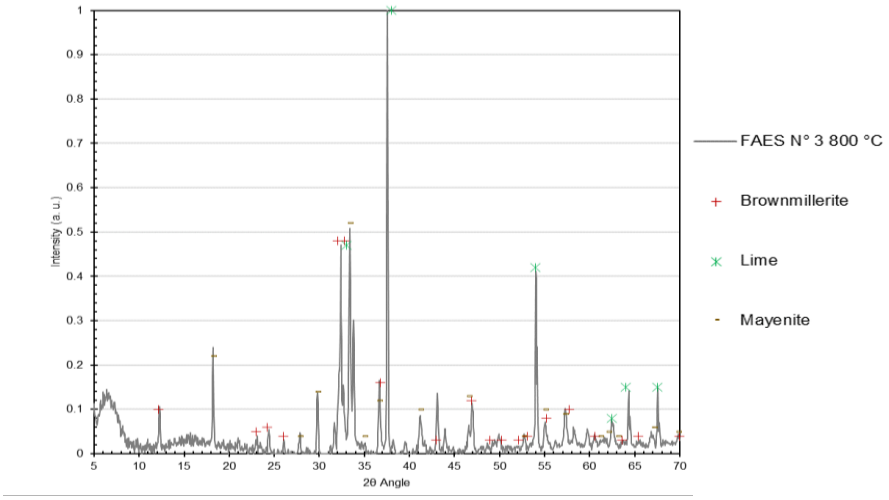

Figure B14 – XRD diffractogram for FAES N° 3 catalyst calcined at 800 °C

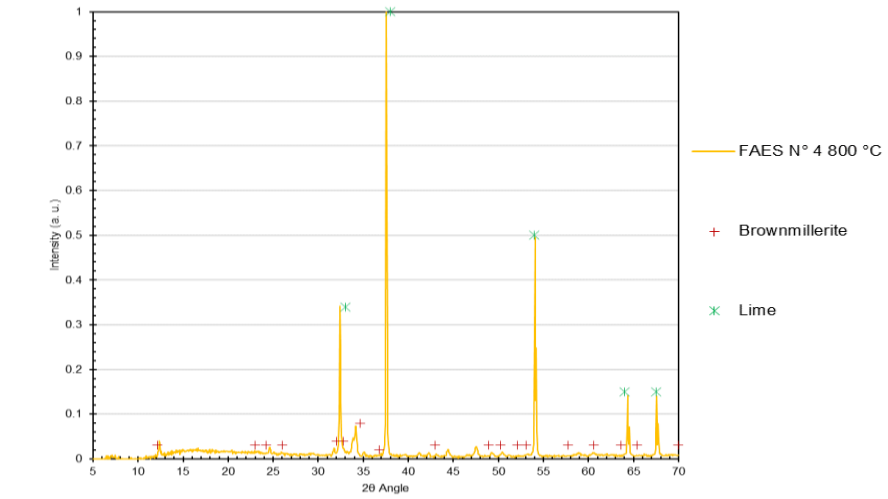

Figure B15 – XRD diffractogram for FAES N° 4 catalyst calcined at 800 °C

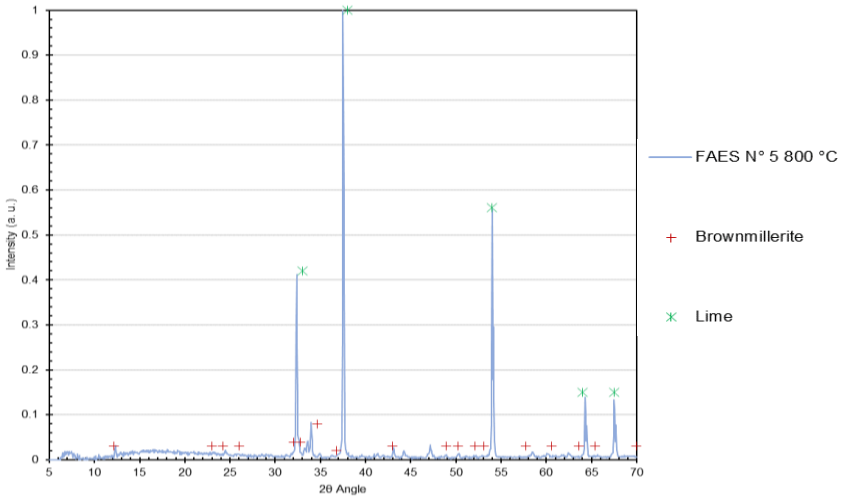

Figure B16 – XRD diffractogram for FAES N° 5 catalyst calcined at 800 °C

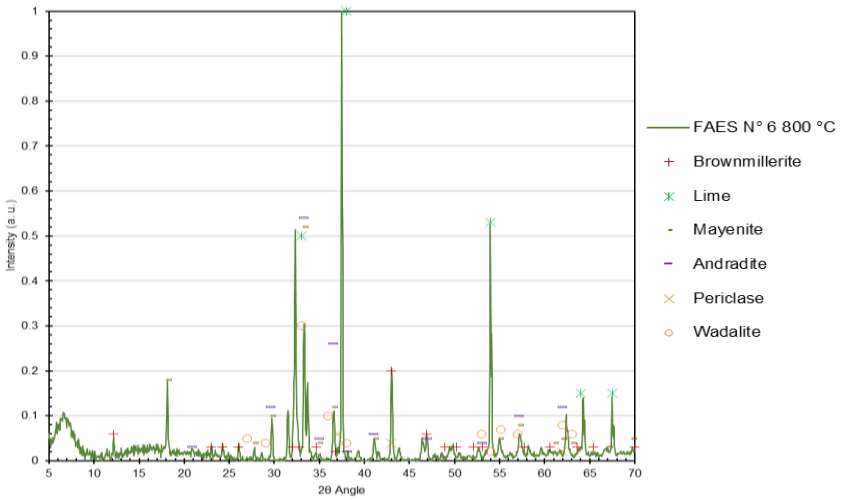

Figure B17 – XRD diffractogram for FAES N° 6 catalyst calcined at 800 °C

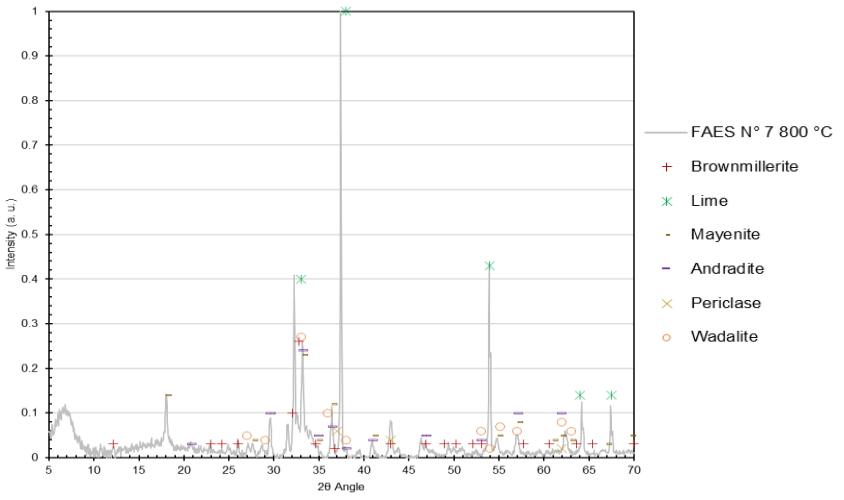

Figure B18 – XRD diffractogram for FAES N° 7 catalyst calcined at 800 °C

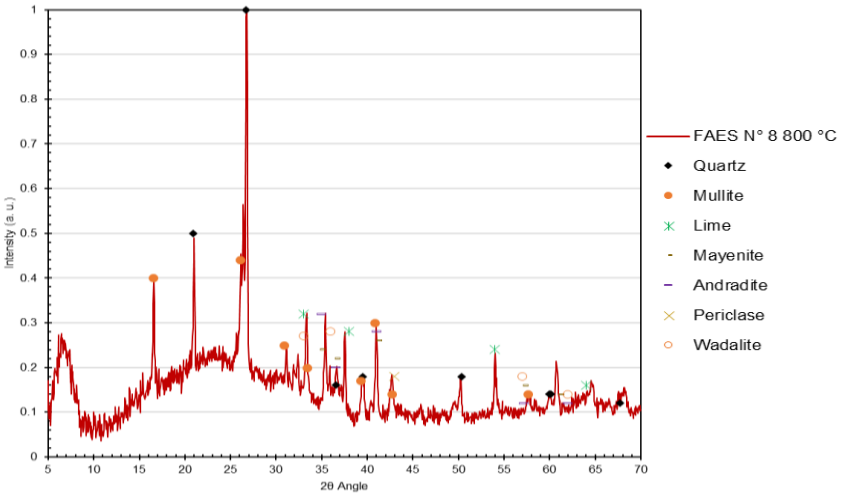

Figure B19 – XRD diffractogram for FAES N° 8 catalyst calcined at 800 °C